NOTICE

AVIS

The quality of this microform is heavily dependent upon the quality of the original thesis submitted for microfilming. Every effort has been made to ensure the highest quality of reproduction possible.

La qualité de cette microforme dépend grandement de la qualité de la thèse soumise au microfilmage. Nous avons tout fait pour assurer une qualité supérieure de reproduction.

If pages are missing, contact the university which granted the degree.

S'il manque des pages, veuillez communiquer avec l'université qui a conféré le grade.

Some pages may have indistinct print especially if the original pages were typed with a poor typewriter ribbon or if the university sent us an inferior photocopy.

La qualité d'impression de certaines pages peut laisser à désirer, surtout si les pages originales ont été dactylographiées à l'aide d'un ruban usé ou si l'université nous a fait parvenir une photocopie de qualité inférieure.

Reproduction in full or in part of this microform is governed by the Canadian Copyright Act, R.S.C. 1970, c. C-30, and subsequent amendments.

La reproduction, même partielle, de cette microforme est soumise à la Loi canadienne sur le droit d'auteur, SRC 1970, c. C-30, et ses amendements subséquents.

Canada

UNIVERSITY OF ALBERTA

NEW CORRELATIONS FOR PREDICTING SIEVE TRAY EFFICIENCIES

by

ALBERT K. M. WONG

©

A thesis submitted to the Faculty of Graduate Studies and Research in partial fulfillment

of the requirements for the degree of **Master of Science.**

DEPARTMENT OF CHEMICAL ENGINEERING

Edmonton, Alberta

Spring, 1993

The author has granted an irrevocable non-exclusive licence allowing the National Library of Canada to reproduce, loan, distribute or sell copies of his/her thesis by any means and in any form or format, making this thesis available to interested persons.

L'auteur a accordé une licence irrévocable et non exclusive permettant à la Bibliothèque nationale du Canada de reproduire, prêter, distribuer ou vendre des copies de sa thèse de quelque manière et sous quelque forme que ce soit pour mettre des exemplaires de cette thèse à la disposition des personnes intéressées.

The author retains ownership of the copyright in his/her thesis. Neither the thesis nor substantial extracts from it may be printed or otherwise reproduced without his/her permission.

L'auteur conserve la propriété du droit d'auteur qui protège sa thèse. Ni la thèse ni des extraits substantiels de celle-ci ne doivent être imprimés ou autrement reproduits sans son autorisation.

UNIVERSITY OF ALBERTA

RELEASE FORM

NAME OF AUTHOR: Albert K. M. WONG

TITLE OF THESIS: New Correlations For Predicting Sieve Tray Efficiencies

DEGREE: Master of Science

YEAR THIS DEGREE GRANTED: 1993

Albert K. M. Wong

1879 - 40th Street,

Edmonton, Alberta

T6L 3H3
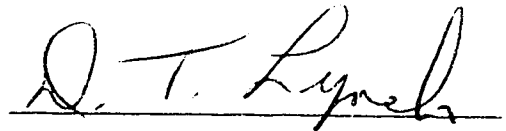
UNIVERSITY OF ALBERTA

FACULTY OF GRADUATE STUDIES AND RESEARCH

The undersigned certify that they have read, and recommend to the Faculty of Graduate Studies and Research for acceptance, a thesis entitled **New Correlations For Predicting Sieve Tray Efficiencies** submitted by **Albert K. M. WONG** in partial fulfillment of the requirements for the degree of **Master of Science**.

_____
Dr. K. T. Chuang, Supervisor

_____
Dr. D. T. Lynch

_____
Dr. R. K. Wood

_____
Dr. J. M. Whiting

Date: _April 14 1993_____

ABSTRACT

Sieve trays have been widely used in distillation for many years. The tray efficiency is often predicted by using empirical or semi-empirical correlations. Extensive studies have been made in developing these correlations, but almost all correlations to date still suffer some limitations.

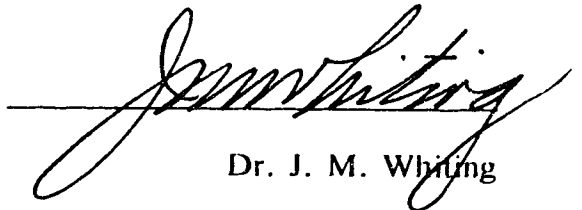One aspect which has not been adequately considered is the effect of surface tension and its gradients on tray efficiencies. Most experimental studies have shown that the effect of surface tension and its gradients can substantially affect the tray efficiency by influencing the interfacial area and the rate of mass transfer in the dispersion. However, no theoretical basis has been established to include those effects in the prediction of tray efficiencies.

Two new semi-empirical correlations have been developed to predict the number of individual phase transfer units in which the effect of surface tension and its gradients was considered explicitly. The correlations were developed under distillation conditions where the number of vapour and liquid mass transfer units were determined based on the same interfacial area. The formulation of an enhancement factor with the Marangoni-index embodies the effect of surface tension gradients. Six binary systems were selected in this investigation in which a wide range of physical properties was covered with different combinations of hydrocarbons, alcohols and aqueous solution. The applicability of the correlations in all systems with different surface tension changes was successful.

The experimental results of this work indicate that the new correlations produce good accuracy in the prediction of tray efficiencies.

ACKNOWLEDGEMENTS

TABLE OF CONTENTS

TABLE

LIST OF FIGURES

NOMENCLATURE

A   Bubbling area, m^2

a   Interfacial area, m^2

$a^{\cdot}$ Interfacial area per unit volume, $1/m$

a_o, b_o, c_o Parameters in Equation (5.3)

b,d   Parameters in Equation (5.2)

c_L Liquid phase concentration, $kmol/m^3$

$c^{\cdot}$ Equilibrium liquid concentration, $kmol/m^3$

De   Eddy diffusivity, m^2/s

D_G Vapour phase diffusion coefficient, m^2/s

D_L Liquid phase diffusion coefficient, m^2/s

E_o Overall efficiency, %

E_{OG} Point efficiency, %

E_{MV} Murphree efficiency, %

FP   Flow parameter, $(m_L/m_G)(\rho_G/\rho_L)^{0.5}$

Fr   Froude number

F_s F-factor based on bubbling area, $= u_s(\rho_G)^{0.5}$, $(kg/m)^{0.5}/s$

g   Acceleration due to gravity, m/s^2

G_M Molar gas flow, $kmol/s$

$G^{\cdot}_M$ Molar gas flow per bubbling area, $kmol/sm^2$

h_f Froth height, m

h_{cl}	Clear liquid height, m
h_w	Weir height, m
K_{OG}	Overall vapour phase mass transfer coefficient, kmol/s m^2 atm
K_{OL}	Overall liquid phase mass transfer coefficient, m/s
k_G	Vapour phase mass transfer coefficient, kmol/s m^2 atm
k_L	Liquid phase mass transfer coefficient, m/s
L_M	Molar liquid flow, kmol/s
L'_M	Molar liquid flow per bubbling area, kmol/sm^2
m	Slope of equilibrium line
M	Marangoni-index, N/m
M_G	Vapour phase molecular weight, kmol/m^3
M_L	Liquid phase molecular weight, kmol/m^3
m_G	Vapour mass flow rate, kg/s
m_L	Liquid mass flow rate, kg/s
N	Rate of diffusion, kmol/s
N_A	Actual number of tray
N_T	Number of theoretical tray
N_G	Vapour phase mass transfer unit
N_L	Liquid phase mass transfer unit
N_{OG}	Overall vapour phase mass transfer unit
P	Total absolute pressure, atm
Pe	Peclet number

p^*	Equilibrium gas partial pressure, atm
p_G	Vapour phase partial pressure, atm
p,q	Hydrodynamic factor in Equation (2.32) and (2.33)
Q_L	Liquid flow rate, m^3/s
R	Gas constant, m^3 atm/kmol K
Sc	Schmidt number, $\mu_G/(\rho_G D_G)$
t_G	Vapour contact time, s
t_L	Liquid contact time, s
T	Temperature, K
u_s	Vapour velocity based on bubbling area, m/s
W	Weir length, m
X_A	Average tray concentration, mol.%
x_n	Liquid composition leaving the tray
x_{n-1}	Liquid composition entering the tray
x_n^*	Liquid composition at equilibrium
y_n	Vapour composition leaving the tray
y_{n-1}	Vapour composition entering the tray
y_n^*	Vapour composition at equilibrium
Z	Height of the column, m
Z_1	Length of liquid travel across the tray, m
Z_L	Liquid phase film thickness, m
Z_G	Vapour phase film thickness, m

Greek Letters

α_e Parameter given in Equation (3.7)

ϵ Vapour hold-up fraction

η Parameter in Equation (3.6)

ρ_G Vapour density, kg/m^3

ρ_L Liquid density, kg/m^3

σ Surface tension, N/m

μ_G Vapour phase viscosity, Ns/m^2

μ_L Liquid phase viscosity, Ns/m^2

ϕ Fraction of open hole area

λ Stripping factor, mG'_M/L'_M

Chapter 1

INTRODUCTION

1. Introduction

One of the important parameters for the design and analysis of a sieve tray column is the mass transfer efficiency. Although it has been extensively studied over the years, significant progress in predicting tray efficiencies has not been achieved since the publication of the AIChE Bubble Tray Design Manual (AIChE, 1958).

The procedure for predicting tray efficiencies involves two parts: (a) the point efficiency prediction based on the transfer-units concept, and (b) its relation to the tray efficiency. The latter part has been a subject of many studies (Porter et. al., 1972; Lockett et. al., 1973; Lockett and Safekourdi, 1976; Lim et. al., 1974) and it was found that reliable calculations can be obtained (Biddulph et. al., 1991). However, the prediction of point efficiencies remains as a rather approximate exercise because of the complexity of the inter-relationships among the parameters that affect tray efficiencies. These parameters can be summarized as physical dimensions of the tray, operating conditions and physical properties of the system. Of all the physical dimensions of the tray only outlet weir height was found to be important enough to affect the mass transfer between phases in the dispersion. (The effect of liquid path length on tray efficiency is taken into account in the correlation to be presented later for the degree of liquid mixing which occurs on the tray.) Other tray design variables such as hole area, hole diameter,

tray spacing, etc., were found to be relatively unimportant as far as the mass transfer is concerned. This is because the vapour and liquid contact usually occurs above the tray deck; thus, those variables have little effect on the mass transfer in the dispersion. In the present study, the effect of outlet weir height on the tray efficiency is implicitly included in the correlation of clear liquid height which will be discussed later.

During distillation, two typical flow regimes (froth and spray regimes) are normally observed in a sieve tray column. These two flow regimes are governed by the operating conditions which in turn influence the hydrodynamic behaviour of the tray such as the vapour-liquid contact time and the interfacial area. Different tray efficiency correlations are generally required to predict efficiencies in separate regimes. However, in practice, sieve tray columns are typically operated in the froth regime rather than the spray regime. The reason is that the problems of entrainment and flooding are usually associated with the spray regime, and operation in such conditions are normally avoided. A separate tray efficiency correlation for predicting efficiencies in the spray regime is really not necessary in most cases; besides, the efficiency changes between the two regimes (from froth to spray) are found to be gradual according to the Fractionation Research Incorporated (FRI) test results and Prado and Fairs' results (1990). Therefore, tray efficiency correlations developed based on the froth regime may also be applied to estimate efficiencies in the spray regime.

For many years, the effects of the physical properties of the system on tray efficiencies are not very clear. Only a few key system properties such as the vapour and liquid viscosities, vapour density and vapour and liquid diffusivities are included in most

2

tray efficiency correlations but the actual effects of these system properties on tray efficiencies are still not apparent. Other important system properties such as the liquid density and the surface tension are somewhat ignored by many researchers in the prediction of the tray efficiency. For the past decade, the effects of system properties have been the subject of many studies, in particular, the effects of the surface tension on tray efficiencies. Previous experimental studies have shown that surface tension can influence the interfacial area and the rate of mass transfer in the dispersion, and consequently the tray efficiency. These effects were regarded as the only confused area in the prediction of the tray efficiency by Lockett (1986); Kister (1992) also stated that there is uncertainty regarding the effects of the surface tension on the tray efficiency because it is often difficult to divorce the surface tension effects from those of other physical properties. More recently, Chen and Chuang (1992) developed two semi-empiricial correlations to predict the number of individual phase transfer units, in which the effects of surface tension were included. However, their analysis was not conclusive because the derivation of their correlations was based on the surface tension neutral system only (i.e. cyclohexane/n-heptane) and was questionable when applying to other systems such as the surface tension positive and negative systems.

Therefore, the focus of this thesis will be devoted to an experimental study of the effects of surface tension on tray efficiencies. The effect of physical properties, such as liquid density, will also be examined. The investigation involves using six different binary systems which represent different categories of surface tension change and cover a wide range of physical properties with different combinations of hydrocarbons, alcohols

and aqueous solutions. The results will allow for developing two reliable tray efficiency

correlations.

Chapter 2

TRAY EFFICIENCY

One of the major parts of a distillation column design is to determine the number of actual trays required for a given separation. This is usually done by first calculating the number of theoretical trays and then modifying the result to the actual number of trays by the use of a measure of efficiency. Many different measures of efficiencies have been defined. Three that are more commonly used than the others are the point efficiency, Murphree efficiency (Murphree, 1925) and overall column efficiency.

2.1 Point efficiency

From Figure 2.1, point efficiency is defined as:

$$E_{OG} = \frac{\overline{y_n} - \overline{y_{n+1}}}{\overline{y_n^*} - \overline{y_{n+1}}}$$

(2.1)

where y_{n+1} is the composition of vapour entering the tray, y_n^* is the composition of vapour in equilibrium with liquid leaving the tray, and y_n is the composition of vapour leaving the tray. The bar on top indicates that all the concentrations are determined at a specific point on the tray.
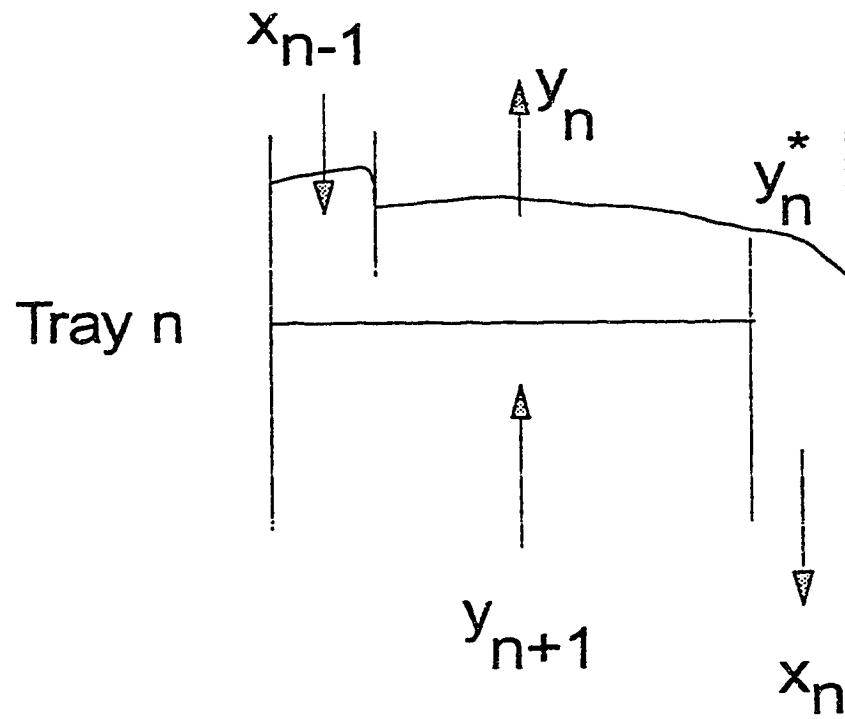
Figure 2.1: Tray Nomenclature

2.2 Murphree tray efficiency

The Murphree tray efficiency (Murphree, 1925) is defined by a ratio of the actual change in a vapour concentration through the tray to the change in vapour concentration at equilibrium. Similar to point efficiency, the vapour phase Murphree tray efficiency can be expressed as:

$$E_{MV} = \frac{y_n - y_{n+1}}{y_n^* - y_{n+1}} \qquad (2.2)$$

Analogous efficiency definitions can also be expressed in terms of the liquid phase:

$$E_{ML} = \frac{x_n - x_{n-1}}{x_n^* - x_{n-1}} \qquad (2.3)$$

At total reflux, from a simple component balance, it follows that the value of y_n is equal to the composition of the liquid entering the tray, i.e. $y_n = x_{n-1}$ and similarly $y_{n+1} = x_n$; therefore, the Murphree vapour efficiency can be expressed as:

$$E_{MV} = \frac{x_{n-1} - x_n}{y_n^* - x_n} \qquad (2.4)$$

If both the liquid and the vapour are perfectly mixed, the liquid composition on the tray is uniform and so is the vapour composition. The Murphree tray efficiency will then coincide with the point efficiency at any point on the tray.

7

2.3 Relation between E_{MV} and E_{OG}

In most cases, especially large-diameter sieve trays, both the vapour and liquid on the tray are not completely mixed, a model of the vapour and liquid mixing patterns is often needed for converting the point efficiency, E_{OG} to the tray efficiency, E_{MV}. One of the mixing models recommended by the AIChE Manual for a partially mixed tray is (AIChE, 1958):

$$\frac{E_{MV}}{E_{OG}} = \frac{1 - e^{-(\eta + Pe)}}{(\eta + Pe)[1 + \frac{\eta + Pe}{\eta}]} + \frac{e^{\eta} - 1}{\eta[1 + \frac{\eta}{\eta + Pe}]} \qquad (2.5)$$

where

$$\eta = \frac{Pe}{2}(\sqrt{1 + \frac{4\lambda E_{OG}}{Pe}} - 1) \qquad (2.6)$$

$$and \qquad \lambda = m G_M' / L_M'$$

$$Pe = \frac{Z_l^2}{De\, t_L} \qquad (2.7)$$

Numerical solutions of Equation (2.5) have been worked out for various values of Pe and λE_{OG} to provide the plot shown in Figure 2.2. De in Equation (2.7) is the eddy diffusion coefficient, which is a measure of the amount of back-mixing. Lockett (1986) suggested the use of the Shore and Haselden (1969) correlation to estimate De for systems other

8
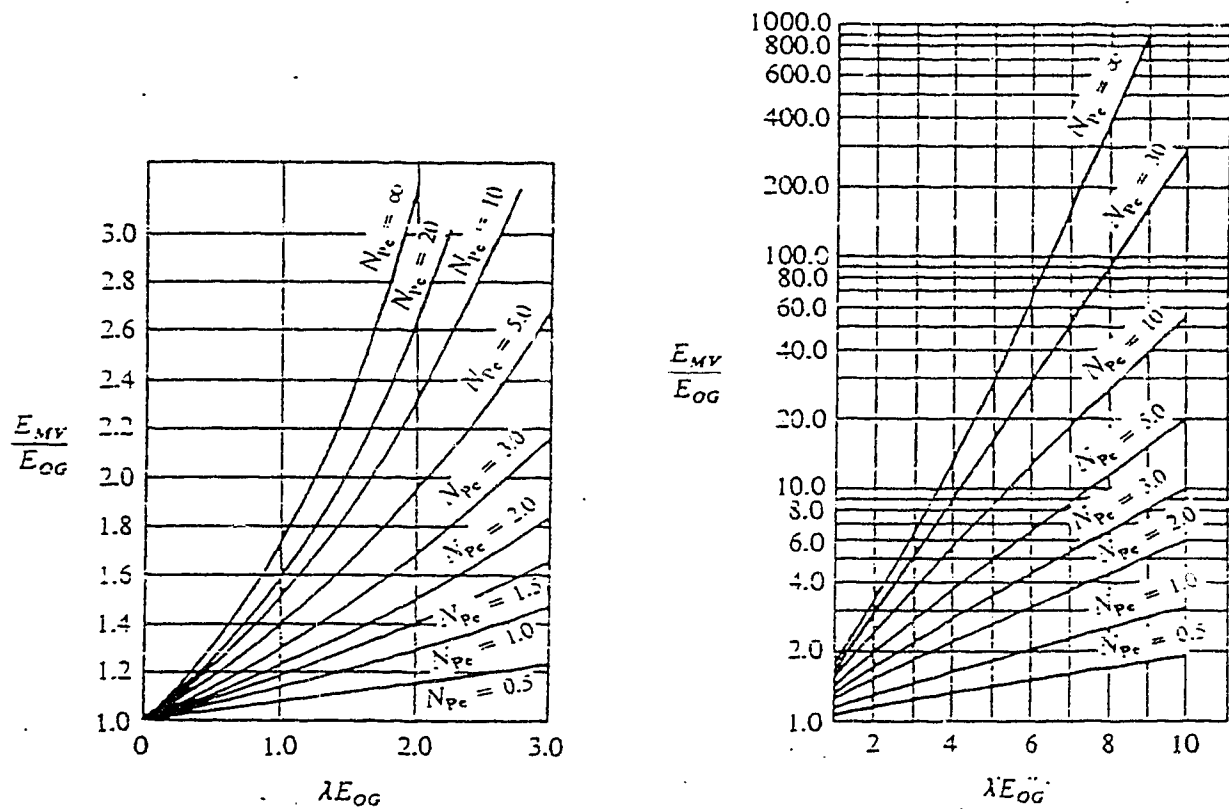
Figure 2.2: E_{MV}/E_{OG} as a function of λE_{OG} and Pe

for the Diffusion Liquid Mixing Model (AIChE 1958)

9

than air-water. The equation is given as:

$$De = 0.31 h_f [u_s (\rho_G/\rho_L)^{0.5}]^{0.63}$$

(2.8)

The Peclet number, Pe, defined in Equation (2.7) is the parameter that characterizes the degree of mixing on the tray. Notice that if the Peclet number approaches zero, Equation (2.5) simplifies to $E_{MV} = E_{OG}$. This implies that the tray is completely mixed. In the present study, tests were carried out using a 0.153 m diameter column. The Peclet number was calculated to be between 0.1 and 0.2 and is shown in Appendix A; hence, the tray is assumed to be completely mixed. With that assumption, less error will be introduced in the correlations for predicting the point efficiency simply because the step of converting the tray efficiency, E_{MV}, to the point efficiency, E_{OG}, or vice versa is eliminated.

The fundamental approach to the prediction of tray efficiencies involves the prediction of point efficiencies from the mass-transfer characteristics of the system and the physical dimensions of the tray. The point efficiencies are then related to the tray efficiencies using the mixing models discussed earlier.

2.4 Overall column efficiency

The tray efficiencies can be related to the overall column efficiency with the following equation:

$$E_o = \frac{\ln[1 + E_{MV}(\lambda - 1)]}{\ln \lambda}$$

(2.9)

10

Equation (2.9) is developed based on an assumption that the equilibrium and operating lines are straight. With the number of theoretical trays, N_T and E_o calculated, the number of actual trays, N_A can be determined as:

$$N_A = \frac{N_T}{E_o} \qquad (2.10)$$

The best way to determine the efficiency of a given tray for a given distillation application is to measure it experimentally; this is usually done on a laboratory scale and then scaled-up to the actual commerical size. From a design point of view, however, this method of obtaining tray efficiencies can be time-consuming and costly. An alternative would be to select tray efficiency data from published literature and compare with the system and tray design on hand. A great deal of care must be exercised in the selection of tray efficiency data in this manner because of the large number of variables which can affect it. There are three main parameters which affect the efficiency of a tray: (1) operating conditions, (2) tray geometry, and (3) system properties. Operating conditions include: gas rate, liquid rate, temperature and pressure. The tray geometry includes: tray spacing, outlet weir height, hole diameter and area, column diameter, etc.. System properties depend upon the type and composition of the components being separated: relative volatility, vapour and liquid viscosity, vapour and liquid density, vapour and liquid diffusivity and surface tension. System properties are also, of course, dependent upon the column pressure and temperature. In most cases each of those parameters affect the tray efficiency to a different degree. Therefore, if the efficiency

data are not available in the literature or for a commercial installation, using empirical or semi-empirical correlations are necessary.

Prior to about 1960, empirical efficiency correlations generally related efficiency to a few key variables, the most important of which was liquid viscosity. The best known of the earlier correlations is that of O'Connell (1946) for bubble-cap trays, which for distillation, can be expressed as:

$$E_o = 9.06 (\mu_L \alpha)^{-0.245} \tag{2.11}$$

where α is the relative volatility

μ_L is the liquid viscosity

Generally, empirical correlations can only be expected to give a very rough estimate of efficiency. They have a place in preliminary studies and when used to support predictions, using other more soundly based mechanistic methods are more appropriate.

2.5 Fundamental Approach In Point Efficiency Prediction

2.5.1 Two-resistance concept

Theoretical prediction methods for the point efficiency are typically based on the two-resistance or two-film theory. Three assumptions are postulated based on this theory:

(1)   the rate of mass transfer of a component within a phase is proportional to the difference in concentration or partial pressure of a composition in the bulk phase and at

12

the interface,

(2) composition at the interface is in equilibrium (i.e. no mass transfer resistance at the interface), and

(3) the hold-up of the transferring component in the boundary layer or region near the phase boundary is negligible with respect to the amount transferred in the process. If these assumptions are valid, then the rate of mass transfer per unit area, may be expressed as:

$$\frac{N}{S} = k_G(p_i - p_G) = k_L(c_L - c_i) \qquad (2.12)$$

where k_G and k_L are known as the mass transfer coefficients for the vapour and liquid phases respectively. S is the planar cross-section area. Based on molecular diffusion, the mass transfer coefficents for the vapour and liquid phases can be defined as:

$$k_G = \frac{D_G}{RTZ_G} \qquad (2.13)$$

$$k_L = \frac{D_L}{Z_L} \qquad (2.14)$$

It should be noted that Equation (2.12) is expressed in terms of interface concentrations and these quantities are generally impossible to measure. Therefore, the definition of overall mass-transfer coefficients are used to bypass this difficulty and

13

Equation (2.12) becomes:

$$\frac{N}{S} = K_{OG}(p^* - p_G) = K_{OL}(c_L - c^*) \qquad (2.15)$$

The p^* is that partial pressure of the diffusing component which would exist in the bulk vapour phase if the vapour were in equilibrium with the bulk liquid phase. Likewise, c^* is that concentration in the liquid which would exist if the bulk liquid phase were in equilibrium with the bulk vapour phase.

Now that the rate of mass transfer has been defined, the next step is to apply it to an actual column. One difficulty that arises immediately is that the area for mass transfer in a column cannot be measured and expressed as a planar cross-sectional area, S. To get around this difficulty, it is customary to define an area term a' by the equation:

$$dS = a'A\,dZ$$

where a' = the interfacial area per unit volume

A = cross-sectional area of contact volume

Z = height of contact volume

Writing Equations (2.12) and (2.15) in differential form, substituting for S, and replacing concentrations, partial pressures with mole fraction terms give the following expressions for the amount of a given component transferred at steady-state:

14

$$dN = K_{OG}a'(y^{\,*}-y)PA\,dZ = k_G a'(y_i-y)PA\,dZ =$$

$$K_{OL}a'(x-x^{\,*})\rho_L A\,dZ = k_L a'(x-x_i)\rho_L A\,dZ \qquad (2.16)$$

It has been found to be convenient in the correlation of mass-transfer data to group several of the variables in Equation (2.16) together to define a single new quantity. This is accomplished as follow. Consider a material balance for the differential element shown in Figure 2.3:

$$dN = G'_M A\,dy = L'_M A\,dx \qquad (2.17)$$

Combination of this material balance with each of the four rate equations in (2.11), followed by an integration from $Z = 0$ to $Z = Z$ (G_M', L_M', P, ρ_L and mass-transfer coefficients are assumed to be constant), gives:

$$\frac{K_{OG}a'PZ}{G'_M} = \int \frac{dy}{y^{\,*}-y} = N_{OG} \qquad (2.18.1)$$

$$\frac{k_G a'PZ}{G'_M} = \int \frac{dy}{y_i-y} = N_G \qquad (2.18.2)$$

15
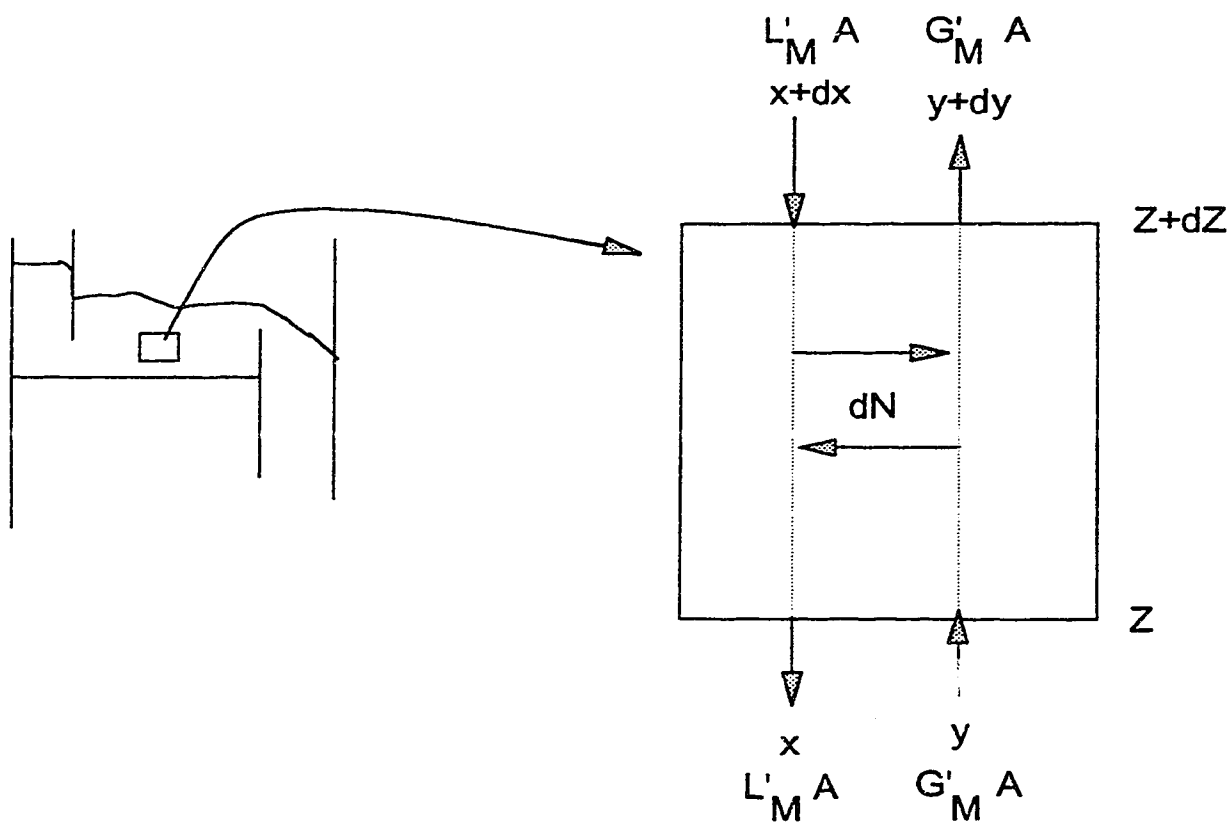
Figure 2.3: Component Balance in a Froth Element

$$\frac{K_{OL}a'\rho_L Z}{L_M'} = \int \frac{dx}{x-x^*} = N_{OL}$$
(2.18.3)

$$\frac{k_L a'\rho_L Z}{L_M'} = \int \frac{dx}{x-x_i} = N_L$$
(2.18.4)

Equations (2.18) define "the number of transfer units". The transfer unit was introduced because it has been found in the correlation of tray efficiency data that a simpler correlation is obtained if the tray variables are related to the number of transfer units rather than to the mass-transfer coefficients.

Additivity of Resistances. The "two-resistance" concept in mass transfer postulates two resistances in series, one in the vapour phase and one in the liquid phase. Each of the two resistances is a function of the physical properties of the system used and based on the same interfacial area under distillation conditions. Assuming that the binary system equilibrium curve at the concentrations in question can be adequately represented by a straight line, then,

$$y^* = mx + b$$
(2.19.1)

where x is the actual bulk phase liquid concentration for the given component. Also if equilibrium is assumed at the interface then

17

$$y_i = mx_i + b \qquad (2.19.2)$$

Combining Equations (2.16) and (2.19) yields:

$$y^* - y = y^* - y_i + y_i - y = \frac{dN}{K_{OG}a'PAdZ} = \frac{mdN}{k_L a' \rho_L AdZ} + \frac{dN}{k_G a'PAdZ} \qquad (2.20)$$

and

$$\frac{1}{K_{OG}a'} = \frac{1}{k_G a'} + \frac{m\dfrac{P}{\rho_L}}{k_L a'} \qquad (2.21)$$

in transfer units from Equations (2.18)

$$\frac{PZ}{N_{OG}G_M'} = \frac{PZ}{N_G G_M'} + \frac{mPZ}{N_L L_M'} \qquad (2.22)$$

$$\frac{1}{N_{OG}} = \frac{1}{N_G} + \frac{\lambda}{N_L} \qquad (2.23.1)$$

$$where \qquad \lambda = m\frac{G_M'}{L_M'}$$

18

At total reflux, $G_M{}'$ is equal to $L_M{}'$, Equation (2.23.1) becomes:

$$\frac{1}{N_{OG}} = \frac{1}{N_G} + \frac{m}{N_L}$$

(2.23.2)

Equations (2.23) are the well-known relationship used for adding vapour and liquid mass transfer resistances. Often in Equations (2.18) for N_G and N_L, the terms $\rho_G Z / G_M{}'$ and $\rho_L Z / L_M{}'$ represent the contact time between the two phases. Equations (2.18.2) and (2.18.4) can also be rewritten as:

$$N_G = k_G{}' a t_G$$

(2.24)

$$N_L = k_L{}' a t_L$$

(2.25)

2.5.2 Relation between E_{OG} and N_{OG}

In order to express the point efficiency in terms of mass-transfer units, Equation (2.18.1) is integrated with the assumptions that in the vertical direction liquid is perfectly mixed and vapour is in plug flow. This gives:

$$N_{OG} = -\ln\left(\frac{y_n^* - y_n}{y_n^* - y_{n+1}}\right)$$

(2.26)

Combining Equation (2.26) with the definition of point efficiency gives:

19

$$E_{OG} = 1 - \exp(-N_{OG}) \qquad (2.27)$$

In Figure 2.4, the sequence of steps in converting mass transfer units into tray efficiency is summarized.

2.6 Review On Correlations For Individual Phase Transfer Units

In order to obtain the overall mass transfer unit, N_{OG}, the values of N_G and N_L are usually determined by using correlations. Various approaches which have been proposed to correlate these quantities are discussed in the following sections.

2.6.1 AIChE Method

The AIChE method was developed over five years in the late 1950s by three universities: University of Delaware, University of Michigan and North Carolina State College. The development of the correlations was based on a great deal of data obtained from absorption and stripping. The vapour and liquid components were chosen such that the resistance to mass transfer could be confined in either the vapour or liquid phase. Using the procedure outlined in Figure 2.4, the tray efficiency is determined by the following transfer-unit correlations:

$$N_G = (0.776 + 4.57 h_w - 0.238 F_s + 104.8 \frac{Q_L}{W}) S_c^{-0.5} \qquad (2.28)$$

and

System
Properties

Operating
Conditions

Tray
Geometry

Correlations for No. of
Mass Transfer Units

N_G, N_L

Sum $\longleftarrow$ m G'_M /L'_M

Overall No. of Mass Transfer
Units, N_{OG}

Point Efficiency

Mixing Models

Murphree Tray Efficiency
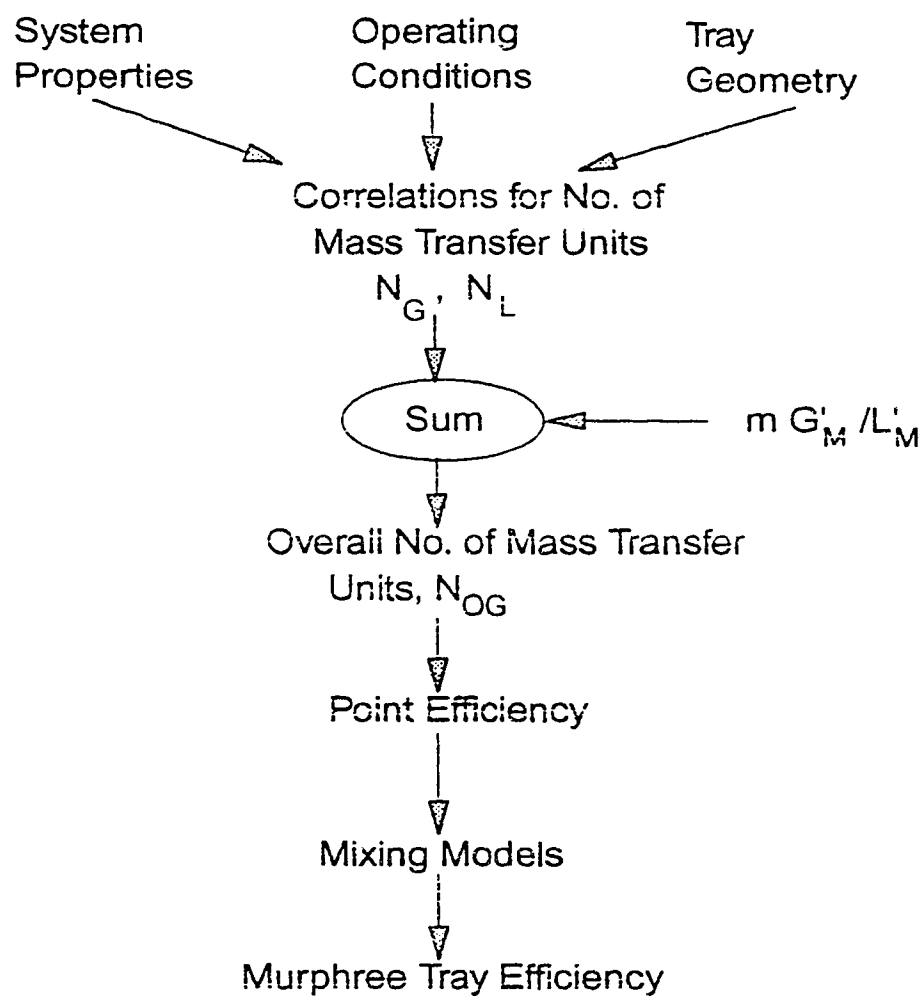
Figure 2.4: Sequence of Steps in Predicting Tray Efficiency

21

$$N_L = 1.97x10^4 D_L^{0.5}(0.4F_s + 0.17)t_L \qquad (2.29)$$

$$where \qquad t_L = \frac{h_{cl}Z_l W}{Q_L}$$

The correlation for N_G was obtained from experiments using the absorption of soluble gases. In this case, the slope of the equilibrium line, m, is usually either close to or equal to zero; therefore, the rate of mass transfer is mainly controlled by the gas phase (i.e. $N_{OG} = N_G$). For N_L, on the other hand, the procedure was to measure the absorption or desorption of slightly soluble gases. Here, only liquid phase resistance exists (i.e. $N_{OG} = N_L$). It can be seen that the correlations for N_G and N_L obtained in this way have a different form than Equations (2.24) and (2.25) and are based on quite different interfacial area. For N_L, the interfacial area, a, is approximately equal to (0.4 F_s + 0.17); and for N_G, the interfacial area term is not even clear. Therefore, the extension of those two correlations to distillation, where mass transfer occurs through one interfacial area, may be questionable. In addition, the important of the Schmidt number, Sc in Equation (2.28) is also open to question. For example, in very careful experiments, Mehta and Sharma (1966) found that N_G depends on D_G but not on Sc. Despite these deficiencies, the AIChE method continues to be used for making predictions of tray efficiencies in many industrial applications.

Over the last few decades, many researchers have attempted to modify the AIChE correlations with more variables or experimental values (Harris, 1965; Asano and Fujita,

22

1966; Jeromin et. al. 1969; Hughmark, 1971); however, no significant progress has been made because the fundamentals of the two correlations for the number of mass transfer units were not considered.

2.6.2 Chan and Fair Correlation

Chan and Fair (1984) derived their correlation based on an extensive distillation data bank. They obtained values of E_{OG} from distillation data then used Equation (2.27) to determine N_{OG}. The AIChE correlation, Equation (2.29) was then used to calculate values for N_L. Given the measured N_{OG} and calculated N_L, the values of N_G can be obtained from Equation (2.23.1). Based on the Higbie's penetration theory (Higbie, 1935) and data regression, they developed a new correlation for N_G:

$$N_G = \frac{1000(D_G)^{0.5}(10.3(FF) - 8.67(FF)^2)t_G}{h_{cl}^{0.5}}$$

(2.30)

$$where \quad t_G = \frac{(1 - \alpha_e)h_{cl}}{(\alpha_e u_s)}$$

(2.31)

$$and \quad FF = \frac{u_s}{u_{s,flood}}$$

Equation (2.30) has a form similar to Equation (2.24). However, the interfacial area in Equation (2.30) (i.e. $a = (10.3\ FF - 8.67\ FF^2)/h_{cl}^{0.5}$) is still different from the N_L correlation (i.e. $a = 0.4\ F_s + 0.17$). Futhermore, in Equation (2.30), the FF term

is the fractional approach to flooding. Lockett (1986) pointed out that the presence of this term in Equation (2.30) implies that the efficiency depends on the tray spacing for fixed vapour and liquid loads. This implication is supported neither by theoretical nor by experimental evidence, and is considered by Lockett as "hardly reasonable". Although the Chan and Fair correlation provided improvements to the AIChE method, at the same time it inherited several theoretical limitations from the AIChE correlation. However, offsetting this is the redeeming feature that the correlation is based on actual distillation data.

Lockett and Plaka (1983) proposed a better approach in obtaining N_G and N_L correlations. They realized the importance in obtaining N_G and N_L under the same distillation conditions. Based on the penetration theory, they postulated the following equations for the mass transfer coefficients:

$$k_G' = p\, \rho_G (D_G)^{0.5} \qquad\qquad (2.32)$$

$$k_L' = q\, \rho_L (D_L)^{0.5} \qquad\qquad (2.33)$$

where p and q are hydrodynamic factors whose values must be determined by experiment. At total reflux, they have the following equations for N_G and N_L:

$$N_G = N_{OG}[1 + m(\frac{\rho_G}{\rho_L})(\frac{p}{q})(\frac{D_G}{D_L})^{0.5}]$$ (2.34)

$$N_L = N_{OG}[m + (\frac{\rho_L}{\rho_G})(\frac{q}{p})(\frac{D_L}{D_G})^{0.5}]$$ (2.35)

In Equations (2.34) and (2.35), the experimental values of N_{OG} were used together with the values of p and q obtained by parameter estimation to evaluate the values of N_G and N_L. They claimed that this method of determining N_G and N_L from experimental distillation data is more accurate than any other previously proposed method. Its power lies in the way that N_G and N_L are obtained directly from a mixed resistance system and the effects of turbulent diffusion have been taken into account by two parameters, p and q. However, their correlations are obtained from one system (methanol/water); therefore, p and q are experimentally dependent and the correlations may not be applicable for any other systems.

2.6.3 Chen and Chuang Correlations

More recently, Chen and Chuang (1992) developed a semi-empirical model to predict the number of individual phase transfer unit. They recognized the fact that the tray efficiency is controlled by the bubble dispersion in the froth, and this bubble dispersion is somewhat similar to that of other gas-liquid dispersion systems in mixing vessels. Thus, based on the well established dispersion theory, they developed a

25

correlation to determine the interfacial area:

$$a = \frac{6\epsilon}{d_{max}} \propto \frac{\epsilon(\rho_L^2 \rho_G)^{0.2} u_s^{0.4}}{\sigma^{0.6} \mu_L^{0.1}}$$ (2.36)

where

$$\epsilon = (\frac{F_s}{F_{s,max}})^{0.28} = [\frac{u_s \rho_G^{0.5}}{2.5(\phi^2 \sigma(\rho_L - \rho_G)g)^{0.25}}]^{0.28}$$

$$\propto \frac{u_s^{0.28} \rho_G^{0.14}}{\phi^{0.14} \sigma^{0.07} \rho_L^{0.07}}$$ (2.37)

substituting ϵ into Equation (2.36) and gives:

$$a \propto \frac{1}{\mu_L^{0.1} \phi^{0.14}} [\frac{F_s^2 \rho_L}{\sigma^2}]^{(1/3)}$$ (2.38)

Notice that in Equation (2.38), liquid viscosity, liquid density and surface tension are all considered to be important parameters that affect the interfacial area in the dispersion, whereas no such considerations have appeared in any of the previously proposed correlations. With that achievement, they developed the final correlations for the number of individual phase transfer units are as follows:

26

$$N_G = C_1 \frac{1}{\mu_L^{0.1} \phi^{0.14}} [\frac{\rho_L F_s^2}{\sigma^2}]^{(1/3)} (D_G t_G)^{0.5} \tag{2.39}$$

$$N_L = C_2 \frac{1}{\mu_L^{0.1} \phi^{0.14}} [\frac{\rho_L F_s^2}{\sigma^2}]^{(1/3)} (M_G G_M / M_L L_M)(D_L t_L')^{0.5} \tag{2.40}$$

where

$$t_G = h_{cl} / u_s \quad and \quad t_L' = t_G \rho_L / \rho_G$$

$$F_s = u_s (\rho_G)^{0.5}$$

Similar to Lockett and Plakas' correlations, they included two parameters C_1 and C_2 whose values must also be determined experimentally. However, in this case, C_1 and C_2 are constants and are independent of the system properties and tray geometry. Additionally, in principle, the two constants can be obtained from one accurate data point. In order to obtain values for C_1 and C_2, they combined Equations (2.23.1), (2.39) and (2.40) to give:

$$N_{OG} = \frac{N_G}{1 + \lambda \dfrac{N_G}{N_L}}$$

$$= \frac{C_1 \dfrac{1}{\mu_L^{0.1} \phi^{0.14}} \left[\dfrac{\rho_L F_s^2}{\sigma^2}\right]^{(1/3)} (D_G t_G)^{0.5}}{\lambda \dfrac{C_1}{C_2} \left(\dfrac{D_G \rho_G}{D_L \rho_L}\right)^{0.5} \left(\dfrac{M_L L_M}{M_G G_M}\right) + 1}$$

$$(2.41)$$

By fitting the above equation to the experimental N_{OG} data as a function of m, the values of C_1 and C_2 have been found to be 11 and 14, respectively. It should be noted that at a total reflux, λ = m, and M_G/M_L = 1. From Equations (2.39) and (2.40), one can observe that these equations include the absolute value of the surface tension effect, N_G and $N_L \propto \sigma^{(-2/3)}$. However, this inclusion of surface tension is open to debate because the data that they tested their correlations with was published by FRI and the surface tension and ph: properties change in unison. Thus, a definite conclusion about the surface tension effect on tray efficiencies is still uncertain. In addition, the values of C_1 and C_2 were obtained based on a surface tension neutral system (i.e. the cyclohexane/n-heptane system) and were questionable when applying to other systems, such as surface tension positive systems and negative systems. But nonetheless, Chen and Chuangs' correlations provided a very good basis for predicting N_G and N_L values because their correlations are based on the same interfacial area.

In most circumstances, the point efficiency can only be predicted to a certain degree of accuracy. This is because of the complex interaction between the transfer units

28

and the system properties. One area which is still remained unreliable as pointed out earlier in the tray efficiency prediction is the effects of surface tension. Therefore, a review on the effects of surface tension on the tray efficiency will be discussed in the next chapter.

Chapter 3

REVIEW ON THE EFFECT OF SURFACE TENSION ON TRAY

EFFICIENCY

One of the factors which can substantially affect the magnitude of tray efficiencies is the effects of surface tension on tray efficiencies. These effects include two parts: (a) the absolute value of surface tension and (b) the surface tension gradients within the dispersion. The absolute value of surface tension refers to the surface tension forces acting on the bubbles in the dispersion. Hinze (1955) conducted work in turbulent flow based on the dispersion theory and found that the size of the bubble was controlled by the inertial forces due to the deform action of the bubbles whereas the surface tension forces tend to resist the deformation. The maximum stable spherical bubble size can be determined by the balance between these two forces. Chen and Chuang (1992) incorporated this idea and developed correlations for the number of mass transfer units which included the effect of the absolute value of surface tension. However, as discussed earlier, their analysis is incomplete because they did not consider the effect of the surface tension gradients. Therefore, in the present study, the focus will be devoted to extend their correlations with the inclusion of the effect of the surface tension gradients.

The development of surface tension gradients within the dispersion due to mass transfer can cause variations in the interfacial area and the rate of mass transfer which in turn affect the tray efficiency. But first, for discussion purposes, let's classify distillation systems into three types (Zuiderweg and Harmens, 1958):

(a)   surface tension positive system, σ^+, where the surface tension increases as the liquid proceeds down the distillation column.

(b)   surface tension negative system, σ^-, where the surface tension decreases as the liquid proceeds down the column.

(c)   surface tension neutral system, σ^o, where the surface tension is virtually unchanged from tray to tray. This can arise either because the components have similar surface tension or the surface tension change from tray to tray is small.

The Change In Interfacial Area. During distillation, it is important to identify the tray operating regime before discussing the effects of surface tension gradient on the tray efficiency because these effects are quite different in different regimes. There are two important regimes:

(1)   froth regime with a continuous liquid phase, and

(2)   spray regime with a continuous vapour phase.

Zuiderweg and Harmens (1958) cite data for the effect of surface tension gradients upon the contacting efficiency for the distillation of a number of different mixtures in different devices. They found that in plate column distillation, operated in the froth regime, surface tension positive systems exhibit higher plate efficiencies than either neutral or negative systems. They also found a higher froth height in positive systems than in negative and neutral systems. In explaining this phenomena, they postulated a mechanism which stated that in the froth regime, a thin liquid film existed between the bubbles. This liquid film is generally rich in the less-volatile components

31

because the concentration of the volatile components in the vapour phase is greater than that in the liquid phase. For a surface tension positive system, the liquid film is of higher surface tension and the surface tension gradients along the surface of the film cause the surface flow of liquid into the film. This thickens and locally reinforces thin parts of the film and results in relative slowness in bursting of the bubbles. Thus, surface tension positive systems tend to have more stable and uniform bubbles. Futhermore, when these bubbles stablize on the tray, the froth height will increase which will in turn generate a larger interfacial area. Conversely, for surface tension negative systems, there is a surface flow out of the film which acts to thin and break the film. Therefore, surface tension negative systems do not tend to have stablized froth to any significant extent. This effect is illustrated in Figure 3.1. Hart and Haselden (1969) also found similar influences of surface tension upon the interfacial area and plate efficiencies.

However, Lockett (1986) argued that the mechanism proposed by Zuiderweg and Harmens (1958) on froth stablization is not conclusive, because the observed maximum point efficiency occurred at very low vapour velocities. He found it hard to accept that when Zuiderweg (1983) attempted to explain this increase in point efficiency by suggesting that the effect of surface tension gradients can cause froth stabilization for positive systems, such as methanol/water, even at vapour velocities bordering on the transition to the spray regime. In fact, experimental results have shown that after increasing vapour velocities to a certain point where no stabilized froth was observed, higher tray efficiency was still noticed. This suggested that the change in interfacial area may not be the only reason that enhances the tray efficiency. Ellis and Biddulph (1967)
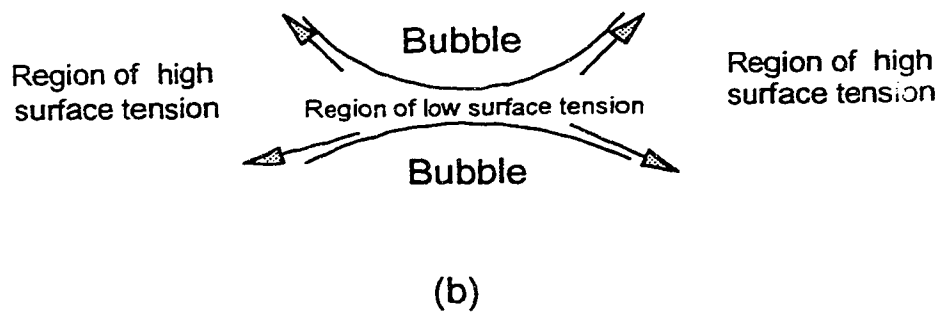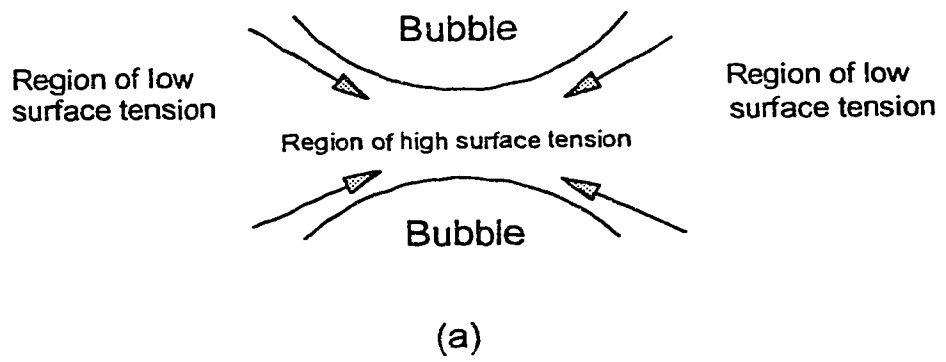
Figure 3.1: Effect of Surface Tension Gradient on Froth Stability

(a) σ^+ systems; (b) σ^- systems

conducted experiments in a pool column where the interfacial area was fixed. They found that surface tension gradients have a major effect on the rate of mass transfer, rather than on the interfacial area alone.

Change In Rate Of Mass Transfer. Surface tension gradients were found to influence the rate of mass transfer by affecting the mixing and surface renewal at the liquid interface. The phenomenon by which surface tension gradients induce interfacial convection and influence the mass transport is called the Marangoni effect.

Consider a surface tension positive system where the bulk liquid has lower surface tension than the liquid at the interface. An eddy arriving at the surface carrying with it liquid having a lower value of surface tension will therefore introduce unbalanced surface tension forces. The liquid of lower surface tension will spread across the interface and cause convection cells or disturbance. The intensity of this effect depends on the surface tension gradient, which is proportional to the difference between the surface tension at the interface and in the bulk, and depends on the magnitude of the concentration driving force. Ellis and Biddulph (1967) measured the eddy spreading velocity at the interface using a photographic technique and found that surface tension positive system exhibits a larger value of N_L than negative system. This larger value of N_L contributes a larger mass transfer coefficient in the liquid phase. Sawistowski (1973) echoed these results and stated that the presence of the Marangoni effect will increase the mass transfer coefficient in the liquid phase several times over those predicted by the molecular diffusion theory or penetration theory. Brian et al. (1971) studied the effect of cellular

34

convection driven by surface tension gradients upon the vapour-liquid mass transfer rate. They found that the mass transfer coefficient in the liquid phase was enhanced several fold by the cellular convection, and at the same time had a negligible effect upon the vapour phase mass transfer coefficient. These results can be attributed to the fact that the linear dimension of the convection cells was too small, and the velocity of the convection was too slow, to affect the vapour phase mass transfer coefficient. Van Der Klooster et. al. (1979) conducted experiments in a wetted wall column in which the effect of surface tension gradients on the mass transfer coefficient were investigated. They found that the effect of cellular convection driven by surface tension gradients upon the mass transfer coefficient was much more pronounced in the liquid phase than in the gas phase because the diffusion coefficient in the gas phase is fourth order of magnitude higher than that in the liquid phase.

Generally speaking, the influence of surface tension gradients on plate performance is somewhat complex depending on a number of factors such as differences in interfacial area, variations in individual phase resistance due to the surface movement effects, etc., which in turn are influenced by system properties, tray geometry, and operating conditions. Therefore, a satisfactory theoretical basis has not yet been established to predict accurately the above effects on the tray efficiency.

3.1   New Correlation Development

Based on the previous discussions on the effect of surface tension gradients upon the liquid phase mass transfer rate, it is apparent that the liquid phase mass transfer

coefficient determined from molecular diffusion or penetration theory alone will not provide satisfactory results in predicting the tray efficiency. Therefore, a factor which can incorporate this enhancement effect on the liquid phase mass transfer coefficient is desired. Moens (1972) suggested a good measure for the effects caused by the surface tension gradients is the stabilizing-index also known as the Marangoni-index. This index is the maximum difference in surface tension that may exist locally at the liquid surface. According to Kalbassi et al. (1987), the Marangoni-index can be defined as:

$$M-index = (y-y^*)(\frac{d\sigma}{dx})$$

(3.1)

where $(y - y^*)$ is the mass transfer driving force, and $d\sigma/dx$ is the rate of change of surface tension with composition.

Based on the Higbie penetration theory (Higbie, 1935), the following equations for the mass transfer coefficients are postulated:

$$k_G' = C_1\sqrt{\frac{D_G}{t_G}}$$

(3.2)

$$k_L' = C_2 S(M)\sqrt{\frac{D_L}{t_L'}}$$

(3.3)

In Equation (3.3), an enhancement factor, $S(M)$, is included in the k_L' equation which

36

will take into account the surface-tension-gradient effect. This enhancement factor, S(M), is a function of the Marangoni-index and will be determined from experimental results. Substitution of Equations (3.12), (3.13) into Equations (2.19), (2.20) respectively gives:

$$N_G = C_1 a \sqrt{D_G t_G} \qquad\qquad (3.4)$$

$$N_L = C_2 S(M) a \sqrt{D_L t_L'} (M_G G_M)/(M_L L_M) \qquad\qquad (3.5)$$

$$where \qquad t_L = t_L'(M_G G_M)/(M_L L_M)$$

By experimentally determining the values of C_1 and C_2 without the Marangoni effect (i.e. use only neutral systems) and utilizing those two values to predict N_G and N_L for positive and negative systems, one will be able to compare the N_L values obtained from Equation (2.18) and those predicted by C_2 value with the variation of the M-index, and determining the function S(M). But first, let's determine the interfacial area, a, and the contact time of liquid, t_L and vapour, t_G.

Interfacial area.   In the present study, the correlation for the interfacial area derived by Chen and Chuang (1992) was used. Notice that in Equation (2.36), ϵ is the gas hold-up fraction which can be determined by many empirical correlations (Gardner and McLean (1969), Kastanek (1970), Stichlmair (1978), Colwell (1979)). Unfortunately

most of the correlations are based on small data banks, only those of Colwell (1979) and Stichlmair (1978) are notable exceptions. Chen and Chuang (1992) selected Stichlmair equation to predict ϵ. However, Stichlmair used the fluidization model of spray as the basis for his correlation; although he found that it also held in the froth regime, his correlation is generally recommended for spray regime. On the other hand, Colwell (1979) developed his correlation by carefully evaluated data from a wide range of systems operating in the froth regime. Since in this study, we only operated in the froth regime; therefore, Colwell's equations were chosen and are shown in Equation (3.6):

$$\epsilon = \frac{\eta}{1+\eta} \qquad (3.6)$$

$$where \quad \eta = 12.6(Fr')^{0.4}\phi^{-0.25}$$

$$Fr' = Fr\rho_G/(\rho_L - \rho_G)$$

$$Fr = u_s^2/(gh_{cl})$$

where h_{cl} is the clear liquid height.

The clear liquid height on a sieve tray plays an important role in mass transfer because of its influence on the contact time t_L and t_G. Many correlations for h_{cl} are available (Colwell (1979), Bennett et al. (1983), Hofhuis and Zuiderweg (1979)). In this study, the correlation of Bennett et al. (1983) was used because the predicted values of h_{cl} show good agreement with the experimental measurements. The correlation is given by:

$$h_{cl} = \alpha_e [h_w + C(\frac{Q_L}{W\alpha_e})^{0.67}]$$ (3.7)

where $\alpha_e = \exp[-12.55(u_s(\frac{\rho_G}{(\rho_L - \rho_G)})^{0.5})^{0.91}]$

$C = 0.5 + 0.438\exp(-137.8h_w)$

Contact Time t_G and t_L.   The vapour residence time or contact time in the two-phase dispersion can be expressed as·

$$t_G = h_{cl}/u_s$$ (3.8)

Similarly for the liquid residence time t_L:

$$t_L = t'_L(M_G G_M)/(M_L L_M)$$

where $t'_L = t_G \rho_L/\rho_G$ (3.9)

Equations (3.8) and (3.9) were also employed by Chen and Chuang (1992). Combining Equations (2.36), (3.4) and (3.5) gives the correlations for the individual mass transfer units at total reflux as follow:

$$N_G = C_1 \frac{\epsilon(\rho_L^2 \rho_G)^{0.2} u_s^{0.4}}{\sigma^{0.6} \mu_L^{0.1}} \sqrt{D_G t_G} \qquad (3.10)$$

$$N_L = C_2 S(M) \frac{\epsilon(\rho_L^2 \rho_G)^{0.2} u_s^{0.4}}{\sigma^{0.6} \mu_L^{0.1}} \sqrt{D_L t_L'} \qquad (3.11)$$

.

Chapter 4

EXPERIMENTAL EQUIPMENT AND OPERATION

4.1 Equipment

A schematic diagram of the experimental equipment which was completely instrumented with conventional industrial control valves, controllers and pressure transmitters is shown in Figure 4.1. The column sections were made of Pyrex glass with an inner diameter of 153 mm and contained four identical trays spaced 318 mm apart. Each tray was made of stainless steel and equipped with thermocouples and sampling points. A total condenser and a thermosiphon partial reboiler completed the distillation system. Detailed dimensions of the column and the trays are shown in Table 4.1.

4.2 Operation

The experiment was conducted at total reflux with the column pressure at 1.8 mm Hg. Six binary systems used were cyclohexane/n-heptane, methanol/water, chloroform/toluene, benzene/n-heptane, methanol/isopropyl alcohol and n-heptane/toluene. They represent different categories of surface tension gradients change and all the systems employed in this study were prepared by mixing the reagent grade chemicals obtained from Fisher Scientific. The second tray from the top was chosen as the test tray where end effects were minimal. An Opto22 process I/O subsystem interfaced to an IBM personal computer was used to record temperatures, flow rates, and liquid levels. The total pressure drop for the test tray was measured with a water

41

Cooling Water

CONDENSER

Vent

2

1

4

6

Steam

3

REBOILER

5

Steam Condensate

1. Cooler
2. Manometer
3. Preheater
4. Flow Recorder Controller
5. Flow Recorder
6. Liquid Level Controller
7. Pressure Controller
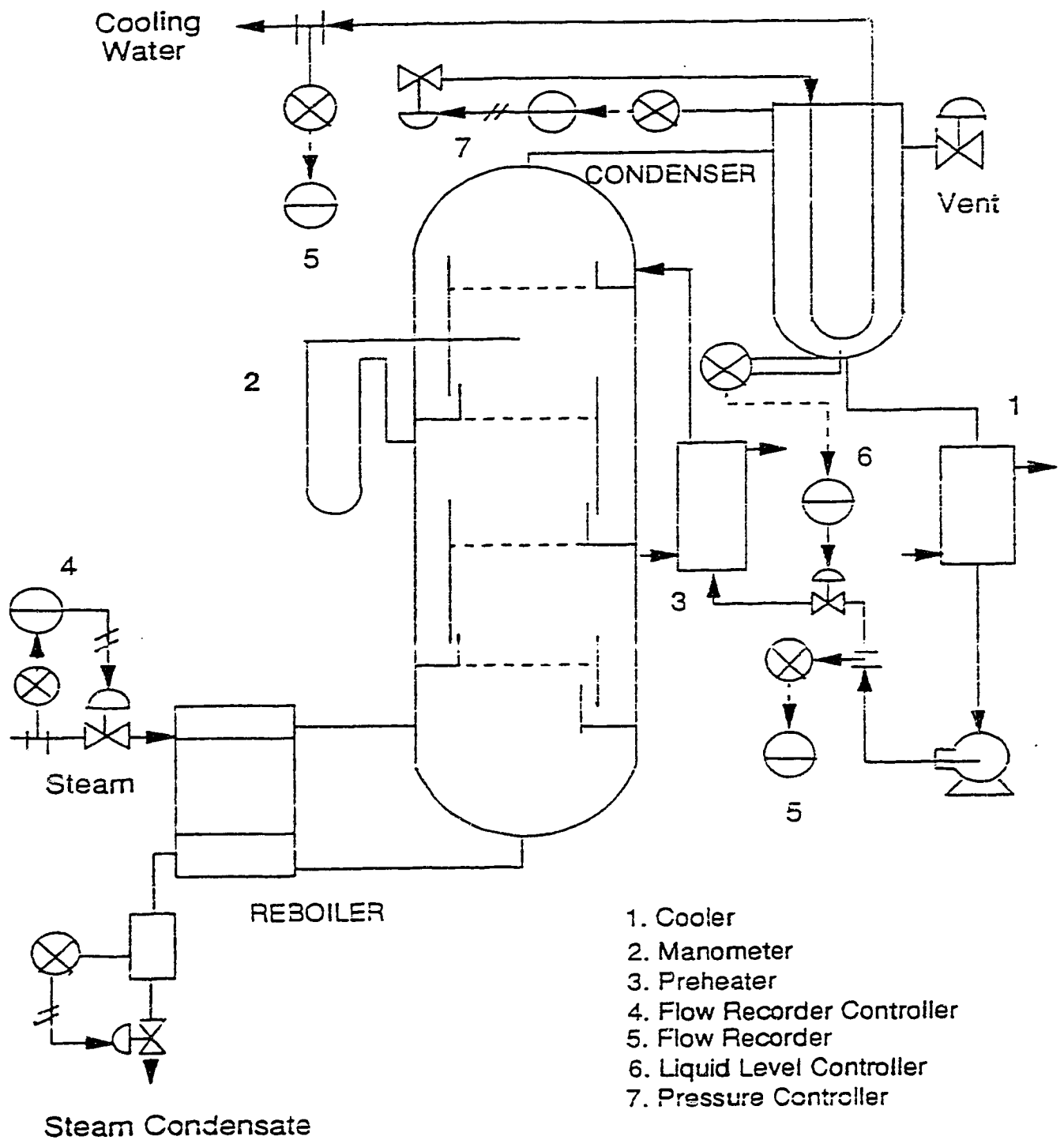
Figure 4.1: Schematic Diagram of the Experimental Equipment

42

manometer. The froth heights on the tray were obtained by visual observations. When the temperature profile and the flow rates of liquid streams were constant for a period of 60 minutes, steady state operation was assumed to exist. Energy balance calculations were also performed to confirm that steady state was reached (discrepancy < ± 5%). Once steady state had been achieved, the liquid samples at the inlet and outlet of the test tray were taken, and other required data, such as the temperature profile, total pressure drop and visual froth height were also recorded. The samples taken were then analyzed by the gas chromatograph (HP 5790A) where the compositions of each sample were determined. Since the sampling technique is essential to this experiment, duplicate samples were taken and analyzed.

The efficiencies for the test tray were measured at various vapour rates and different concentrations of the more volatile component of the binary systems used. The vapour rates were changed from just above the weep point to below the spray point; therefore, all systems were operated at the froth regime with negligible weeping and entrainment effects. One important note is that when the vapour rate reaches the spray point, liquid sampling becomes difficult because the spray bed has a poorly defined upper surface (i.e. liquid is thrown up into the inter-tray space where samples cannot be collected). Additionally, problems of entrainment immediately occur for small increases in vapour rate after the spray point been reached. Therefore, this confirms what has been said in the introduction, namely that the spray regime is not a favorable operating regime for a sieve tray column. A detailed step-by-step experimental procedure is listed in Appendix A.

Table 4.1 COLUMN AND TRAY DIMENSIONS	
Column Diameter	0.153 m
Total Column Cross-sectional Area	0.0171 m^2
Bubbling Area	0.0119 m^2
Downcomer Area	0.0026 m^2
Hole Diameter	4.76 mm
Open Hole Area	0.000784 m^2
Tray Thickness	10 mm
Outlet Weir Height	0.063 m
Weir Length	0.122 m
Tray Spacing	0.318 m

Chapter 5

RESULTS AND DISCUSSION

To investigate the effect of surface tension gradients on the tray efficiency, six binary mixtures were employed in this study. Careful attention was given to the accurate measurement of the vapour and liquid flows and the compositions. The reproducibility of individual liquid and vapour composition samples was better than $\pm$ 0.5 %. The test mixtures were classified on the basis of their changes in direction of surface tension at their boiling point as follows:

(i)   Surface-tension positive systems

- Methanol/water (surface tension 18.2 dyn/cm, 61 dyn/cm respectively)

- n-Heptane/toluene (surface tension 12 dyn/cm, 18.2 dyn/cm respectively)

(ii)   Surface-tension negative system

- Benzene/n-heptane (surface tension 21 dyn/cm, 12 dyn/cm respectively)

(iii)   Surface-tension neutral systems

- Chloroform/toluene (surface tension 21.5 dyn/cm, 18.2 dyn/cm respectively)

- Methanol/isopropyl alcohol (surface tension 18.2 dyn/cm, 15.1 dyn/cm respectively)

- Cyclohexane/n-heptane (surface tension 15.5 dyn/cm, 12 dyn/cm respectively)

Equilibrium data of the above mixtures are shown in Appendix C. All physical properties were either extrapolated from published experimental data or estimated based on the procedure suggested by Reid et al. (1977). Tables of the physical properties for

45

each system are listed in Appendix B.

5.1   Effect of F-factor on Tray Efficiency

Figures 5.1 to 5.6 show the measured Murphree tray efficiency as a function of the F-factor, F_s for all systems. In all cases, it can be seen that the tray efficiency decreases slightly with an increasing F-factor. This can be attributed to the fact that when the weeping and entrainment effects were eliminated, the tray efficiency is not a strong function of vapour rate. However, if the F-factor continues to increase until entrainment occurs, the tray efficiency drops because entrainment causes a reduction in the driving force for mass transfer between liquid and vapour.

5.2   Effect of Liquid Compositions on Tray Efficiency

Discussions in Chapter 3 show how the surface tension gradients affect the interfacial area and the rate of mass transfer in the dispersion. In this section, we will relate those findings to the experimental results.

Figure 5.7 shows the variation of the liquid composition with the Murphree tray efficiency for the methanol/water system at two different F-factors. The Murphree tray efficiency increased as the tray concentration increased from about 10 mol.% to 90 mol.% of methanol. Visual observation of the tray operation suggested that more stablized and uniform bubbles exist with increasing methanol concentration at low vapour rates ($F_s \leq 0.7$). However, no such observation was noticed when F_s is greater than 0.7; yet higher tray efficiencies were still observed. This suggests that Zuiderweg and

46

Figure 5.1: Effect of the F-factor on Tray Efficiency for the Methanol/Water System
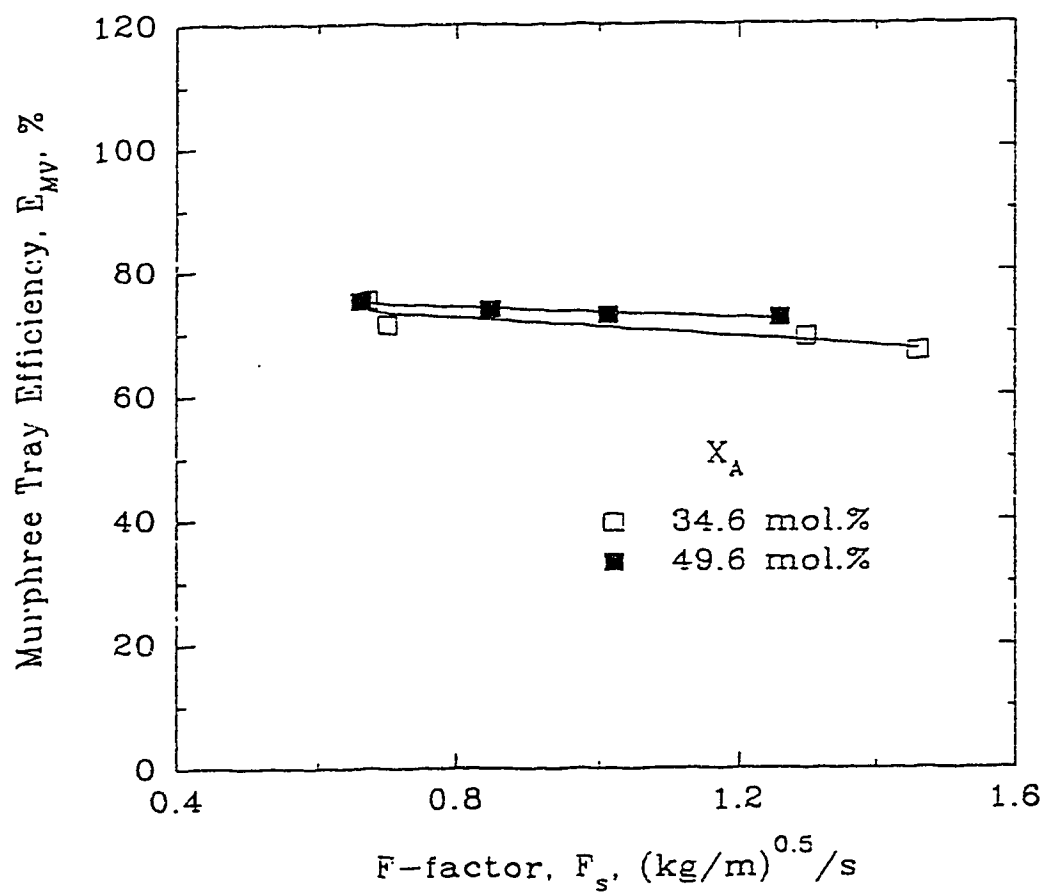
Figure 5.2: Effect of the F-factor on Tray Efficiency for the n-Heptane/Toluene System
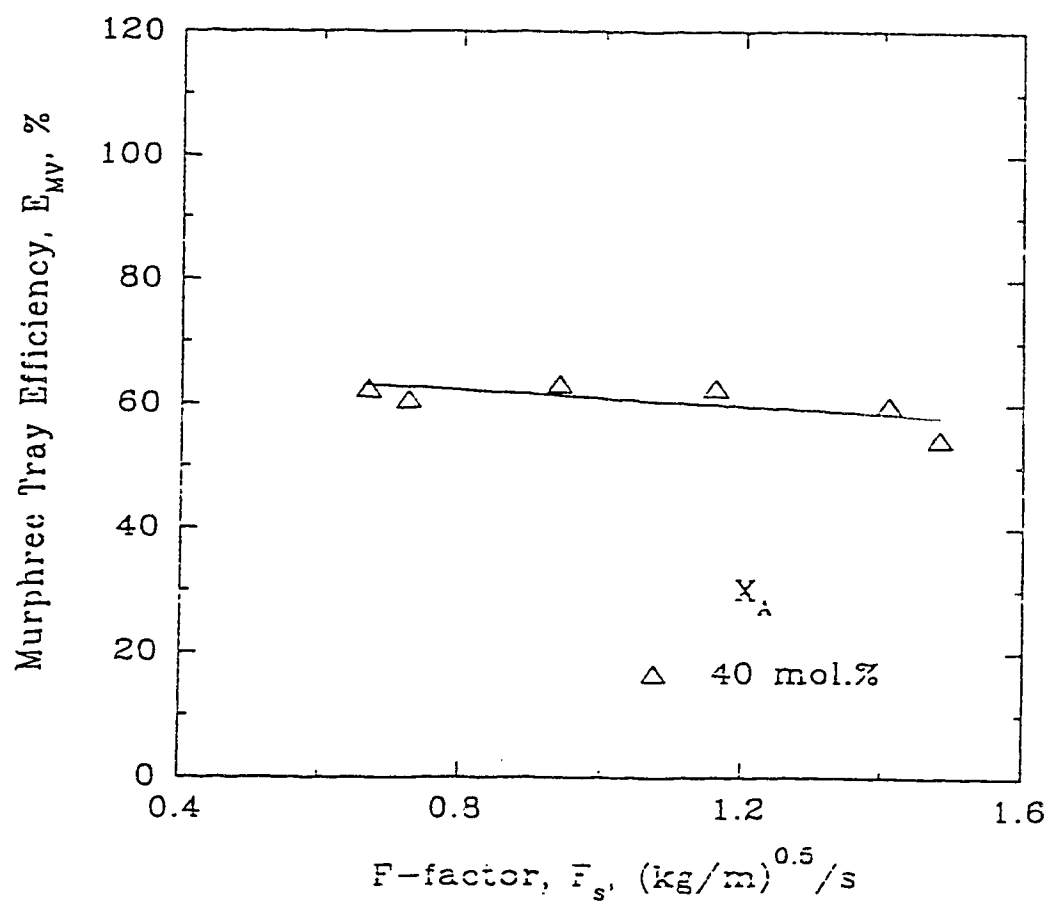
Figure 5.3: Effect of the F-factor on Tray Efficiency for

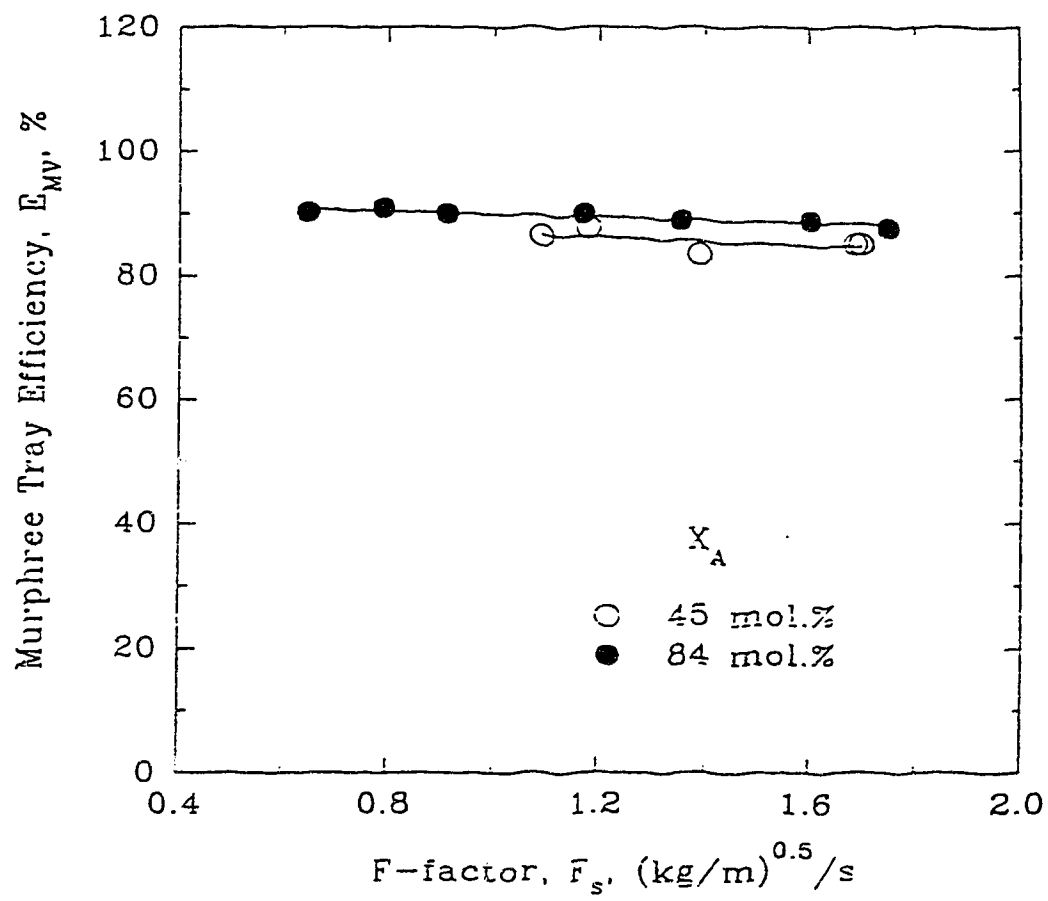the Benzene/n-Heptane System

Figure 5.4: Effect of the F-factor on Tray Efficiency for

the Cyclohexane/n-Heptane System
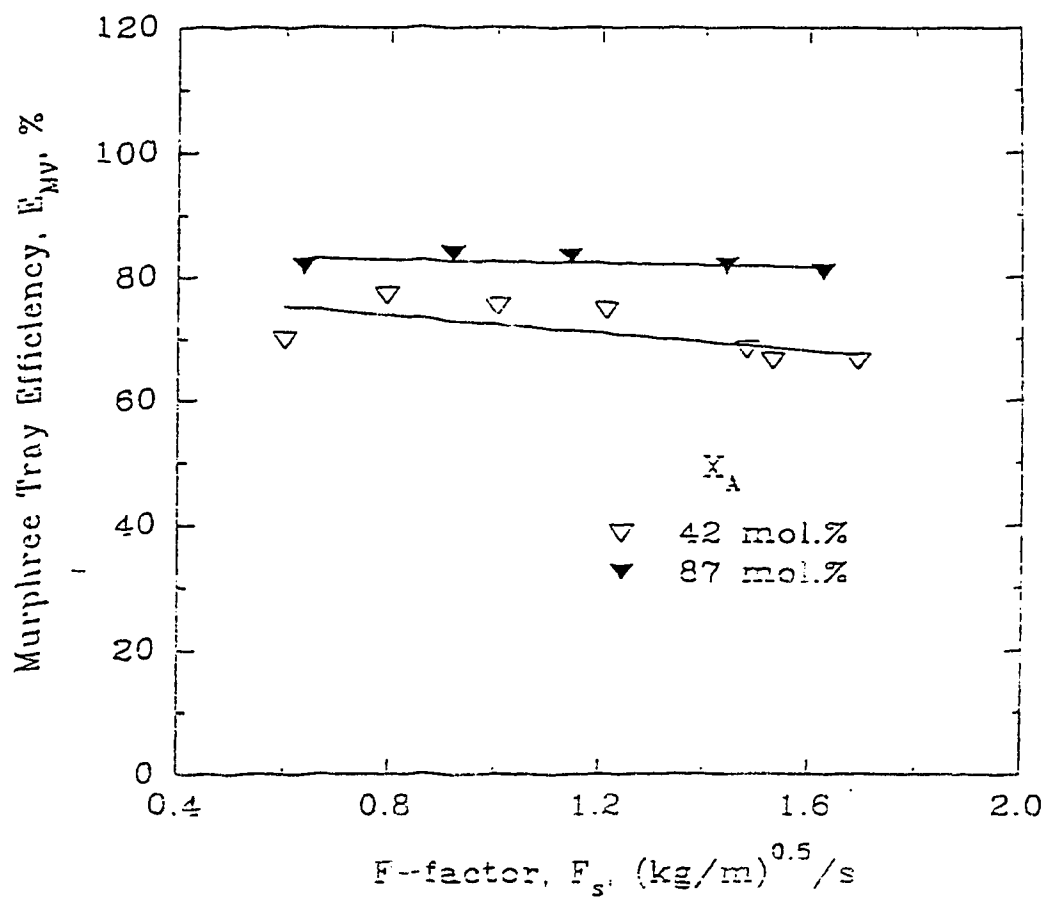
Figure 5.5: Effect of the F-factor on Tray Efficiency for
the Methanol/Isopropyl Alcohol System
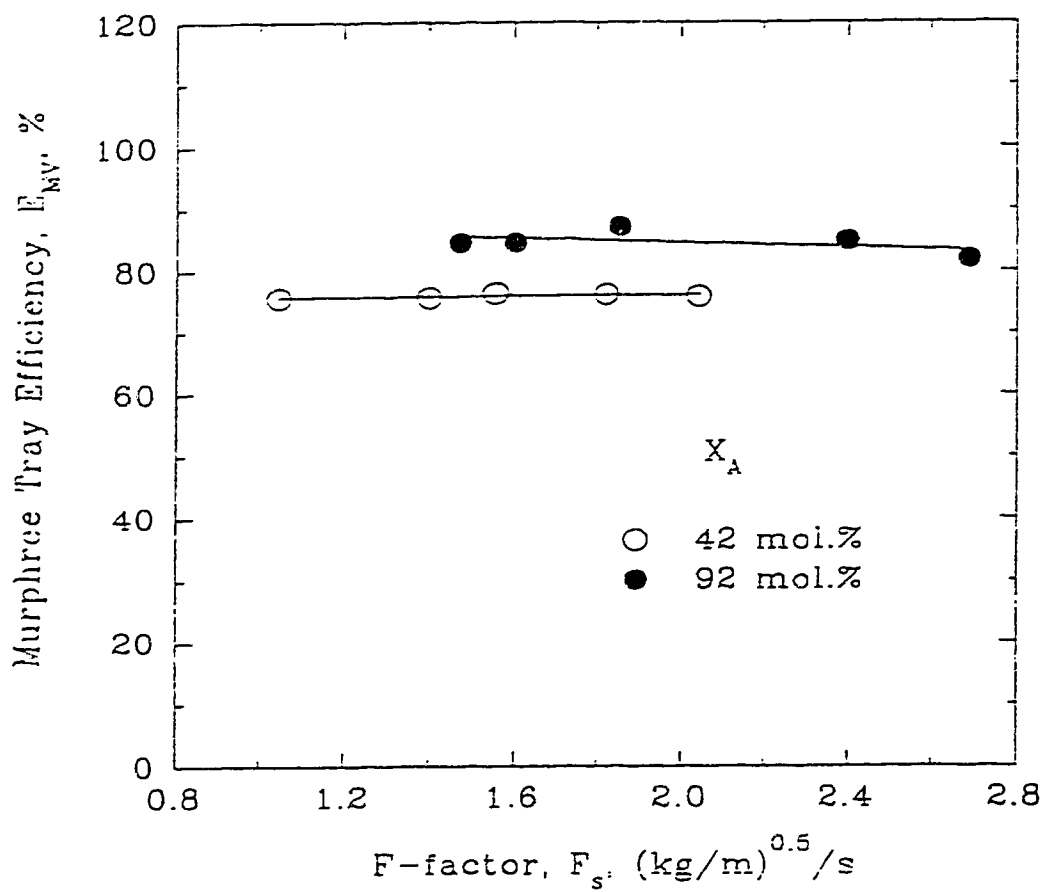
Figure 5.6: Effect of the F-factor on Tray Efficiency for

the Chloroform/Toluene System
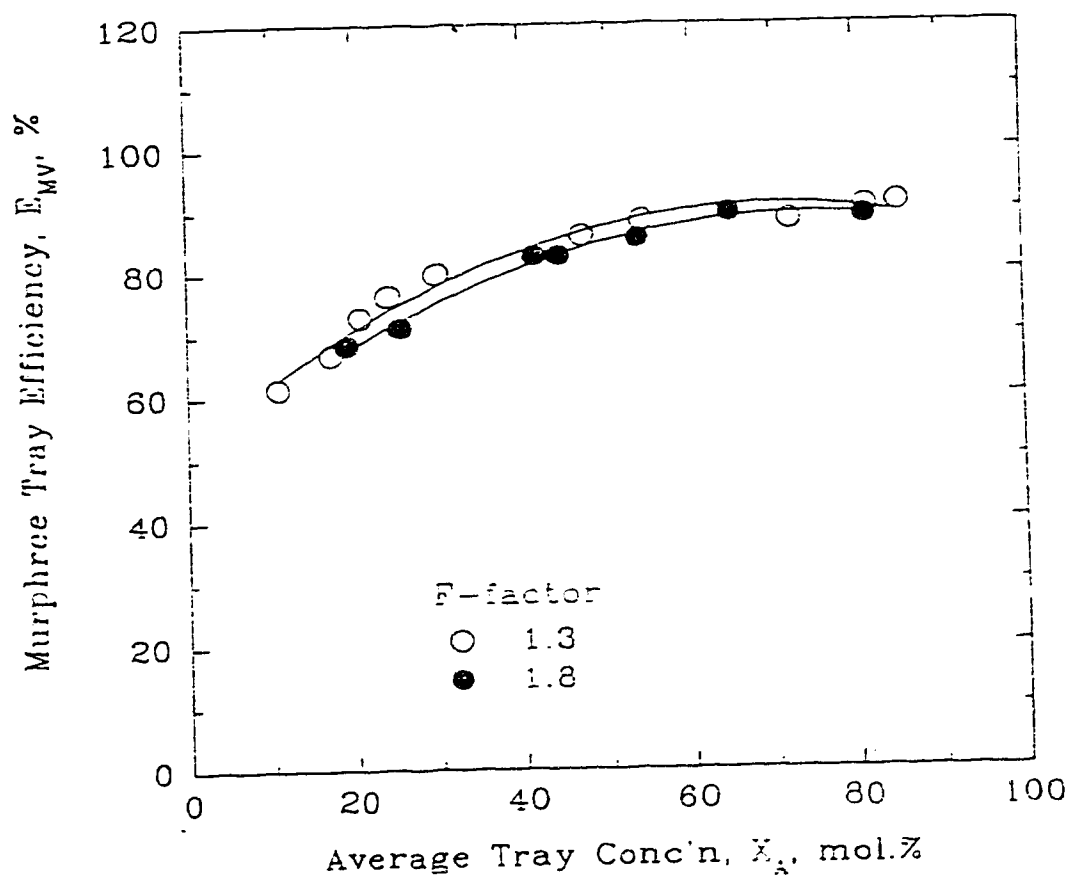
Figure 5.7: Effect of Liquid Composition on Tray Efficiency

for the Methanol/Water System

Harmens' (1958) proposed froth stabilization mechanism may not be the only explanation for enhancing the tray efficiency. Other explanation may come from the discussion in Chapter 3 of the Marangoni effect on the liquid phase mass transfer coefficient. Because of the large difference in surface tension between methanol and water, this promotes interfacial cellular convection in the liquid phase which enhances the rate of mass transfer and the tray efficiencies. These efficiency results are consistent with those observed by Lockett and Ahmed (1983).

The additional surface tension positive system chosen for this study was the n-heptane/toluene system. Unlike the methanol/water system, the n-heptane/toluene system is a hydrocarbon system and has a smaller surface tension gradient (12 to 18.2 dyn/cm compares with 18.2 to 61 dyn/cm for methanol/water system). Figure 5.8 shows the variation of Murphree tray efficiency with liquid composition. It can be seen that the tray efficiency does not increase with increasing concentration as sharply as that for the methanol/water system. Also the tray efficiencies were lower than for the methanol/water system. By comparing the physical properties between the two systems given in Appendix B, it was found that the n-heptane/toluene system has a smaller value of the vapour-phase diffusivity (one order of magnitude smaller). This significantly reduces the rate of mass transfer and prohibits higher tray efficiency for the n-heptane/toluene system.

Figure 5.9 shows the variation of Murphree tray efficiency for a surface tension negative system, the benzene/n-heptane system, as a function of the liquid composition. Notice that as the benzene concentration increases from 10 mol.% to about 70 mol.%,

54
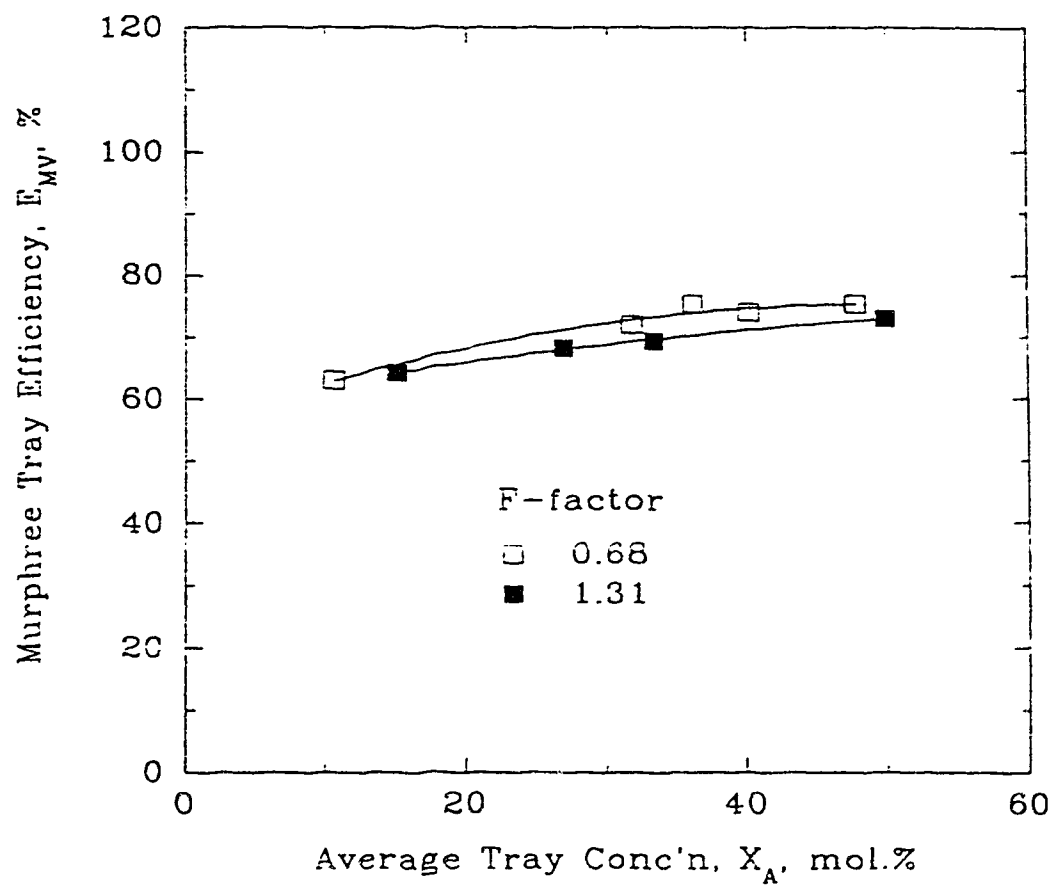
Figure 5.8: Effect of Liquid Composition on Tray Efficiency

For the n-Heptane/Toluene System
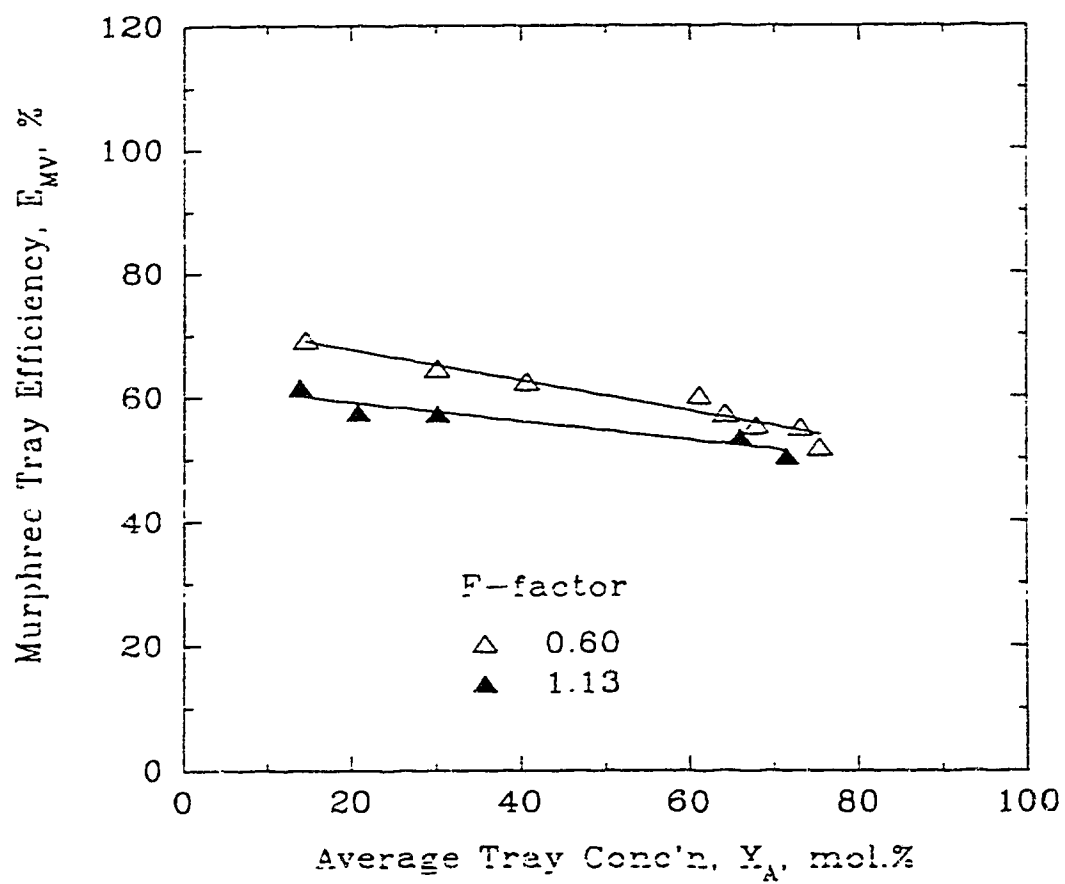
Figure 5.9: Effect of Liquid Composition on Tray Efficiency
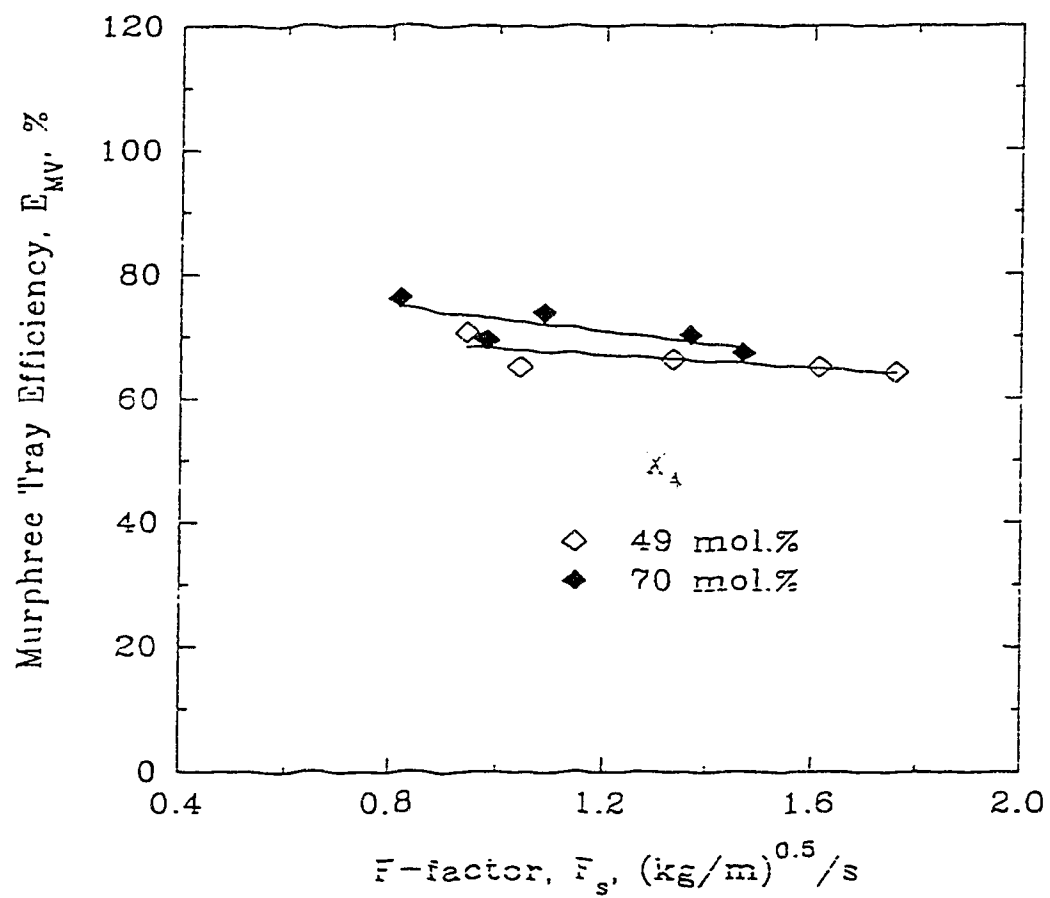
For the Benzene/n-Heptane System

the tray efficiency decreases from about 68 % to 50 %. In addition, this system exhibits lower value of tray efficiencies than the surface tension positive systems. Similar results were also obtained by Zuiderweg and Harmens (1958). From what has been said about the instability of liquid films when distilling a surface tension negative mixture based on Zuiderweg and Harmens' (1958) mechanism, it will be clear that in this case, the bubble stabilizing factor is absent; hence providing a smaller interfacial area and lower efficiency. In addition, cellular convection at the liquid phase is not favourable for negative systems which results in a lower mass transfer rate and efficiency.

Figure 5.10 shows the variation of Murphree tray efficiency for the cyclohexane/n-heptane (neutral) system as a function of liquid composition. As the liquid composition increases from 49 mol.% to 70 mol.% a slight increase in tray efficiency is noticed. Biddulph et al. (1991) reported similar efficiencies (in a range of 60 % to 70 %) for the cyclohexane/n-heptane system using a 0.43 metre diameter sieve tray. Unlike positive and negative systems, this system has no drastic change in the tray efficiency as the liquid composition increases. These results are expected because of the similar physical properties of the two hydrocarbons.

Figure 5.11 shows the variation of Murphree tray efficiency with liquid composition for the methanol/isopropyl alcohol system. The trend in efficiency is similar to that observed for the cyclohexane/n-heptane system except that the methanol/isopropyl alcohol system exhibits the tray efficiency which is 7 % higher than those for the cyclohexane/n-heptane system. Examination of the physical properties of the two systems reveals that the methanol/isopropyl alcohol system has higher values of
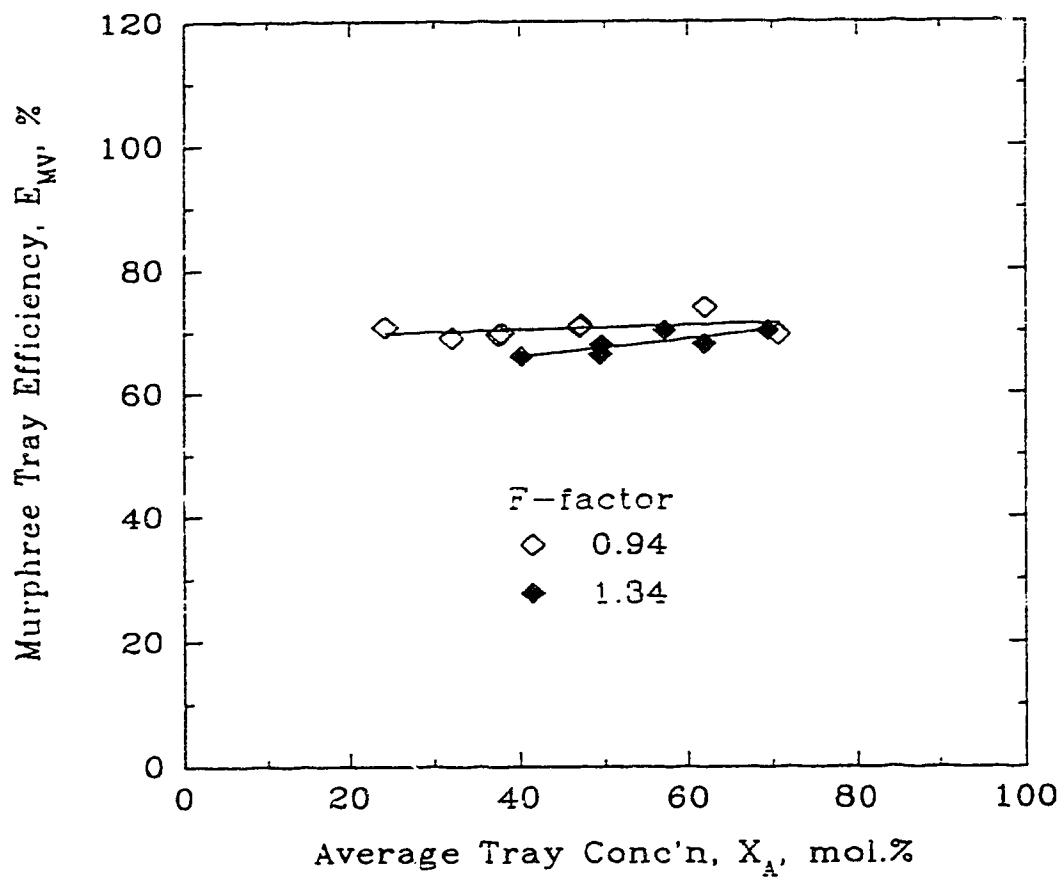
Figure 5.10: Effect of Liquid Composition on Tray Efficiency

for the Cyclohexane/n-Heptane System

58
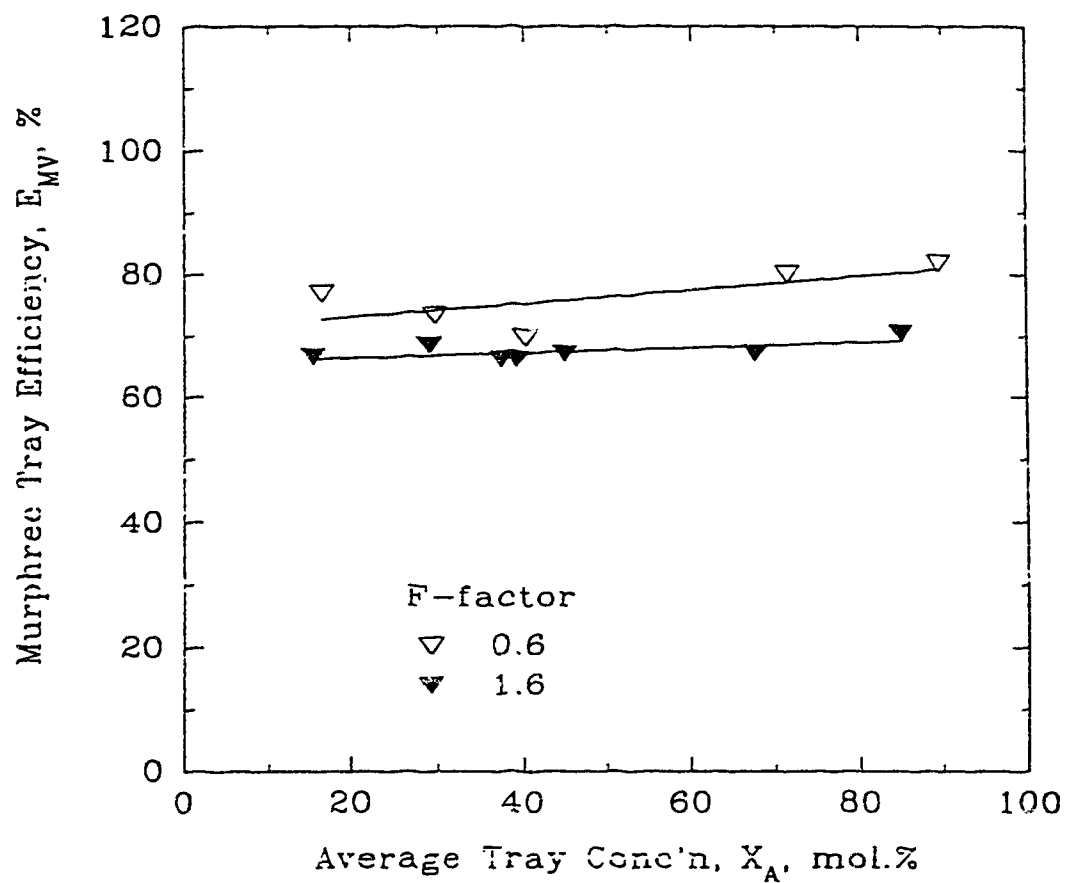
Figure 5.11: Effect of Liquid Composition on Tray Efficiency

for the Methanol/Isopropyl Alcohol System

D_G (2.5 times higher) than the cyclohexane/n-heptane system which results in higher values of k_G and consequently higher tray efficiency. These results also agree with those reported by Biddulph et al (1991) for alcohol/alcohol systems (77 % to 81 % for methanol/n-propanol system).

Figure 5.12 shows the variation of Murphree tray efficiency with liquid composition for the chloroform/toluene (neutral) system. It is interesting to note that because of the high liquid density of chloroform, the tray can only be operated at a F-factor greater than 1.4 at high chloroform concentrations (i.e. 92 mol.%), otherwise the problem of weeping occurs. As shown in Figure 5.12, tray efficiency increases drastically as chloroform concentration increases. These results are similar to those for the methanol/water mixture, however in this case, the surface tension change is minimal whereas the density change is significant. In this case, the density gradients (which are similar to surface tension gradients) create an unstable situation in the liquid phase which will favour cellular motion and as a result, increase the liquid phase mass transfer coefficient and the tray efficiency. This cellular motion can be explained by considering the example of the desorption of a light component (e.g. water) from a heavy component (e.g. ethylene glycol). There, as the light component (water) is being desorbed from a heavier, less volatile component (ethylene glycol), into a gas phase which lies above the liquid phase, a region of greater density develops near the interface because of the evaporation of the light component. This results in a region of high-density liquid occurring above a region of low-density liquid, and this will tend to be relieved through cellular motion in which the heavy interface liquid flows downward and the lighter bulk
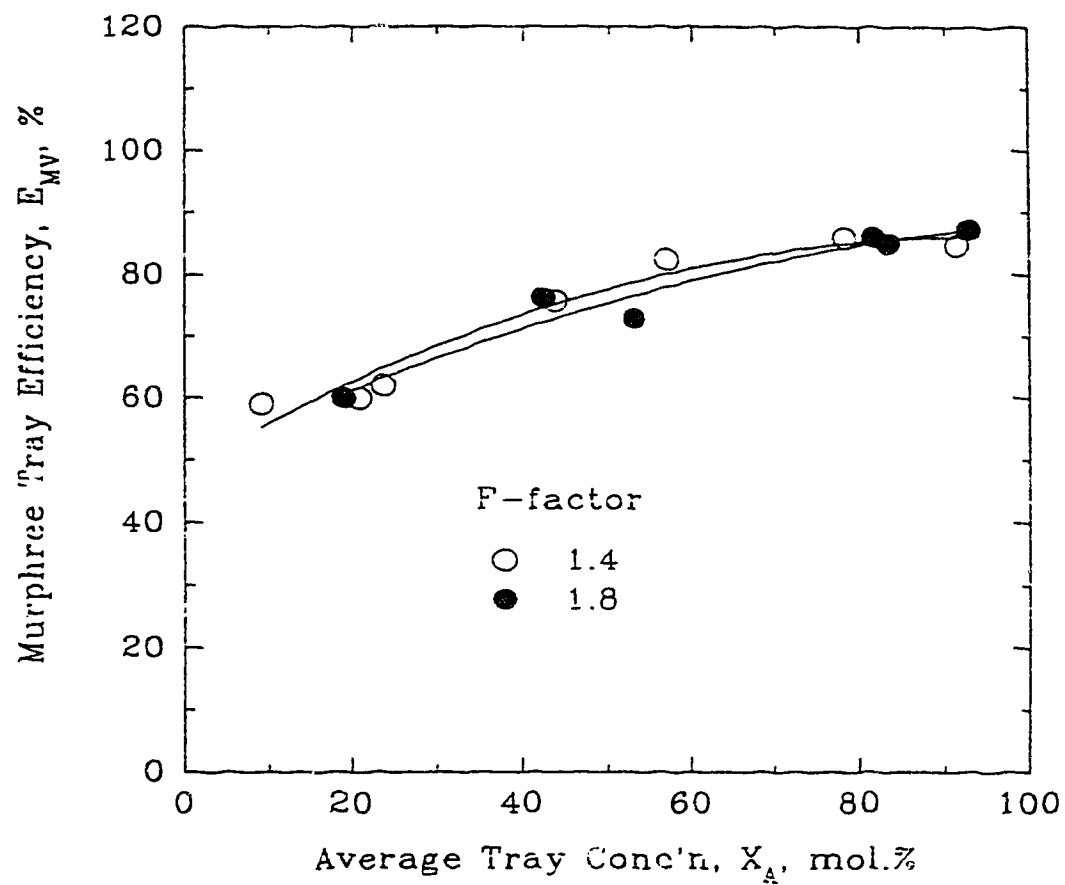
Figure 5.12:   Effect of Liquid Composition on Tray Efficiency

for the Chloroform/Toluene System

liquid flows upward.

Figure 5.13 shows the Murphree tray efficiency as a function of F-factor for three different surface tension gradients systems. The figure suggests that different surface tension gradient systems give different value of efficiencies and therefore should be considered seriously in the correlations development.

5.3 Determination Of Constants C_1 and C_2

In order to determine C_1 and C_2 in Equations (3.10) and (3.11), experimentally measured efficiency data must be used. Combining Equations (2.23.2), (3.10) and (3.11), the overall mass transfer unit at total reflux can be expressed as:

$$N_{OG} = \frac{N_G}{1+m\dfrac{N_G}{N_L}} = \frac{C_1\dfrac{\epsilon(\rho_L^2\rho_G)^{0.2}u_s^{0.4}}{\sigma^{0.6}\mu_L^{0.1}}\sqrt{D_G t_G}}{1+m\dfrac{C_1\sqrt{D_G t_G}}{C_2 S(M)\sqrt{D_L t_L'}}} \tag{5.1}$$

It should be noted that the enhancement factor, S(M) which is a function of the M-index; and for the limiting case when the M-index equals zero (i.e. neutral systems), S(M) becomes unity. Based on this limiting case, a parameter estimation method is required to determine C_1 and C_2 with neutral systems only.

The parameter estimation method was carried out by using Sigmaplot version 4.0 (Jandel Scientific, 1988). Since all the variables except C_1 and C_2 are defined in Equation (5.1), a functional form can be expressed as:

62
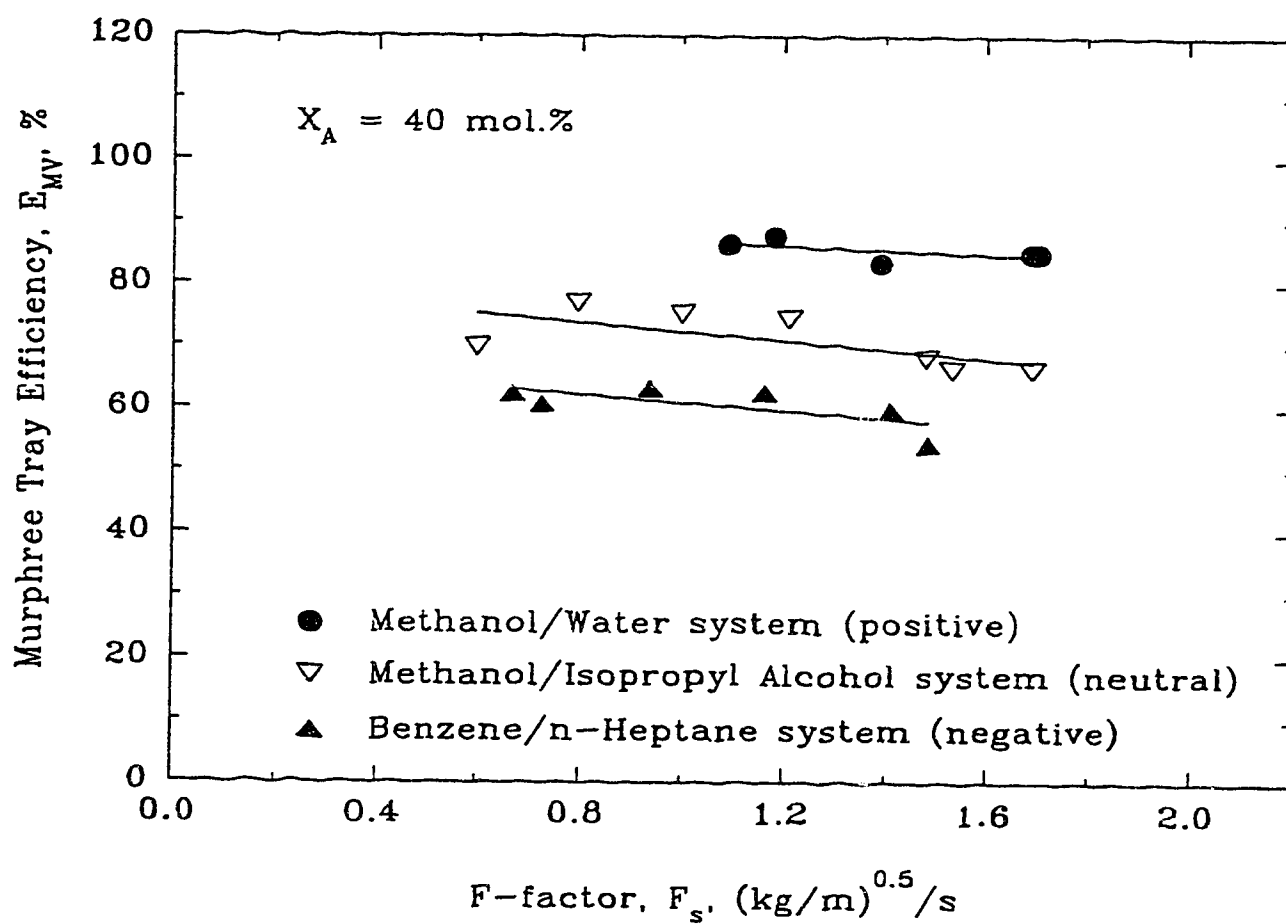
Figure 5.13: Comparison of Tray Efficiency for Three

Different Surface Tension Gradients Systems

63

$$N_{OG} = \frac{C_1 b}{1 + \frac{C_1}{C_2} d}$$

(5.2)

Simply write the above function into Sigmaplot 4.1 and assume an initial value for C_1 and C_2 with an iteration tolerance set at 1×10^{-6}, C_1 and C_2 were found to be 17.6 and 33.6, respectively, over 71 data points. In order to examine the aptness of the two constants, a residual analysis was used. Figure 5.14 shows a standardized residual plot with the calculated N_{OG} values. The figure suggests that with constants, C_1 and C_2, the correlations fit almost all values of surface tension neutral systems and these two values can be used to calculate the N_G and N_L for systems free of the Marangoni effect.

5.4   Determination Of Function S(M)

Given $C_1 = 17.6$, N_G can be calculated by using Equation (3.10) for positive and negative systems. Subtracting these N_G values from Equation (2.23.2), experimental N_L values can be determined. Notice that these N_L values represent systems with the Marangoni effect. Similarly using $C_2 = 33.6$, N_L can be calculated by using Equation (3.11) (i.e. S(M) = 1); with these values applicable to systems which do not exhibit the Marangoni effect. By comparing these two different N_L values over the range of M-index, the function S(M) can then be determined. Figure 5.15 reveals the relationship of the ratio N_L exp./N_L cal. with M-index. From the figure, the function S(M) was assumed to take the form:
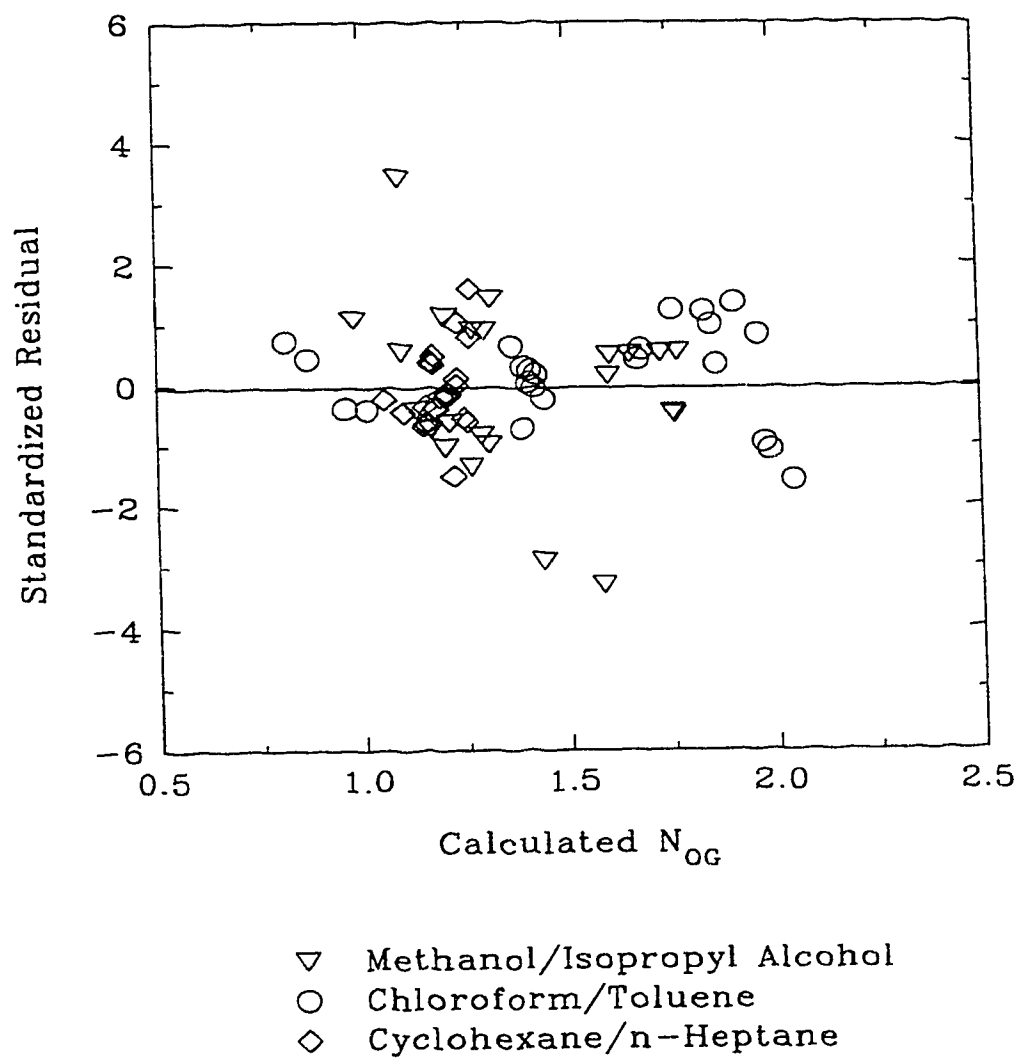
Figure 5.14: Standardized Residual Plot with the Calculated N_{OG} Values
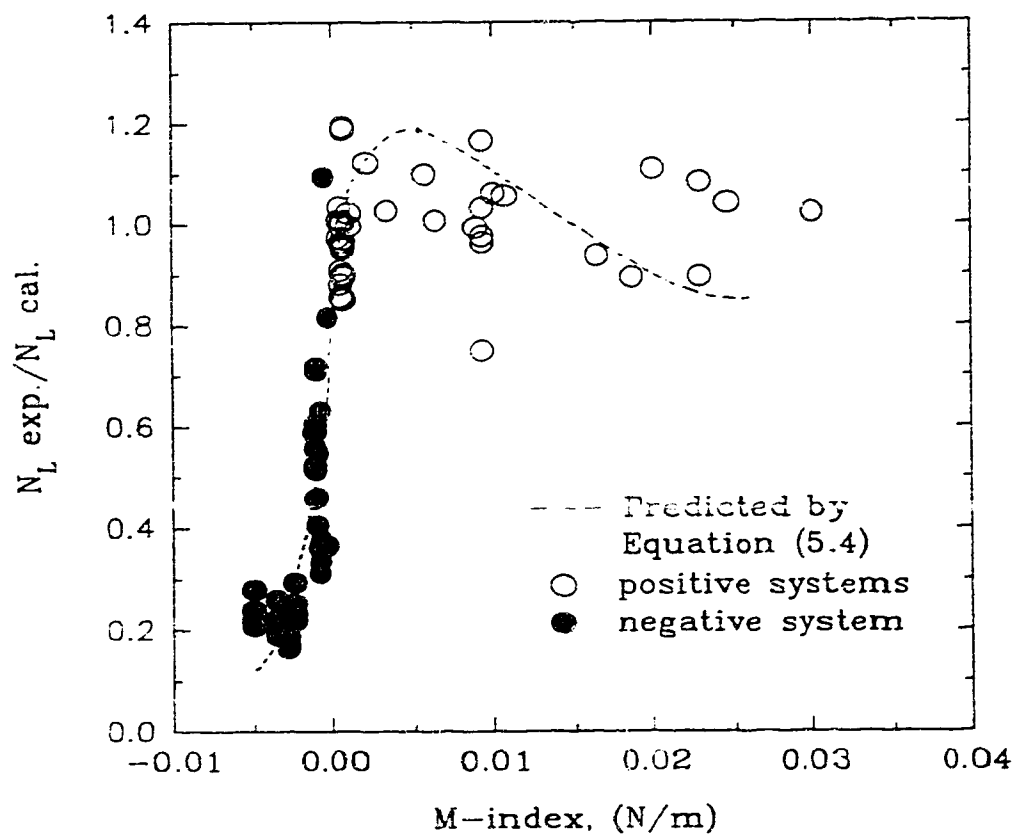
Figure 5.15: The Ratio N_L exp./N_L cal. as a Function of M-index

$$S(M) = \frac{e^{-b_sM}}{1+a_s|M|^{c_s}e^{-b_sM}}$$

(5.3)

The best fit over 83 experimental data point for the positive and negative systems gave:

$$S(M) = \frac{e^{417.96M}}{1+4.67|M|^{0.357}e^{417.96M}}$$

(5.4)

The range of applicability of Equation (5.4) is for $-0.005 < M < 0.03$. The standardized

residual plot with the Marangoni-index is shown in Figure 5.16.

With S(M) defined, the final correlations can be expressed as:

$$N_G = 17.6\frac{\epsilon(\rho_L^2\rho_G)^{0.2}u_s^{0.4}}{\sigma^{0.6}\mu_L^{0.1}}\sqrt{D_G t_G}$$

(5.5)

$$N_L = 33.6(\frac{e^{417.96M}}{1+4.67|M|^{0.357}e^{417.96M}})\frac{\epsilon(\rho_L^2\rho_G)^{0.2}u_s^{0.4}}{\sigma^{0.6}\mu_L^{0.1}}\sqrt{D_L t_L}$$

(5.6)

Figure 5.17 shows a plot of the experimental N_{OG} values versus the predicted N_{OG}

values. The scatter tends to be equally distributed about the straight line having a slope

of unity, indicating no bias in the proposed correlations for all three different systems.

Also, in order to test the validity of the correlations, experimental data of the acetic

acid/water mixture taken from the similar tray by Chen et al. (1992) were compared.

From Figure 5.17, the proposed correlations show good agreement with the experimental

results.
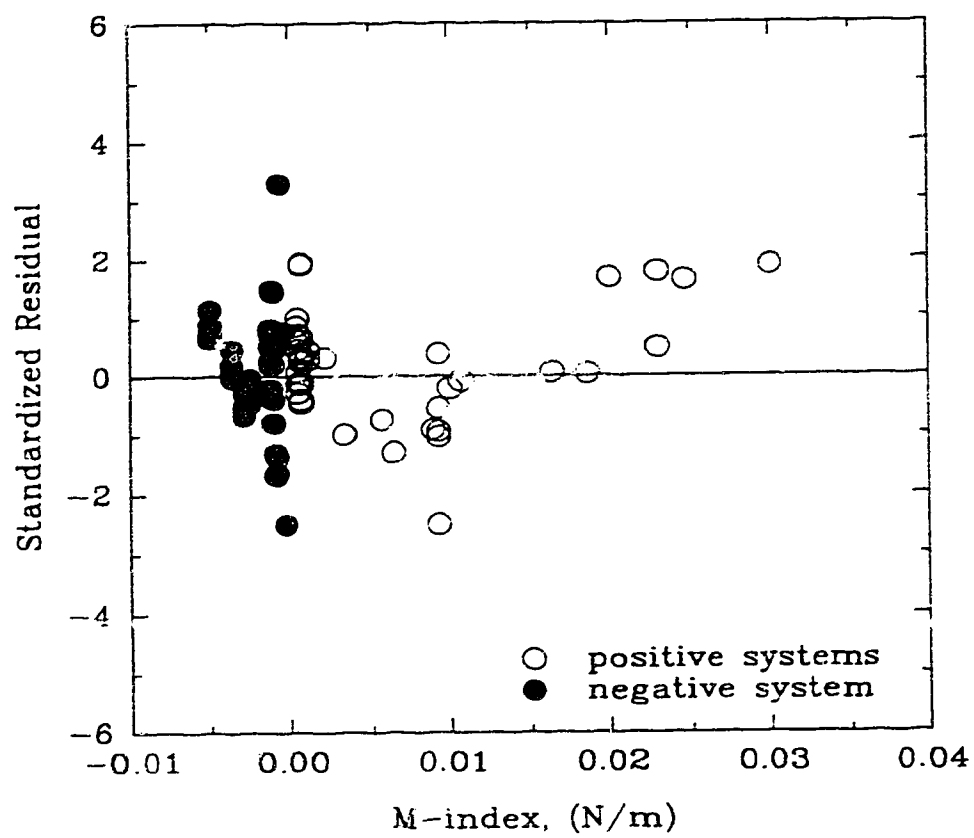
Figure 5.16: Standardized Residual Plot with the Marangoni-index
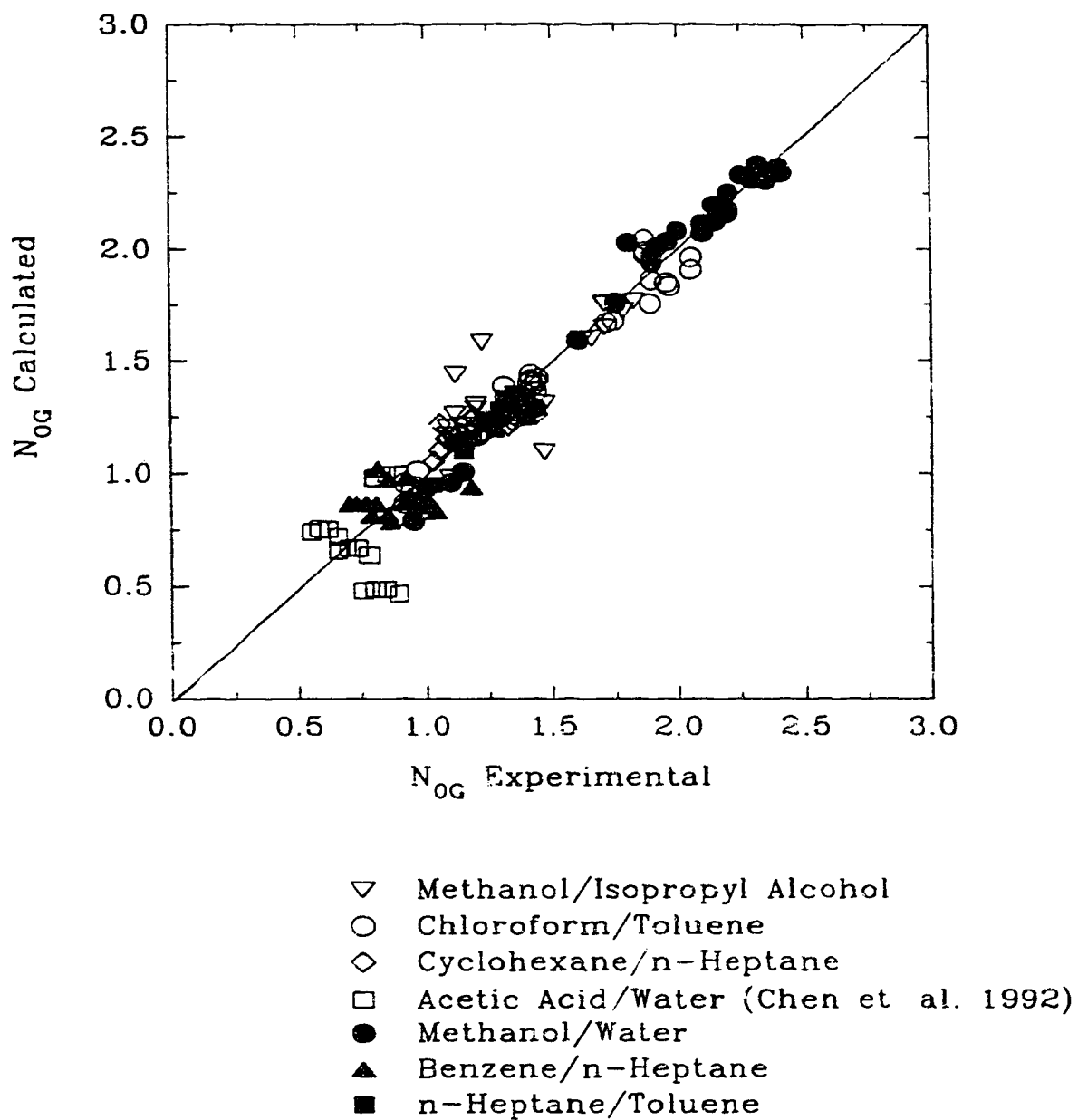
Figure 5.17: Comparison of Experimental Values of N_{OG} with those predicted from the Proposed Correlations

Figure 5.18 shows a plot of the experimental E_{MV} values versus the predicted values. The correlations predict the measured E_{MV} values within ± 15 %.

As shown in Equations (5.5) and (5.6), the new correlations provide a clear picture of some of the physical properties that affect the tray efficiency. The correlations predict higher tray efficiency for increasing values of liquid density. This prediction can be seen clearly in Figure 5.19 for chloroform/toluene system. When the chloroform concentration increases (i.e. liquid density increases as well) from 10 mol.% to 90 mol.%, the tray efficiency increases from about 60 % to 90 %. With other correlations such as that in the AIChE method (1958) and the Chan and Fair (1984) correlation, this kind of tray efficiency behaviour will not be predicted because the liquid density was not explicitly considered in their equations. Similarly, for the methanol/water system, surface tension changes significantly from 0.0417 N/m (i.e. 10.8 mol.% methanol) to 0.0196 N/m (i.e. 85.2 mol.% methanol), while the tray efficiency changes from about 50 % to 90 % as well. As indicated in Figure 5.20, both the AIChE (1958) and the Chan and Fair (1984) correlations cannot predict these efficiency trends. In fact, both of those correlations will only predict a fairly constant efficiency regardness of any given change in concentrations.

5.5   Comparison With Other Correlations

Figures 5.21 and 5.22 show a comparison between the experimental E_{MV} values versus those predicted by the AIChE method and the Chan and Fair correlations. It can be seen that in Figure 5.21, the AIChE method cannot predict the experimental tray
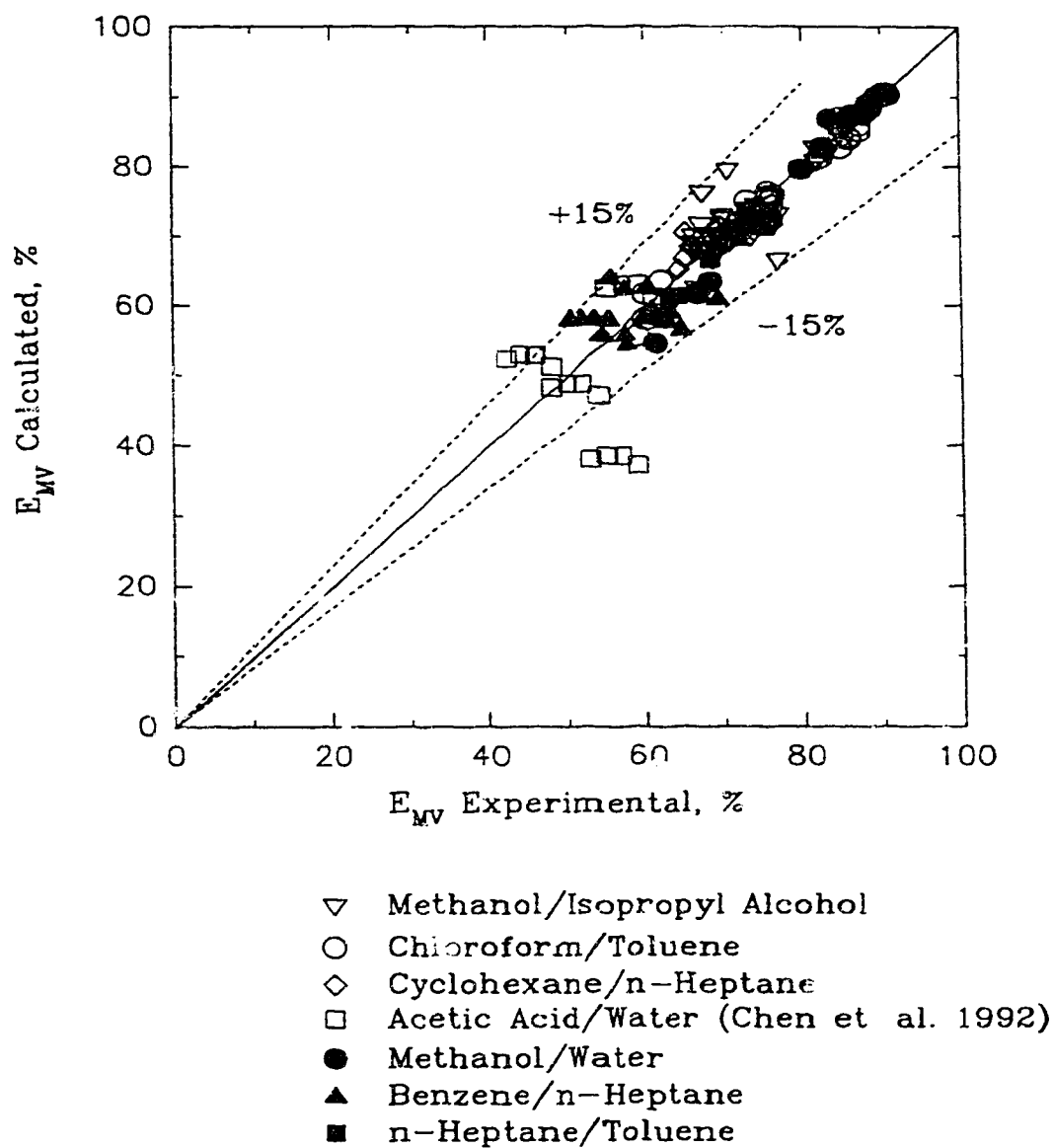
Figure 5.18: Comparison of Experimental Values of E_{MV} with those

predicted from the Proposed Correlations
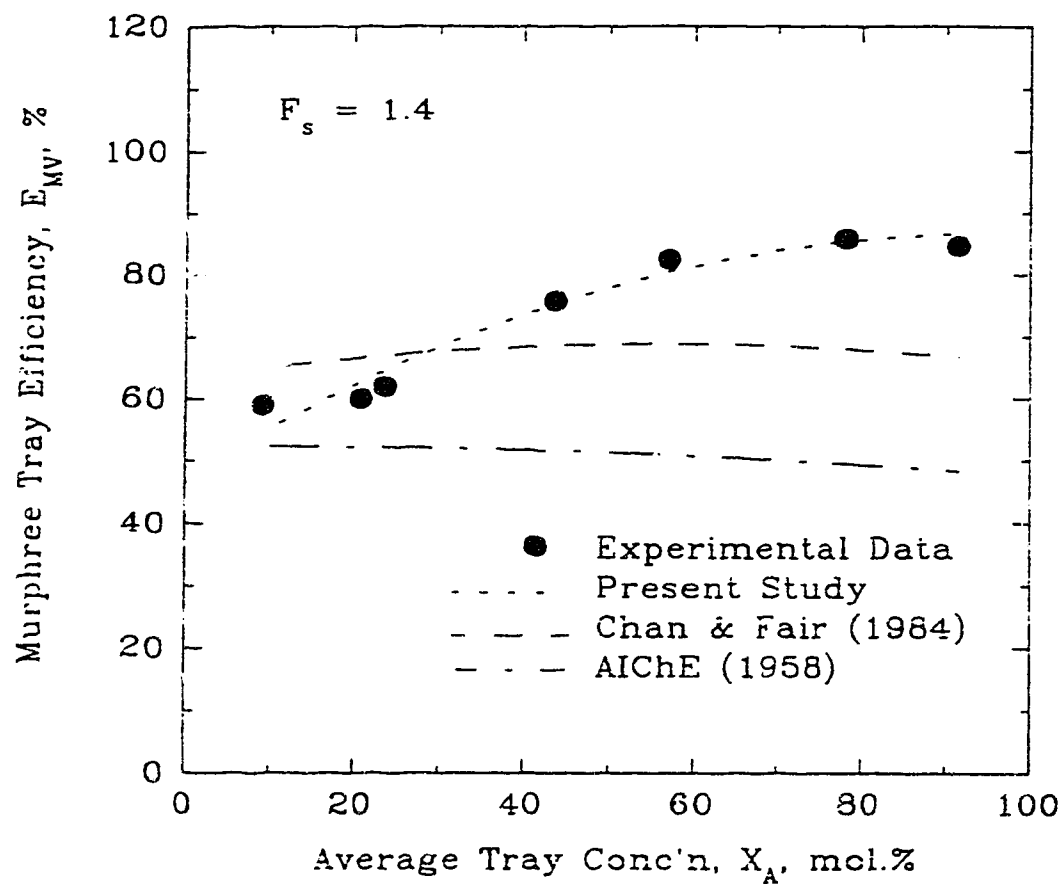
Figure 5.19: Comparison of Tray Efficiency predicted by the New

Correlations and Other Correlations for the Choroform/Toluene System

72
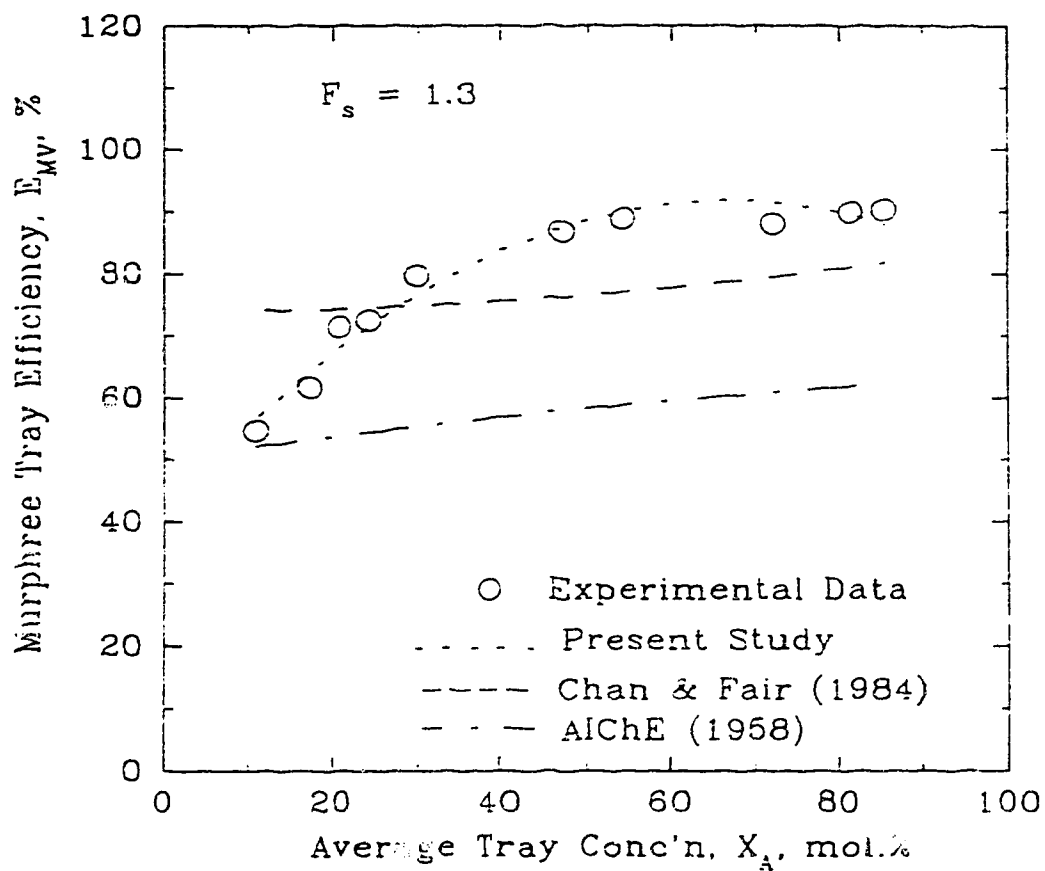
Figure 5.20: Comparison of Tray Efficiency predicted by the New

Correlations and Other Correlations for the Methanol/Water System
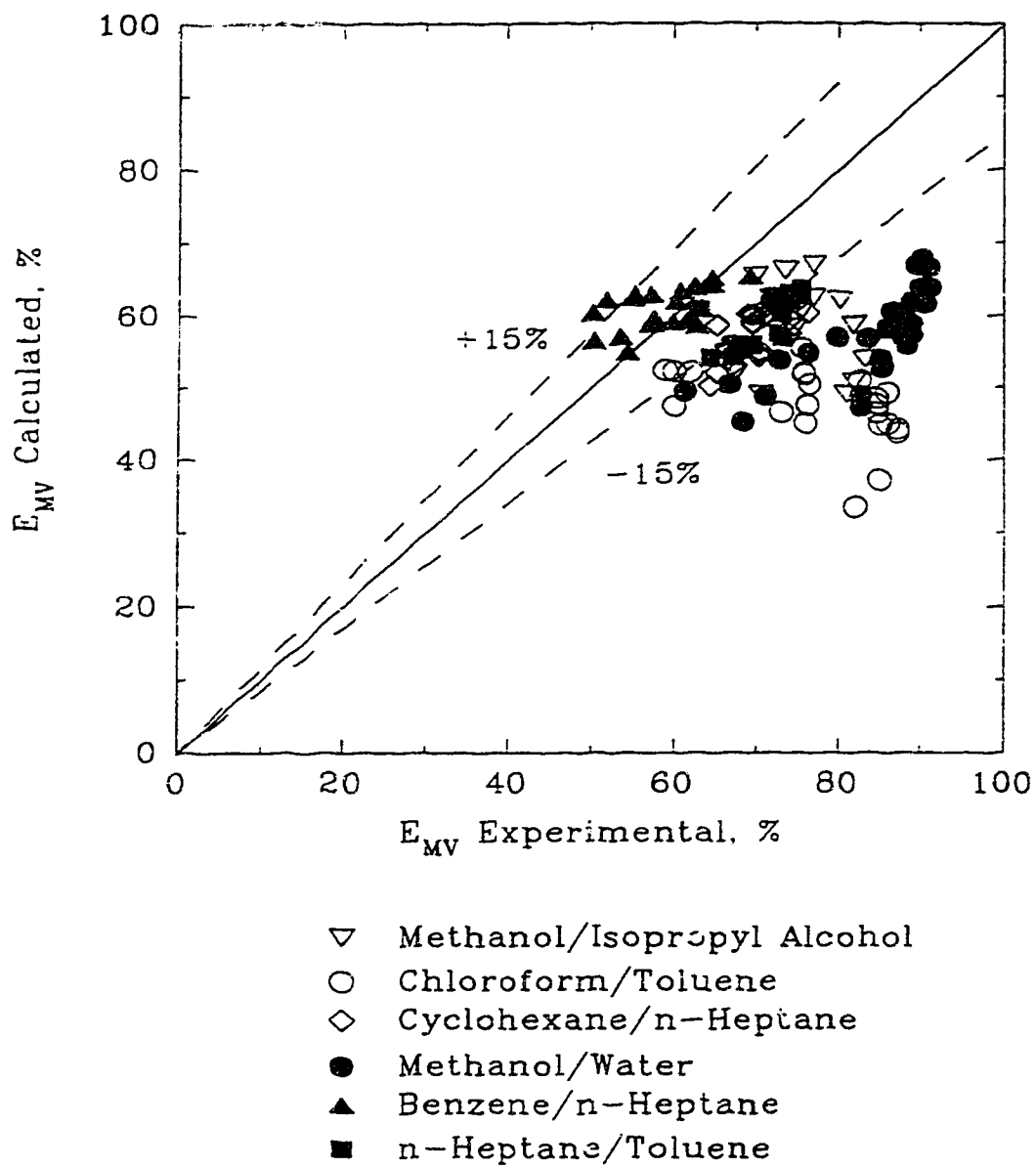
Figure 5.21: Comparison of Experimental Values of E_{MV} with those predicted from the AIChE Method

efficiency within the same degree of accuracy ($\pm$ 15 %) in most cases, whereas in Figure 5.22, the Chan and Fair correlations provide a fairly good prediction of the experimental values. However, the scatter tends not to be e(....ally distributed about the straight line having a slope of unity. This indicates that their correlations will always provide a sort of average fit with the experimental data; the actual tray efficiency trend of the system will not be predicted by their equations as shown in Figures 5.19 and 5.20. Therefore, it is clear from the comparisons that the present correlations are a much better representation of the experimental efficiencies than the other two correlations.
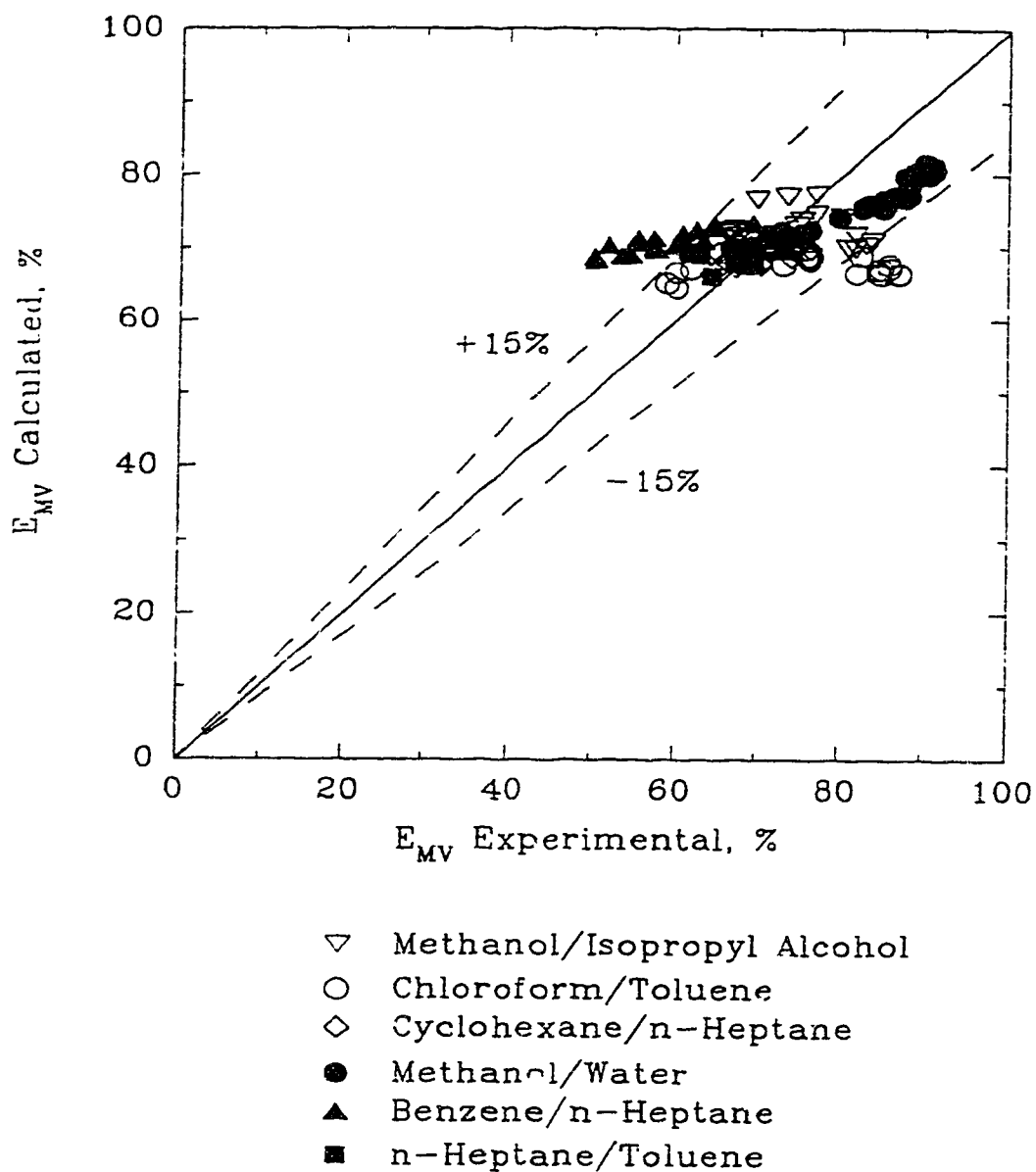
Figure 5.22: Comparison of Experimental Values of E_{MV} with those

predicted from the Chan and Fair Correlations

Chapter 6

CONCLUSION

Experimental results have shown that the effect of surface tension and its gradients can substantially affect the effici icy of a sieve tray. These effects have been experimentally studied by using six different binary mixtures and the results indicate a more reliable prediction method is needed.

Two new correlations for the prediction of the number of mass transfer units, hence tray efficiency, have been developed. The correlations include the effect of surface tension a radients explicitly. The interfacial area of the sieve tray dispersion is estimated by using the Chen and Chuang (1992) equation and the mass transfer coefficients are obtained from the penetration theory. The applicability of the correlations in all systems with different surface tension changes has been demonstrated.

The test results indicate that the correlations predict the point efficiency in good accuracy (within ± 15 %) for all three different surface-tension-gradients systems. This achievement shows that the correlations overcome some of the limitations experienced by the previously proposed tray efficiency prediction methods and therefore can generally be applicable for the prediction of the sieve tray efficiency in distillation.

RECOMMENDATIONS AND POSSIBLE FUTURE WORK

This study only provided a fairly empirical approach in establishing the effect of surface tension gradient into the tray efficiency prediction. The quantitative aspect of the

Marangoni effect on the liquid phase mass transfer coefficient still needs to be studied.

This includes the determination of the formation of roll cells in the liquid interface.

Some related references are:

Brian, P.L.T., (1971), "Effect of Gibbs Adsorption on Marangoni instability", AIChE J., **17**, No. 4, p.765-772.

Imaishi, N., Hozawa M., Fujinawa, K., and Suzuki, Y., (1983), "Theoretical study of interfacial turbulence in gas-liquid mass transfer, appling Brian's linear-stability analysis and using numerical analysis of unsteady Marangoni convection", International Chemical Engineering, **23**, No. 3, p. 466-476.

Chapter 7

REFERENCES

AIChE, (1958), "Bubble tray design manual", AIChE, New York.

Asano, K. and Fujita, S., (1966),"Vapour and liquid phase mass transfer coefficients in tray towers", Kagaku Kogatu 4, 330 & 369.

Bainbridge, G. S. and Sawistowski, H., (1964), "Surface tension effects in sieve plate distillation columns", Chem. Eng. Sci., 19, 992.

Bennett, D. L., Agrawal, R. and Cook, P. J., (1983), "New pressure drop correlation for sieve tray distillation columns", AIChE J., 29, No. 3, 434.

Biddulph, M. W., Rocha, J. A., Bravo, J. L. and Fair, J. R., (1991), "Point efficiencies on sieve trays", AIChE J., 37, No. 8, 1261.

Brian, P. L. T., Vivian, J. E. and Mayr, S. T., (1971), "Cellular convection in desorbing surface tension lowering solutes from water", Ind. Eng. Chem. Fundam., 10, No. 1, 75.

Chan, H. and Fair, J. R., (1984), "Prediction of point efficiencies on sieve trays", Ind. Eng. Chem. Proc. Des. Dev., 23, 814.

Chen, G. X. and Chuang, K. T., (1992), "Prediction of number of mass transfer units in distillation", Ind. Eng. Chem. Res.. (in press)

Chen, G. X., Chuang, K. T., Chien, C. and Ye, Y., (1992), "Mass transfer and hydraulics of packed sieve trays", Gas Separation and Purification, 6, No. 4, 207.

Colwell, C. J., (1979), "Clear liquid height and froth density on sieve trays", Ind. Eng.

Chem. Proc. Des. Dev., **20**, No. 2, 298.

Danckwerts, P. V., Sawistowski, H. and Smith, W., (1960), "The effects of heat transfer and interfacial tension in distillation", International symposium on distillation.

Dribika, M. M. and Biddulph, M. W., (1986), "Scaling-up distillation efficiencies", AIChE J., **32**, No. 11, 1864.

Ellis, S. R. M. and Biddulph, M. W., (1967), "The effect of surface tension characteristics on plate efficiencies", Trans. Instn Chem. Engrs., **45**, T223.

Fane, A. G. and Sawistowski, H., (1969), "Plate efficiencies in the foam and spray regimes of sieve-plate distillation", I. Chem. E. Symp. Ser., No. 32, p.1:8.

Fane, A. and Sawistowski, H. (1968), "Surface tension effects in sieve-plate distillation", Chem. Eng. Sci., **23**, 943.

Fell, C. J. D. and Pinczewski, W. V., (1977), "New considerations in the design of high-capacity sieve trays", The Chem. Engr., (Jan.), 45.

Gardner, R. G. and McLean, A. Y., (1969), "Effect of system properties on sieve-plate froths", I. Chem. E. Symp. Ser., No. 32, p.2:39

Gerster, J. A., (1963), "Tray efficiencies...is more research needed?", Chem. Eng. Prog. **59**, No. 3, 35.

Hala, E., Wichterle, I., Polak, J. and Boublik, T., (1968), "Vapour-liquid equilibrium data at normal pressures", Pergamon, Toronto.

Harris, I. J., (1965), "Optimum design of sieve tray", Br. Chem. Eng., **10**, No. 6, 377.

Hart, D. J. and Haselden G. G., (1969), "Influence of mixture composition on distillation-plate efficiency", I. Chem. Eng. Symp. Ser., No. 32, p.1:19.

Higbie, R., (1935), "The rate of absorption of a pure gas into a still liquid during short periods of exposure", Trans. Am. Inst. Chem. Engrs., 31, 365.

Hirata, M., Ohe, S. and Nagahama, K., (1975), "Computer aided data book of vapour-liquid equilibria", Elsevier, New York.

Hinze, J. O., (1955), "Fundamentals of the hydrodynamic mechanism of splitting in dispersion processes", AIChE J., 1, 289.

Hofhuis, P. A. M. and Zuiderweg, F. J., (1979), "Sieve plates: dispersion density and flow regimes", Inst. Chem. Eng. Symp. Ser., No. 56, p.2.2/1.

Hovestreijdt, J., (1963), "The influence of the surface tension difference on the boiling of mixtures", Chem. Eng. Sci., 18, 631.

Hughmark, G.A., (1971), "Models for vapour phase and liquid phase mass transfer on distillation tray", AIChE J., 17, No. 6, 1295.

Jackson, M. L. and Ceaglske, N. H., (1950), "Distillation, vaporization, and gas absorption in a wetted-wall column", Ind. Engng. Chem., 42, No. 6, 1188.

Jeromin, L., Holik, H. and Knapp, H., (1969), "Efficiency calculation method for sieve-plate columns of air separation plants", Inst. Chem. Engrs. Symp. Series No.32, p.5:45.

Kalbassi, M. A., Dribika, M. M., Biddulph, M. W., Kler, S. and Lavin, J. T., (1987), "Sieve tray efficiencies in the absence of stagnant zones", Inst. Chem. Engr. Symp. Ser., No. 104, A511.

Kastanek, F., (1970), "Efficiencies of different types of distillation plate", Coll. Czech. Chem. Comm., 35, 1170.

81

Kister, H. Z., (1992), "Distillation Operation", 2nd Edition, McGraw-Hill, Toronto.

King, C. J., (1971), "Separation Processes", McGraw-Hill, Toronto.

Koziol, A. and Mackowiak, J., (1992), "A new method for determining the efficiency of tray columns with downcomers", Chem. Eng. Technol., 15, 103.

Levich, V. G., (1962), "Physiochemical hydrodynamics", Prentice Hall, Englewood Cliffs, NJ, 464.

Lewis, W. K., (1936), "Rectification of binary mixtures", Ind. Engng. Chem., 28, No. 1, 399.

Lim, C.T., Porter, K.E., and Lockett, M.J., (1974), "The effect of liquid channeling on two-phase distillation plate efficiency", Trans. Inst. Chem. Engrs., 52, 193

Lockett, M. J. and Ahmed, I. S., (1983), "Tray and point efficiencies from a 0.6 meter diameter distillation column", Chem. Eng. Res. Des., 61, 110.

Lockett, M. J. and Plaka, T., (1983), "Effect of non-uniform bubbles in the froth on the correlation and prediction of point efficiencies", Chem. Eng. Res. Des., 61, 119.

Lockett, M.J., Lim, C.T. and Porter, K.E., (1973), "The effect of liquid channeling on distillation column efficiency in the absence of vapour mixing", Trans. Inst. Chem. Engrs., 51, 61.

Lockett, M.J. and Safekourdi, A., (1976), "The effect of the liquid flow pattern on distillation plate efficiency", Chem. Eng. J., 11, 111.

Lockett, M. J., (1986), "Distillation tray fundamentals", Cambridge University Press, New York.

MacFarland, S. A., Sigmund, P. M. and Van Winkle, M., (1972), "Predict distillation

efficiency", Hydrocarbon Processing, 111.

Mehta, V.D. and Sharma, M.M., (1966), "Effect of diffusivity on gas-side mass transfer coefficient, Chem. Eng. Sci., **21**, 361.

Moens, F. P., (1972), "The effect of composition and driving force on the performance of packed distillation columns--I", Chem. Engng. Sci., **27**, 275.

Mostafa, H. A., (1979), "Effect of concentration on distillation plate efficiency", Trans. I. Chem. E., **57**, 55.

Murphree, E. V., (1925), "Rectifying column calculations with particular reference to N component mixtures", Ind. Engng. Chem., **17**, No. 7, 747.

Porter, K.E., Lockett, M.J. and Lim, C.T., (1972),"Effect of liquid channeling on distillation plate efficiency", Trans. Inst. Chem. Engrs., **50**, 91.

Plaka, T., Ehsani, M. R. and Korchinsky, W. J., (1989), "Determination of individual phase transfer units, N_G and N_L, for a 0.6 meter diameter distillation column sieve plate: methylcyclohexane-toluene system", Chem. Eng. Res. Des., **67**, 316.

Prado, M. and Fair, J. R., (1990), "Fundamental model for the prediction of sieve tray efficiency", Ind. Eng. Chem. Res., **29**, No. 6, 1031.

Reid, R. C., Prausnitz, J. M. and Sherwood, T. K., (1977), "The properties of gases and liquids", McGraw-Hill, Toronto.

Ruckenstein, E., (1964), "Influence of the Marangoni effect on the mass transfer coefficient", Chem. Eng. Sci., **19**, 505.

Ruckenstein, E. and Smigelschi, O. (1964), Chem. Eng. Sci., **19**, 505.

Sawistowski, H., (1973), "Surface-tension-induced interfacial convection and its effect

on rates of mass transfer", Chemie-Ing.-Techn., 45, 1093-1098.

Shore, D., and Haselden, G. G., (1969), "Liquid mixing on distillation plates

and its effect on plate efficiency", I. Chem. E. Symp. Ser., No. 32, p.2:54.

Stichlmair, J. (1978). Bodenkolonne. Verlag Chemie.

Spekuljak, Z., (1987), "A criterion to determine the occurrence of the "Marangoni

effect" in a thin liquid film", Chem. Eng. Sci., 42, 163.

Szekely, J., (1963), "Notes on the transfer at the interface of two independently stirred

liquids", Int. J. Heat Mass Transfer, 6, 833.

Van Der Klooster, H. W. and Drinkenburg, A. A. H., (1979), "The influence of

gradients in surface tension on the mass transfer in a packed column", I.

Chem. E. Symp. Ser., No. 56, 2.5/21.

Van Wijk, W. R. and Thijssen, H. A., (1954), "Concentration and plate efficiency in

distillation columns", Chem. Eng. Sci., 3, 153.

Wankat, P. C., (1988), "Equilibrium staged separations", Elsevier, New York.

Young, T. C. and Stewart, W. E., (1992), "Correlation of fractionation tray

performance via a cross-flow boundary-layer model", AIChE J., 38, No. 4, 592.

Zuiderweg, F. J. and Harmens, A., (1958), "The influence of surface phenomena on the

performance of distillation columns", Chem. Eng. Sci., 9, 89.

Zuiderweg, F. J., (1982), "Sieve trays--a view on the state of the art", Chem. Eng.

Sci., 37, No. 10, 1441.

Zuiderweg, F. J., (1983), "Marangoni effect in distillation of alcohol-water mixtures",

Chem. Eng. Res. Des., **61**, 388.

APPENDIX A: DETAILED EXPERIMENTAL PROCEDURE AND DATA

Gas Chromatograph (HP 5790A) Preparation

The compositions of the samples were determined by using the gas chromatograph, G.C., (HP 5790A). For different binary systems, different G.C. columns were used in order to achieve the required separation. Table A.1 summaries the G.C. operating conditions and the columns used for all the test systems.

Table A.1: G.C. Operating Conditions and Columns Used	
Injection temperature: 250°C	
Detector temperature: 200°C	
Oven temperature: range of 50 to 70°C	
Carrying gas: purified helium	
flow rate: 30 ml/min.	
Systems	Columns
methanol/water	6.6% CBX 20m 80/100 Carbopark 6' R21044
methanol/isopropyl alcohol	3% Aprezon L on W 36" 1/8 ss column
cyclohexane/n-heptane	20% sp2100 80/100 supelcoport 6' 03605
n-heptane/toluene	20% sp2100 80/100 supelcoport 6' 03605
chloroform/toluene	20% sp2100 80/100 supelcoport 6' 03605
benzene/n-heptane	20% wp2100 80/100 supelcoport 6' 03605

For each binary system, known samples are prepared from a range of 5 wt.% to 95 wt.% of the more volatile components. Then 1 μl of each sample is injected into the G.C. for analysis. The G.C. would provide compositions in terms of area %. Duplicate samples were injected and the average of the two samples were used to construct the calibration curve. The difference between the two duplicated samples was better ± 0.5%. The procedure was repeated for each prepared sample and a calibration curve was constructed. The G.C. calibration curves for each system are provided in the subsequent pages.
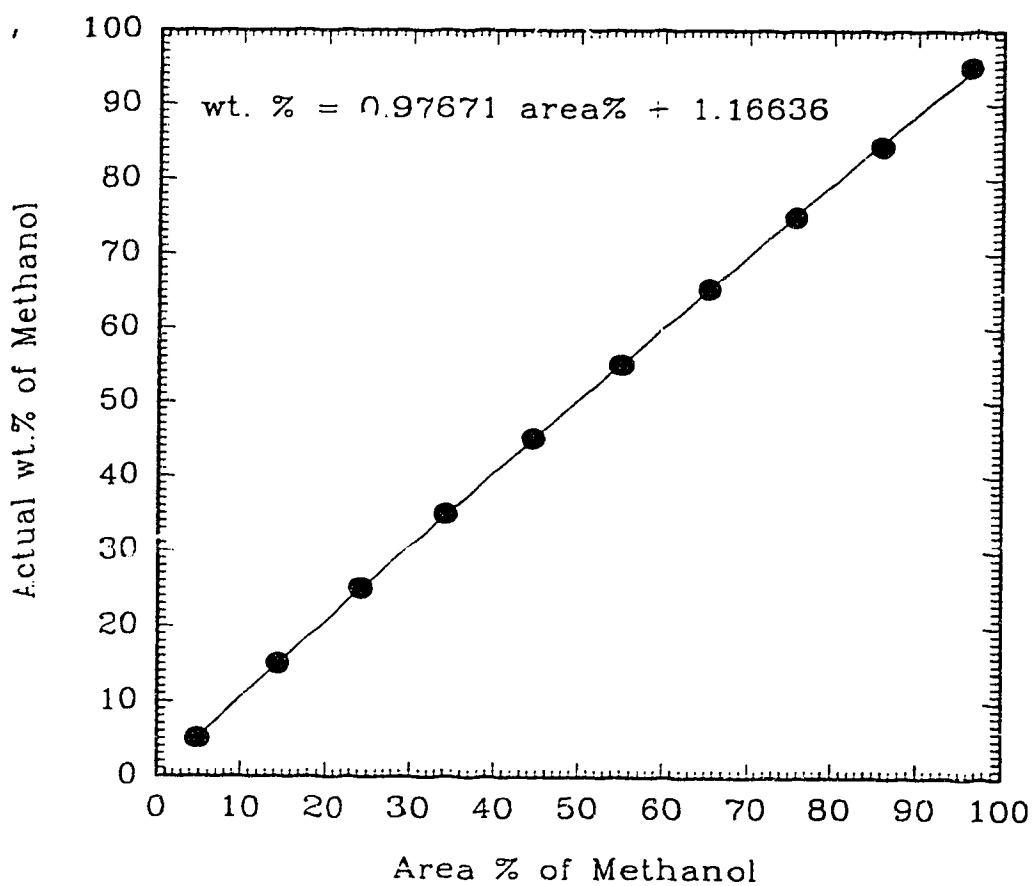
Figure A.1: G.C. Calibration for Methanol/water system
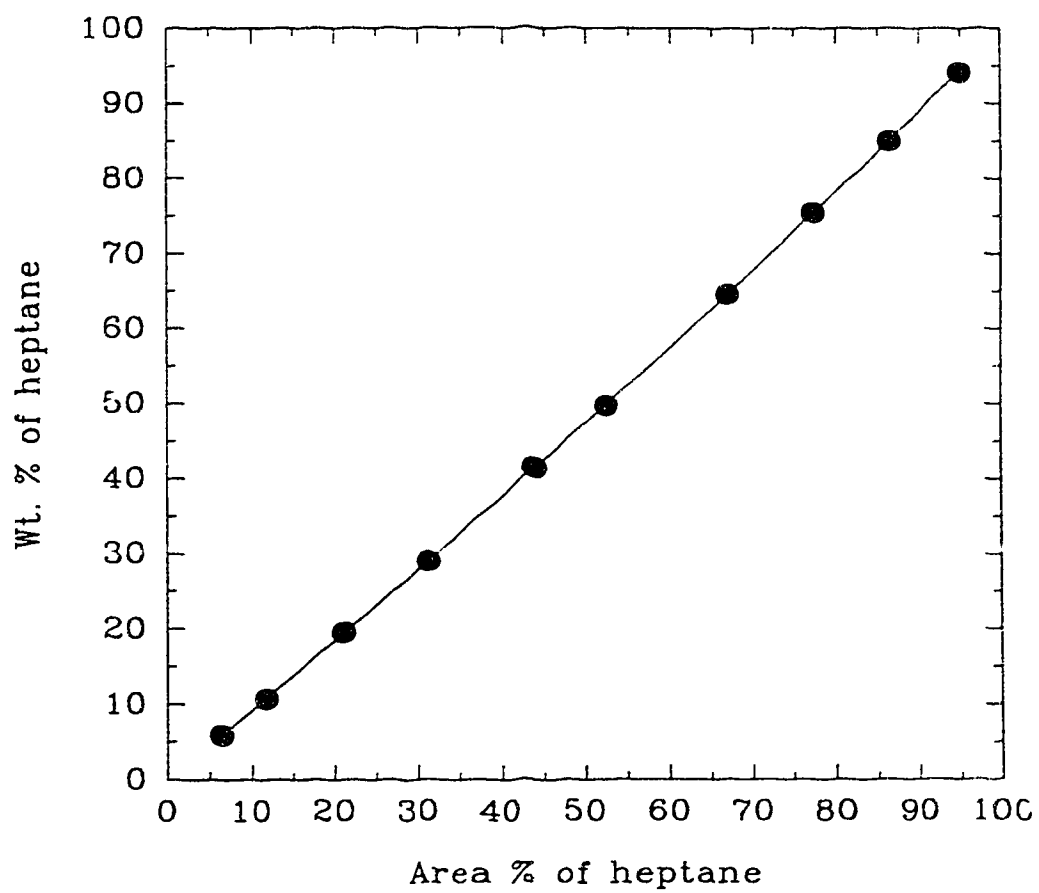
Figure A.2: G.C. Calibration for n-heptane/toluene system
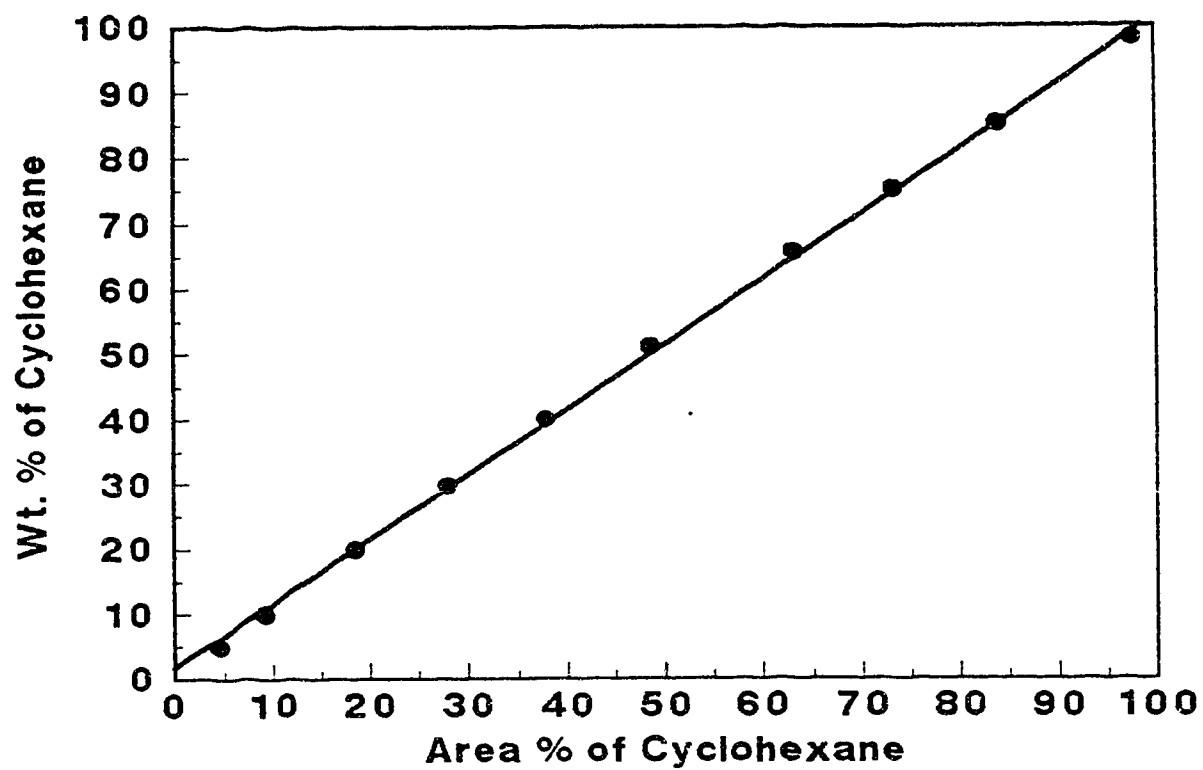
Figure A.3: G.C. Calibration for Cyclohexane/n-heptane system
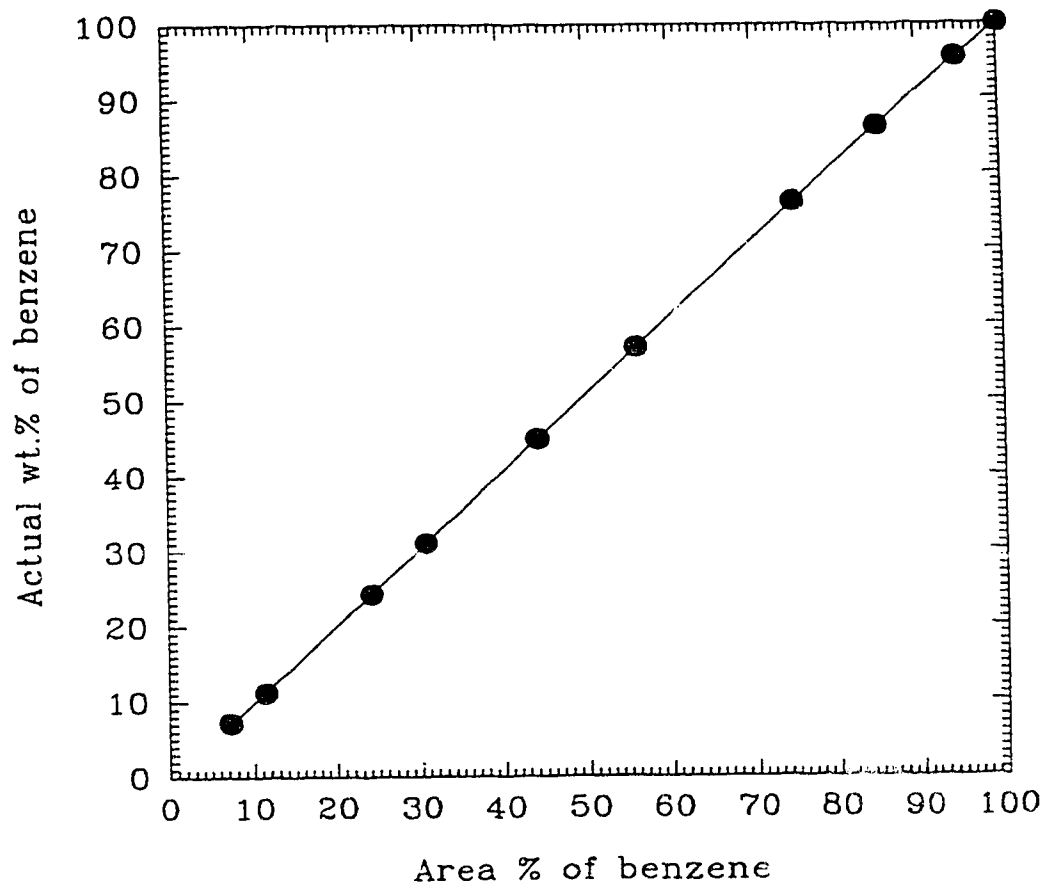
Figure A.4: G.C. Calibration for Benzene/n-heptane system

92
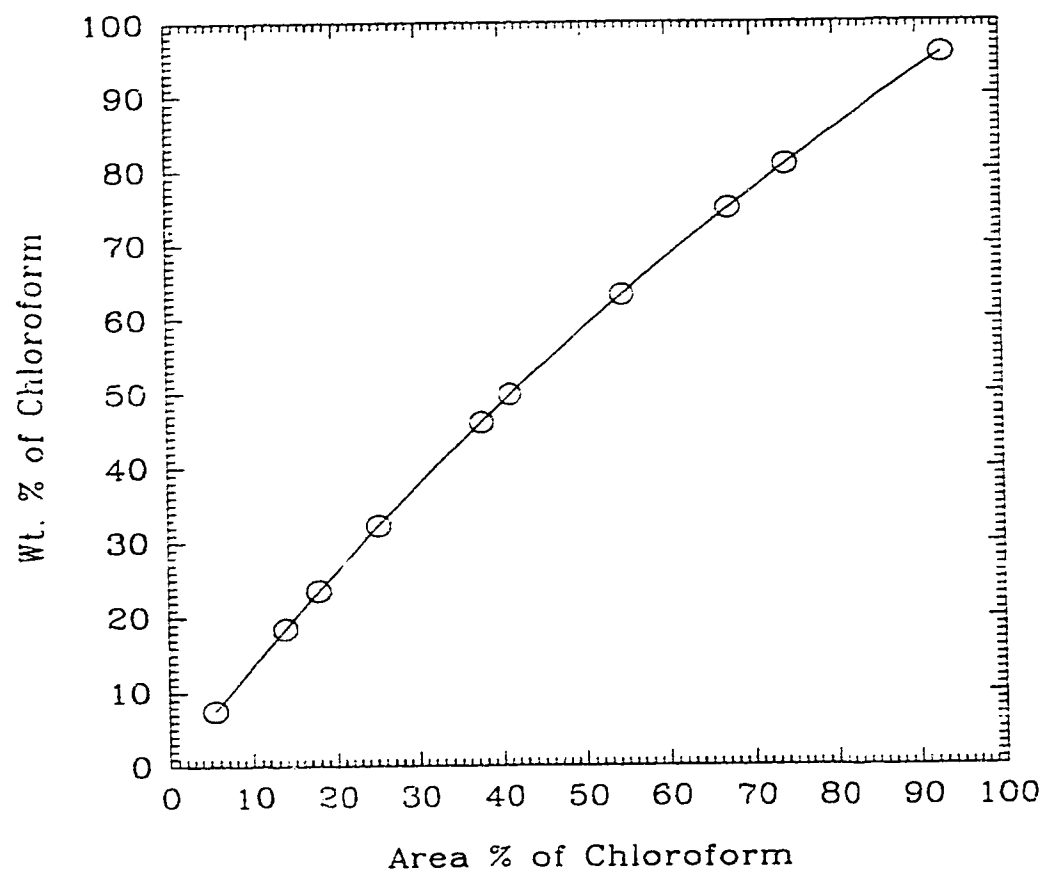
Figure A.5: G.C. Calibration for Chloroform/Toluene system
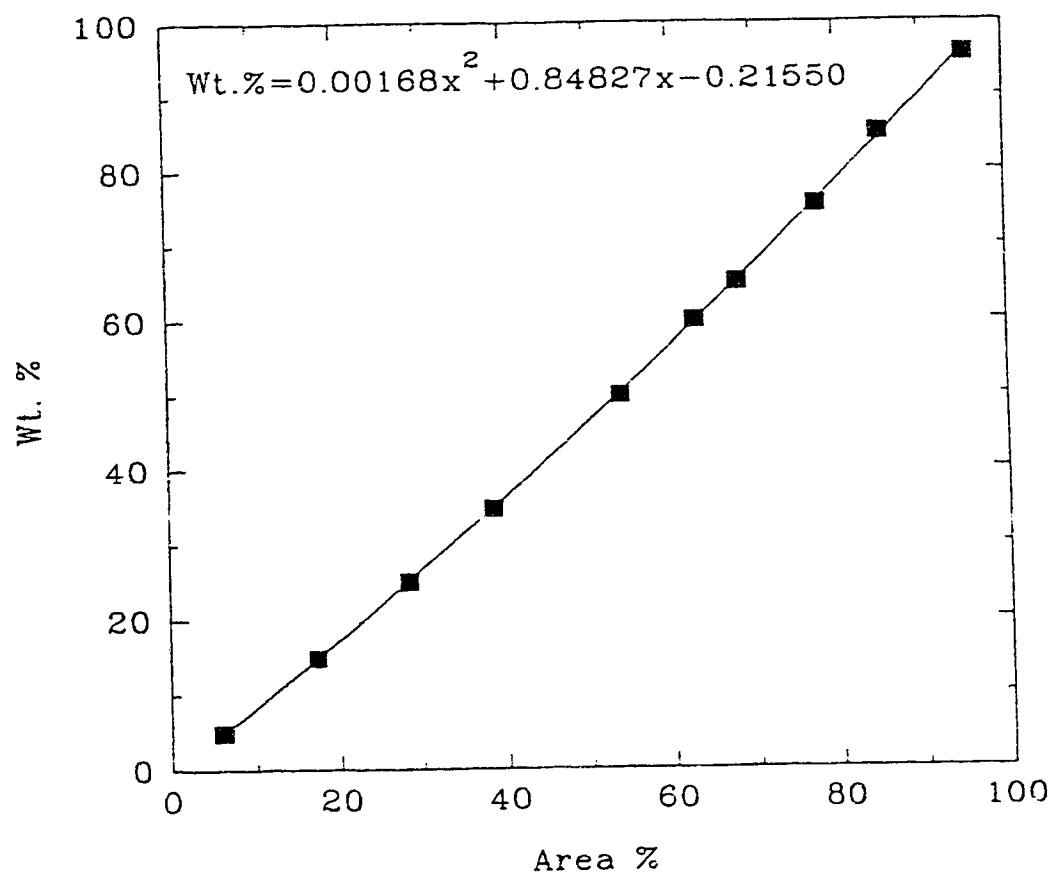
Figure A.6: G.C. Calibration for Methanol/Isopropyl Alcohol system

Once the G.C. is calibrated, mixtures are prepared and put into the distillation column.

START-UP

(3)   Open the steam valve through the controller and the mixtures will gradually start to boil. When the vapour is rising up through the column, open the vent to release any build-up of pressure inside the column.

(4)   Turn on the liquid level controller, flow recorder and set them on automatic mode. Also turn on the IBM computer, and the Opto22 process I/O subsystem. A program is available to record temperatures, flow rates, and liquid levels. One simply follows the instructions given by the computer.

(5)   When vapour starts to condense, turn on the reflux pump to circulate liquid back to the column.

(6)   Shut off the vent and the start-up is completed.

Since the column is completely instrumented, after a period of 60 minutes, the approach to the steady-state condition was assumed. Energy balance calculations are performed by using the computer to confirm that steady state is reached (discrepancy $< \pm 5\%$). Once steady state has been achieved,

(7)   Record temperature profile, total pressure drop, and froth height

(8)   Liquid samples at the inlet and outlet of the test tray, outlet of tray #1, and reflux are taken using 3 ml syringes. The sampling points are illustrated in Figure A.7. The reason that syringes are used is to eliminate any vapour loss.

Sampling
Point
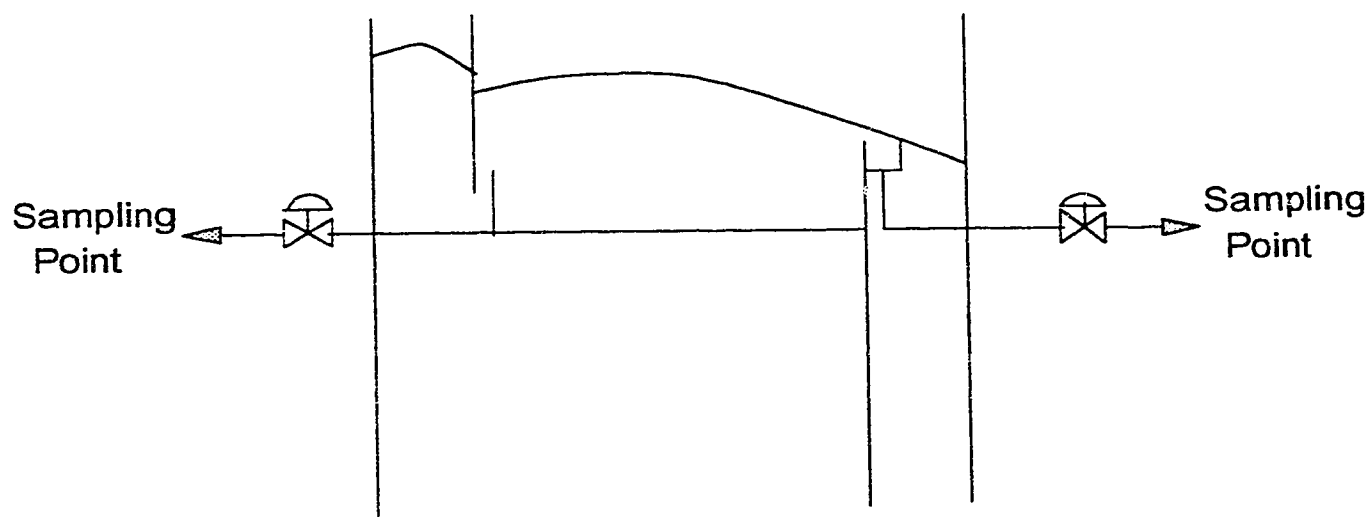
Sampling
Point

Figure A.7: Sampling Points on the Test Tray

(9)   1 μl of each sample is injected into the G.C. where the concentration will be determined. The average of the inlet and outlet concentrations gives the average liquid composition, X_A, on the tray.

(10)   The Murphree tray efficiency, E_{MV}, is calculated using Equation (2.4). The equilibrium concentration is determined by reading the corresponding x_n value from the equilibrium curve provided in Appendix C.

(11)   The F-factor, F_s, is calculated as:

$$F_s = u_s\sqrt{\rho_G}$$

where u_s is determined based on the bubbling area of the tray

(12)   For each mixture, one series of experiments is conducted by keeping the concentration on the tray constant and varying the vapour rates from just above the weep point to below the spray point. The other series of experiments are conducted by keeping the vapour rate constant and varying the concentration on the tray.

(13)   Repeat step 1 to 12 for each mixture

Experimental data are provided in Table A.2 to A.7 for each binary system.

Table A.2: Experimental Data for Methanol/Water System									
Run #	temp, °C	P_T, cm of H_2O	h_f,cm	x_{in},mol.%	x_{out}, mol.%	y_n^*	E_{MV}	F_s	De	Pe
1	66.2	3.3	8.8	90.7	80.48	91.71	91.04	1.3	0.0059	0.089
2	74.5	3.1	6.8	63.23	32.24	68.32	85.9	1.3	0.0054	0.075
3	81.3	3.5	7.0	45.49	16.12	52.93	79.8	1.3	0.0063	0.11
4	66.3	3.3	7.5	88.21	75.55	89.54	90.46	1.3	0.006	0.071
5	84.5	3.9	7.1	32.46	9.68	41.01	72.7	1.3	0.0059	0.08
6	90.9	4.3	7.2	16.02	4.16	23.5	61.3	1.3	0.0059	0.092
7	66.7	4.2	~	88.13	75.81	89.66	88.92	1.75	0.0076	0.137
8	77	4.2	8.0	57.96	27.48	64.38	82.6	1.72	0.0076	0.14
9	75.6	4.0	8.1	59.85	29.64	66.21	82.62	2.03	0.0083	0.138
10	65.5	2.3	7.7	91.43	82.16	92.44	90.18	0.65	0.0033	0.063
11	65.0	~	~	91.99	83.16	92.87	90.93	0.79	0.004	0.076
12	65.8	2.8	8.0	90.86	81.06	91.96	89.97	0.91	0.0046	0.084
13	66.2	3.3	8.8	90.58	80.48	91.71	89.97	1.17	0.066	0.099
14	66.0	3.5	8.4	90.56	80.68	91.79	88.92	1.35	0.0063	0.112
15	66.3	4.0	9.2	89.33	78.22	90.72	88.92	1.60	0.0072	0.131
16	66.7	4.2	~	87.96	75.81	89.66	87.75	1.75	0.0077	0.143
17	75.6	4.0	8.1	59.85	29.64	66.21	85.04	1.7	0.0082	0.16
18	75.6	3.5	7.5	59.0	28.29	65.08	83.47	1.39	0.0063	0.093
19	74.0	2.75	7.2	65.68	35.13	70.46	86.47	1.09	0.0052	0.079
20	74.5	3.1	6.8	63.9	32.24	68.32	87.75	1.18	0.0055	0.083

Run#	Temp	P_T	h_f	x_{in}	x_{out}	y_n^*	E_{MV}	F_s	De	Pe
1	98.85	2.5	8.5	50.95	44.24	53.15	75.3	0.66	0.0036	0.129
2	98.4	2.8	8.6	53.69	47.47	55.87	74	0.844	0.0044	0.149
3	98.25	3.5	9.7	53.85	47.75	56.1	73	1.01	0.0052	0.169
4	98.55	4.0	10.3	53.22	47.09	55.55	72.5	1.26	0.0062	0.202
5	99.75	2.4	8.7	39.88	32.33	42.34	75.4	0.67	0.0036	0.126
6	100.2	2.4	8.6	37.66	30.48	40.52	71.5	0.7	0.0037	0.128
7	101	4.2	10	37.09	30.13	40.16	69.4	1.3	0.0062	0.198
8	99.6	5	11	38.9	32.19	42.21	67	1.46	0.0036	0.119
9	105.2	2.4	8.4	11.92	8.51	13.93	62.99	0.68	0.0036	0.121
10	99.75	2.4	8.5	43.52	36.26	46.07	74	0.68	0.0036	0.127
11	98.85	2.5	8.5	50.95	44.24	53.15	75.32	0.68	0.0037	0.128
12	101.4	2.4	8.5	35.14	27.95	37.94	72	0.68	0.0063	0.20
13	101.7	4.5	10	30.59	23.96	33.66	68.3	1.314	0.0062	0.196
14	103.8	4.7	10.3	17.4	12.78	19.96	64.3	1.355	0.0062	0.189

Table A.3: Experimental Data for n-Heptane/toluene system

Table A.4: Experimental Data for Benzene/n-heptane system										
Run#	Temp	P_T	h_f	x_{in}	x_{out}	y_n^*	E_{MV}	F_s	De	Pe
1	74.3	3.1	7.5	77.23	73.61	80.58	51.94	0.6	0.0032	0.111
2	75.9	3	7.4	75.34	70.98	78.89	55.12	0.6	0.0032	0.112
3	78.2	3	7.4	70.55	65.02	75	55.4	0.6	0.0032	0.113
4	77.5	3.2	7.0	67.48	61.01	72.3	57.3	0.6	0.0034	0.118
5	82.5	2.8	7.2	34.92	25.33	40.17	64.6	0.6	0.0033	0.127
6	88.6	3.3	8.3	17.76	11.32	20.62	69.2	0.6	0.0034	0.131
7	81.3	3	7.5	45.58	35.65	51.53	62.5	0.6	0.0037	0.132
8	84.8	3	7.5	35.65	25.98	40.95	64.6	0.6	0.0037	0.134
9	76.5	2.7	7.8	88.96	87.82	90.08	50.22	0.6	0.0033	0.11
10	88.7	4	8.8	16.65	11.03	20.15	61.6	1.13	0.0056	0.193
11	85	4	8.8	24.3	17.21	29.51	57.6	1.13	0.0056	0.191
12	75.9	3.9	8.2	73.62	69.34	77.83	50.4	1.13	0.0057	0.175
13	78.6	3.96	8.2	68.74	63.04	73.68	53.57	1.13	0.0059	0.195
14	85.9	3.4	7.9	35.16	25.81	40.75	57.36	1.13	0.0037	0.132
15	81.3	3	7.5	45.58	35.65	51.53	62.5	0.667	0.0040	0.137
16	80.9	2.9	7.1	46.07	36.42	52.29	60.8	0.724	0.0049	0.162
17	81.4	3.2	7.8	45.67	35.63	51.50	63.3	0.937	0.0059	0.192
18	81.3	3.4	7.9	45.11	34.38	50.25	62.7	1.16	0.0057	0.187
19	81.4	4.5	8.4	43.45	33.96	49.81	59.87	1.41	0.0071	0.24

Table A.5: Experimental Data for Cyclohexane/n-heptane system										
Run#	Temp	P_T	h_f	x_{in}	x_{out}	y_n^*	E_{MV}	F_s	De	Pe
1	86.6	3.5	8.5	51.33	42.57	55.39	70.7	0.943	0.0050	0.168
2	84.8	3.2	8.0	57.02	48.8	61.41	65.2	1.04	0.0054	0.178
3	85.7	4.0	9.2	53.63	45.16	57.94	66.3	1.33	0.0066	0.22
4	86.2	4.5	9.5	53.04	44.71	48.82	65.1	1.61	0.0050	0.17
5	86.2	5.0	–	51.25	43.01	55.83	64.3	1.76	0.0050	0.172
6	88.2	3	7.7	42.16	33.57	45.93	69.5	0.94	0.0050	0.167
7	89.4	3.2	7.8	35.3	27.96	39.51	69.0	0.94	0.0050	0.17
8	86.2	3.3	8.8	51.65	42.54	55.36	71.1	0.94	0.005	0.167
9	88.2	3.3	8.8	42.14	33.52	45.88	69.7	0.94	0.0049	0.159
10	82.6	3.3	8.7	74.16	67.29	77.18	59.5	0.94	0.0049	0.162
11	84.5	3.3	8.7	66.19	57.56	69.23	73.95	0.94	0.0051	0.175
12	91.6	3.2	7.8	27.64	20.69	30.52	70.7	0.94	0.0066	0.22
13	84.7	4.0	9.1	61.36	52.74	65.01	70.25	1.34	0.0066	0.22
14	86.6	4.0	9.1	53.86	45.17	57.96	67.9	1.34	0.0065	0.214
15	82.8	4.0	9.1	72.88	65.7	75.93	70.19	1.34	0.0066	0.217
16	84.6	4.0	9.1	65.74	57.83	69.46	68.01	1.34	0.0066	0.224
17	85.7	4.0	9.2	56.56	45.16	57.94	66.3	1.34	0.0066	0.23
18	88.2	4.0	9.2	44.27	35.96	48.54	66.0	1.34	0.0043	0.14
19	81.7	3.1	.1	74.96	67.45	77.3	76.2	0.816	0.0051	0.16
20	82.1	3.5	7.5	73.42	65.92	76.1	73.9	1.09	0.0055	0.177
21	82.2	3.3	8.7	73.87	67.2	77.11	67.3	1.47	0.0066	0.217

Table A.6: Experimental Data for Chloroform/toluene system									
Run#	Temp	P_T	h_f	x_{in}	x_{out}	y_n^*	E_{MV}	F_s	De	Pe
1	62.7	5.4	7.7	95.88	87.48	97.41	84.6	1.474	0.00536	0.147
2	61.4	5.5	8.8	97.26	91.38	98.33	84.6	1.60	0.0057	0.156
3	61.4	6	8.3	96.91	89.63	97.98	87.2	1.85	0.0064	0.179
4	62.7	6.9	8.7	96.07	87.66	97.56	84.9	2.4	0.0077	0.24
5	63.6	7.4	9.5	94.83	85.07	96.97	82.0	2.68	0.0058	0.166
6	87.3	4.8	8.0	56.49	31.52	64.51	75.7	1.4	0.0063	0.183
7	88.4	5.3	8.6	56.6	31.38	64.38	76.4	1.56	0.0071	0.215
8	88.0	5.7	8.9	56.4	31.27	64.26	76.2	1.82	0.0046	0.135
9	88.6	6.5	~	55.09	30.28	62.97	75.9	2.04	0.0051	0.141
10	89.6	4.4	7.7	51.37	27.48	59.08	75.6	1.04	0.0053	0.148
11	62.7	5.4	7.7	95.88	87.48	97.41	84.6	1.4	0.0056	0.159
12	70.1	10.0	7.5	88.36	69.08	91.52	85.9	1.4	0.0058	0.166
13	80.7	4.8	8.8	71.93	45.13	77.61	82.5	1.4	.00061	0.178
14	87.3	4.8	8.0	56.49	31.52	64.51	75.7	1.4	0.00612	0.18
15	87.3	4.8	8.0	29.0	15.42	37.32	62.0	1.4	0.0063	0.187
16	99.2	~	~	25.67	13.72	33.64	60.0	1.4	0.0064	0.181
17	104.5	~	~	10.76	5.58	14.36	59.0	1.4	0.0063	0.174
18	67.4	5.9	8.5	91.7	76.38	94.4	85.0	1.8	0.0064	0.182
19	68.3	6.0	8.3	90.84	74.06	93.57	86.0	1.8	0.007	0.213
20	82.7	~	~	65.69	41.39	74.68	73	1.8	0.0069	0.204
21	99.6	~	~	24.64	13.14	32.31	60	1.8	0.0074	0.233

Run#	Temp	P_T	h_f	x_{in}	x_{out}	y_n^*	E_{MV}	F_s	De	Pe
							Table A.7: Experimental Data for Methanol/isopropyl alcohol system			
1	63.9	2.9	6.6	92.4	86.87	93.63	81.8	0.633	0.0034	0.075
2	64.6	3.4	7.1	91.3	84.87	82.53	83.9	0.91	0.0046	0.093
3	64.6	3.8	8.0	91.0	84.49	92.32	83.2	1.14	0.0056	0.109
4	64.8	4.6	8.6	90.59	84.01	82.05	81.8	1.45	0.0067	0.134
5	65.3	5.3	--	89.1	81.87	90.81	80.9	1.64	0.0073	0.152
6	73.1	2.9	7.2	44.61	34.3	49.07	69.8	0.615	0.0033	0.087
7	72.4	3.3	7.3	54.24	42.01	57.9	76.97	0.817	0.0042	0.099
8	72.6	3.8	7.7	51.78	39.99	55.67	75.2	1.044	0.0051	0.115
9	73.1	4.0	8.0	49.42	37.95	53.35	74.5	1.24	0.0059	0.135
10	73.3	4.7	9.4	46.84	36.5	51.67	68.17	1.52	0.007	0.163
11	73.6	4.7	~	44.03	34.24	49.0	66.34	1.57	0.0071	0.171
12	74.0	5.1	~	42.05	32.51	46.9	66.34	1.734	0.0076	0.192
13	67.9	2.9	7.1	77.09	65.74	79.9	80.1	0.6	0.0030	0.076
14	75.2	2.9	7.0	33.66	24.7	36.91	73.4	0.6	0.0029	0.079
15	76.8	2.9	7.3	19.09	13.28	20.83	76.9	0.6	0.0032	0.073
16	68.7	5.5	~	72.8	62.85	77.64	67.3	1.65	0.0072	0.159
17	74.0	5.1	~	42.05	32.51	46.9	66.34	1.65	0.0071	0.171
18	75.2	4.7	9.'	33.2	24.81	37.06	68.54	1.65	0.0071	0.175
19	77.2	5.15	~	17.7	12.82	20.15	66.66	1.65	0.0067	0.155
20	65.3	5.3	11.0	88.18	81.87	90.81	70.53	1.65	0.007	0.153

103

SHUT-DOWN

(14) turn off the steam slowly and ̤he vent.

(15) Shut off all equipment.

SAMPLE CALCULATIONS:

Conversion from wt.% to mol.%

Example: run#2 of cyclohexane/n-heptane system

x_{in} = 52.7 wt.%

MW_{C6} = 84.162

MW_{C7} = 100.21

$x_{in}(mol.\%) = \{(52.7/84.162)/[(52.7/84.162)+(47.3/100.21)]\} * 100\% = 57.02$ mol.%

Calculation of E_{MV}

Example: run#1 chloroform/toluene system

x_{in} = 95.88 mol.%

x_{out} = 87.48 mol.%

$y_n^{\bullet}$ = 97.41

From Equation (2.4), $x_{n-1} = x_{in}$; $x_n = x_{out}$

$E_{MV} = (95.88 - 87.48)/(97.41 - 87.48) * 100 = 84.6$ %

Calculation of F-factor

Example: run#1 methanol/isopropyl alcohol system

$$F_s = u_s (\rho_v)^{0.5}$$

$$\rho_v = 1.429 \text{ kg/m}^3$$

$$u_s = 0.5295 \text{ m/s based on the liquid flow rate}$$

$$F_s = 0.5295 (1.429)^{0.5} = 0.633 \text{ (kg/m)}^{0.5}/s$$

APPENDIX B: PHYSICAL PROPERTIES EMPLOYED IN THIS STUDY

(Reid et al. 1977)

Table B.1:   Physical Properties for the Methanol/Water System

Table B.2:   Physical Properties for the n-Heptane/Toluene System

Table B.3:   Physical Properties for the Benzene/n-Heptane System

Table B.4:   Physical Properties for the Cyclohexane/n-Heptane System

Table B.5:   Physical Properties for the Methanol/Isopropyl Alcohol System

Table B.6:   Physical Properties for the Chloroform/Toluene System

Table B.1: Physical Properties For the Methanol/Water System							
X_A, mol.%	μ_L, Ns/m^2	ρ_L, kg/m^3	ρ_G, kg/m^3	σ,N/m	D_G, m^2/s	D_L, m^2/s	m
10.8	2.98e-4	911.8	0.652	0.0417	2.03e-5	7.79e-9	1.75
20.8	3.14e-4	879.6	0.710	0.0344	1.96e-5	7.55e-9	1
29.9	3.19e-4	854.5	0.758	0.0300	1.92e-5	7.61e-9	0.778
41.5	3.26e-4	828.2	0.824	0.0272	1.88e-5	7.65e-9	0.496
53.6	3.44e-4	807.8	0.906	0.0234	1.80e-5	7.40e-9	0.475
64.5	3.49e-4	792.3	0.97	0.0222	1.76e-5	7.48e-9	0.46
72.0	3.43e-4	781.1	1.01	0.0211	1.76e-5	7.79e-9	0.45
81.1	3.34e-4	768.9	1.05	0.0200	1.77e-5	8.24e-9	0.43
85.2	3.33e-4	764.3	1.08	0.0196	1.76e-5	8.37e-9	0.444

Table B.2: Physical Properties For the n-Heptane/Toluene System							
X_A, mol. %	μ_L, Ns/m^2	ρ_L, kg/m^3	ρ_G, kg/m^3	σ, N/m	D_G, m^2/s	D_L, m^2/s	m
10.6	2.46e-4	753.6	3.0	0.0173	3.48e-6	5.43e-9	1.41
15.7	2.45e-4	741.6	3.03	0.0168	3.45e-6	5.47e-9	1.29
26.9	2.40e-4	727.5	3.07	0.0160	3.42e-6	5.65e-9	1.05
36.1	2.37e-4	712.7	3.11	0.0153	3.38e-6	5.77e-9	0.93
40.1	2.35e-4	705.3	3.12	0.0151	3.38e-6	5.88e-9	0.89
47.8	2.31e-4	692.3	3.15	0.0146	3.36e-6	6.03e-9	0.83
49.9	2.30e-4	688.9	3.16	0.0145	3.36e-6	6.07e-9	0.82

X_A	μ_L	ρ_L	ρ_G	σ	D_G	D_L	m
Table B.3: Physical Properties for the Benzene/n-Heptane System							

X_A	μ_L	ρ_L	ρ_G	σ	D_G	D_L	m
13.8	2.22e-4	629.7	3.3	0.0128	3.59e-6	6.72e-9	1.53
20.8	2.33e-4	642.9	3.3	0.0132	3.52e-6	6.25e-9	1.33
30.1	2.38e-4	655.3	3.2	0.0138	3.54e-6	6.04e-9	1.11
40.6	2.55e-4	676.0	3.1	0.0146	3.45e-6	5.44e-9	0.92
61.1	2.82e-4	717.3	3.01	0.0163	3.36e-6	4.67e-9	0.69
65.9	2.82e-4	724.9	2.97	0.0168	3.39e-6	4.65e-9	0.68
73.2	2.96e-4	743.9	2.93	0.0176	3.34e-6	4.33e-9	0.65
88.4	3.08e-4	780.4	2.8ʼ	0.0195	3.35e-6	4.03e-9	0.73
89.7	3.08e-4	783.6	2.8	0.0196	3.36e-6	4.02e-9	0.74

X_A	μ_L	ρ_L	ρ_G	σ	D_G	D_L	m
24.2	2.36e-4	629.7	3.24	0.01269	3.38e-6	5.89e-9	1.24
31.9	2.51e-4	635.6	3.2	0.01293	3.34e-6	5.46e-9	1.128
37.4	2.61e-4	641.4	3.18	0.01311	3.32e-6	5.2e-9	1.06
47.0	2.79e-4	651.3	3.14	0.01342	3.29e-6	4.79e-9	0.95
57.1	3.0e-4	665.5	3.12	0.01377	3.26e-6	4.37e-9	0.863
61.8	3.08e-4	670.0	3.1	0.01395	3.25e-6	4.23e-9	0.82
70.7	3.31e-4	680.8	3.06	0.01428	3.22e-6	3.87e-9	0.76

Table B.4:   Physical Properties For the Cyclohexane/n-Heptane System

Table B.5: Physical Properties For the Methanol/Isopropyl Alcohol System							
X_A	μ_L	ρ_L	ρ_G	σ	D_G	D_L	m
15.3	4.87e-4	711.2	1.9	0.0155	8.60e-6	4.35e-9	1.4
29.0	4.63e-4	716.5	1.82	0.0159	8.50e-6	4.5e-9	1.27
37.4	4.47e-4	719.8	1.74	0.0161	8.44e-6	4.61e-9	1.15
40.2	4.46e-4	721.7	1.72	0.0162	8.40e-6	4.60e-9	1.115
49.8	4.28e-4	725.7	1.63	0.0165	8.33e-6	4.75e-9	0.97
67.6	3.95e-4	733.9	1.46	0.017	8.18e-6	5.02e-9	0.74
71.4	3.88e-4	736.0	1.43	0.017	8.15e-6	5.08e-9	0.7
89.5	3.57e-4	746.4	1.26	0.0178	7.95e-6	5.38e-9	0.52

Table B.6: Physical Properties For the Chloroform/Toluene System							
X_A	μ_L	ρ_L	ρ_G	σ	D_G	D_L	m
9.1	2.57e-4	812.8	3.05	0.0185	4.22e-6	7.88e-9	2.4
19.0	2.69e-4	862.0	3.18	0.0187	4.11e-6	7.23e-9	1.9
23.6	2.7e-4	882.2	3.22	0.0189	4.11e-6	7.11e-9	1.68
42.4	2.99e-4	988.97	3.5	0.0195	3.86e-6	5.9e-9	0.77
57.0	3.19e-4	1078.8	3.7	0.0199	3.70e-6	5.18e-9	0.50
78.1	3.5e-4	1226.6	4.0	0.0207	3.48e-6	4.27e-9	0.34
83.2	3.59e-4	1266.14	4.11	0.021	3.43e-6	4.07e-9	0.26
91.4	3.74e-4	1332.99	4.25	0.0212	3.33e-6	3.75e-9	0.19

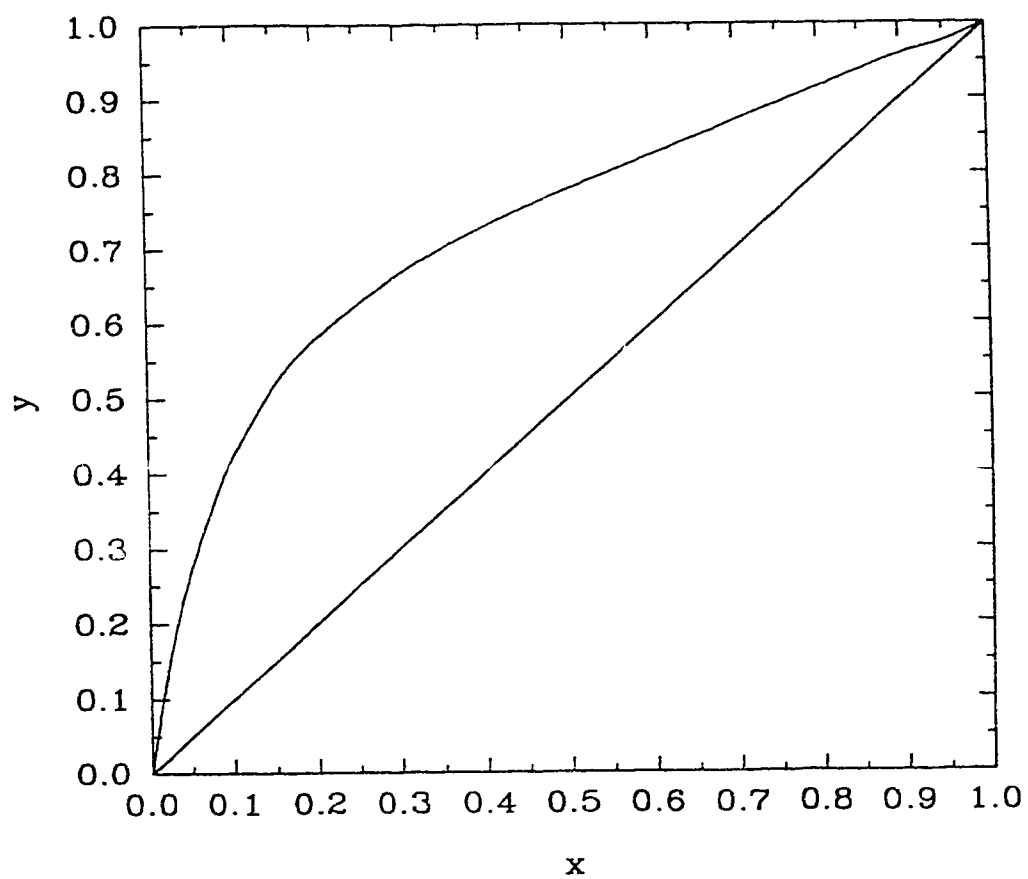APPENDIX C: EQUILIBRIUM DATA (Hirata et. al., 1975)

113

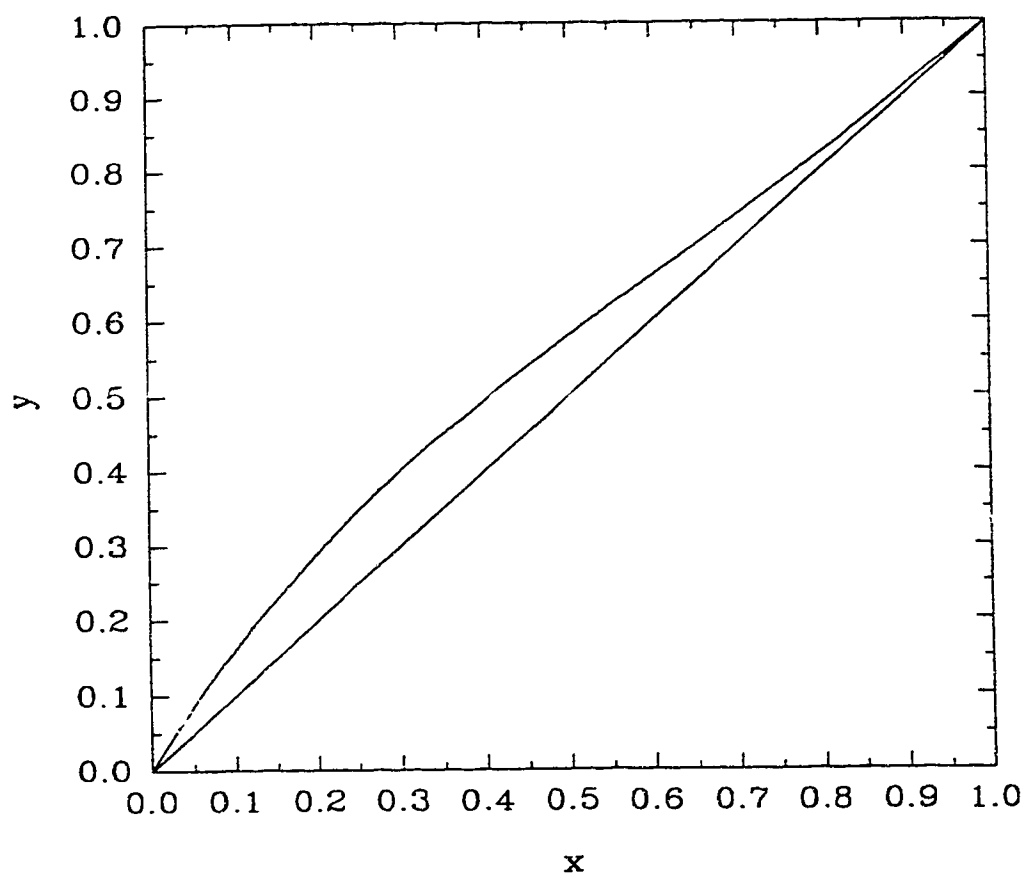Figure C.1: Equilibrium Curve for Methanol/Water System at 720 mmHg

114

Figure C.2: Equilibrium Curve for n-Heptane/Toluene System at 720 mmHg
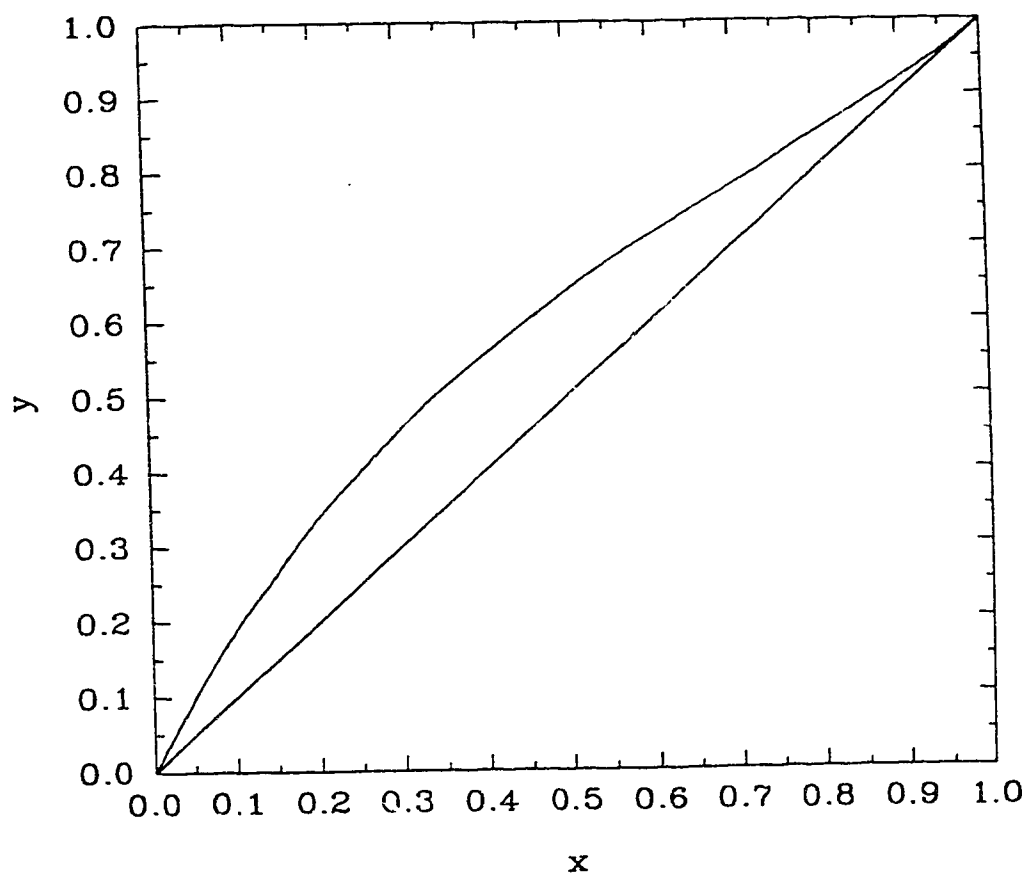
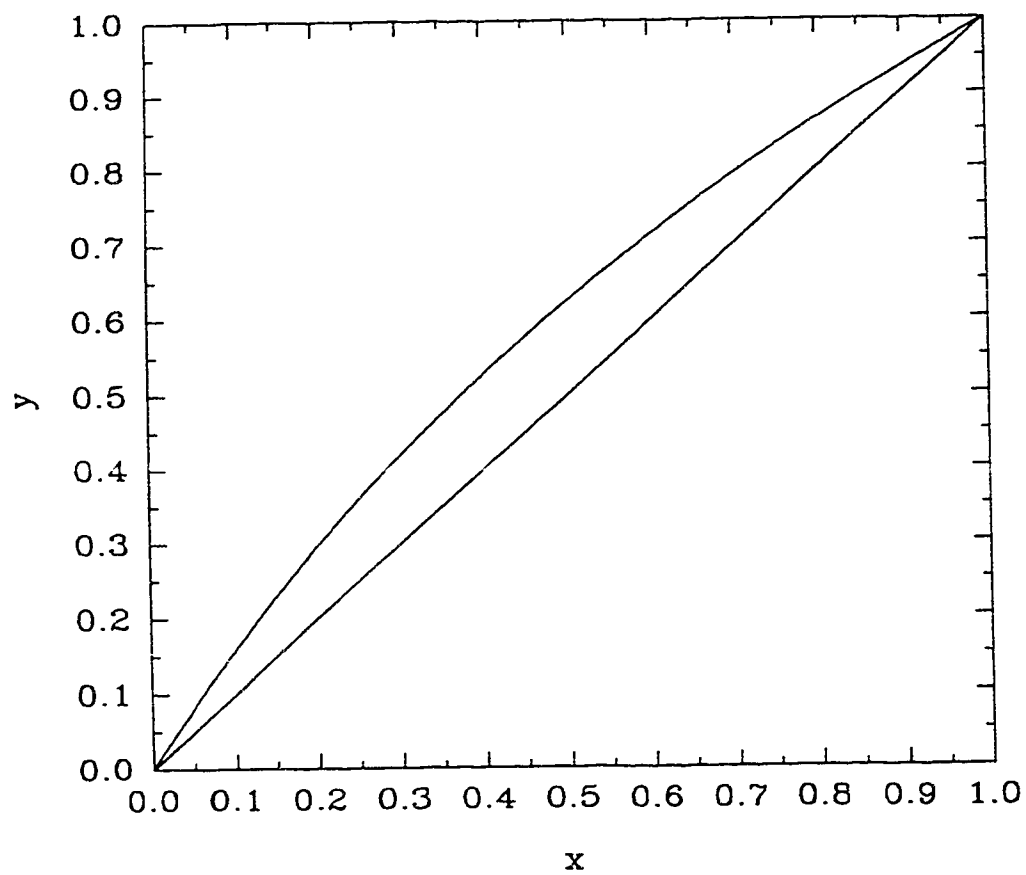Figure C.3: Equilibrium Curve for Benzene/n-Heptane System at 720 mmHg

116

Figure C.4: Equilibrium Curve for Cyclohexane/n-Heptane System
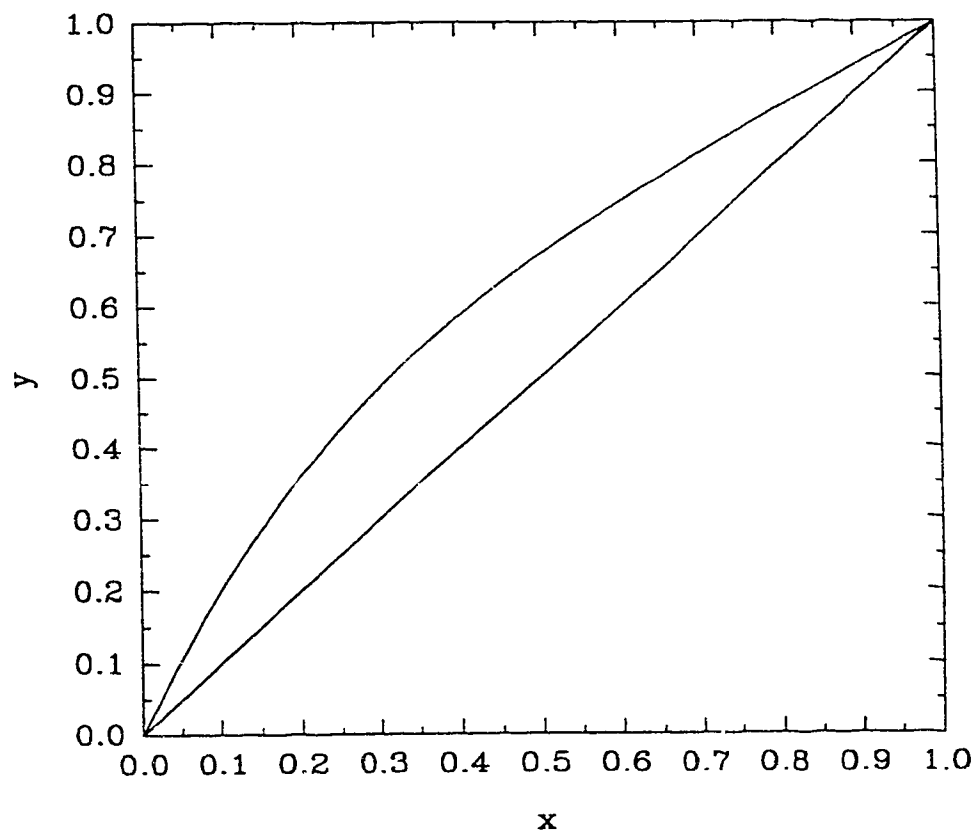
at 720 mmHg

117

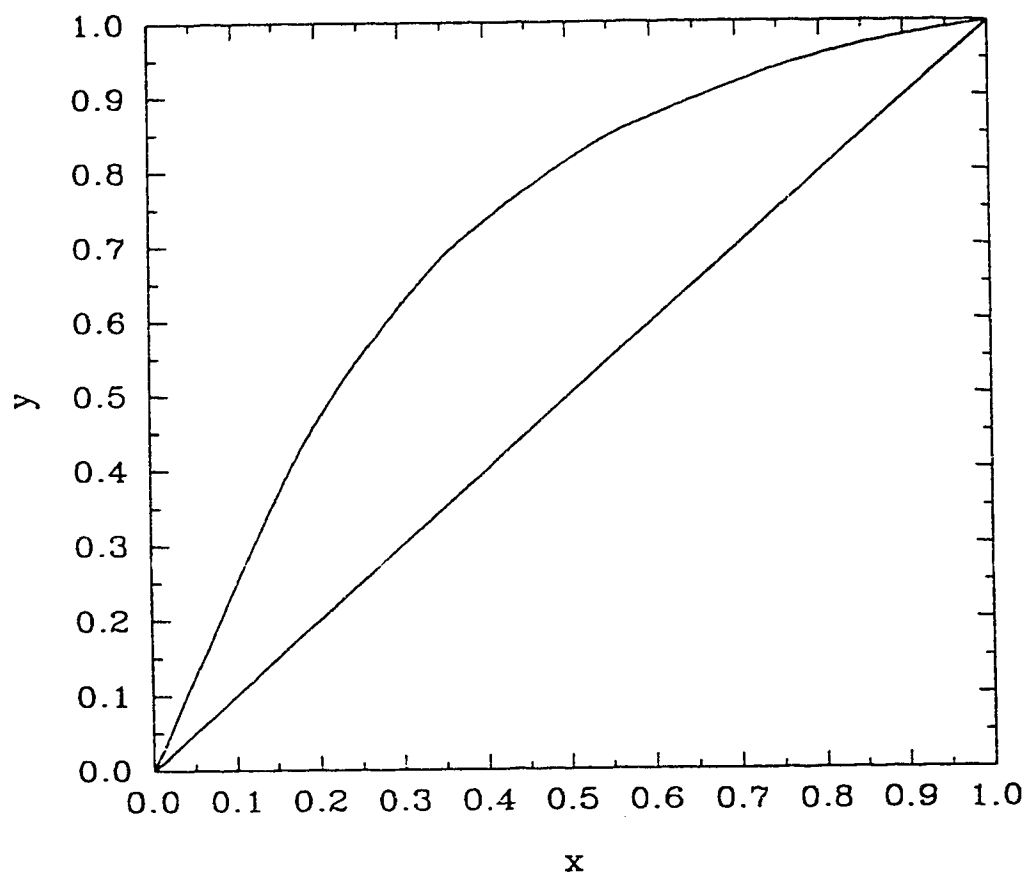Figure C.5: Equilibrium Curve for Methanol/Isopropyl Alcohol System at 720 mmHg

118

Figure C.6: Equilibrium Curve for Chloroform/Toluene System

at 720 mmHg

APPENDIX D: MARANGONI-INDEX DATA (Equation 3.1)

Table D.1: M-index For the Methanol/Water System

Table D.2: M-index For the n-Heptane/Toluene System

Table D.3: M-index For the Benzene/n-Heptane System

Table D.1: M-index For the Methanol/Water System Employed In This Study	
X_A, (mol. %)	M-index, (N/m)
10.8	0.03
19.1	0.023
20.8	0.023
24.2	0.02
29.9	0.0164
41.5	0.011
47	8.93×10^{-3}
53.6	6.43×10^{-3}
64.5	3.39×10^{-3}
72	2.14×10^{-3}
84.2	7.14×10^{-4}

Table D.2: M-index For the n-Heptane/Toluene System Employed In This Study	
X_A, (mol.%)	M-index, (N/m)
10.6	3.765×10^{-4}
15.7	5×10^{-4}
31.76	3.82×10^{-4}
34.6	7×10^{-4}
40.1	6.5×10^{-4}
47.8	5.67×10^{-4}
49.9	5.5×10^{-4}

Table D.3: M-index For the Benzene/n-Heptane System Employed In This Study	
X_A, (mol. %)	M-index, (N/m)
14.5	-6.02×10^{-4}
20.8	-8.5×10^{-4}
30.1	-1.03×10^{-3}
40.0	-1.18×10^{-3}
61.1	-1.04×10^{-3}
71.5	-8.61×10^{-4}
75.4	-7.9×10^{-4}
89	-2.04×10^{-4}